

Composition and Performance of Multi-layer Liner Systems to Inhibit Contaminant Transport in a Fly-ash Dump

Lehlohonolo Mokhahlane

Submitted in fulfilment of the requirements for the degree

Magister Scientiae in Geohydrology

in the

Faculty of Natural and Agricultural Sciences

(Institute for Groundwater Studies)

at the

University of the Free State

Supervisor: Prof G Steyl

Bloemfontein

July 2013

Declaration

I, Lehlohonolo Mokhahlane, declare that the dissertation hereby submitted by me for the Magister Scientiae degree at the University of the Free State is my own independent work except where due references are provided, furthermore this work has not previously been submitted by me at another University/Faculty.

I further cede copyright of the dissertation in favour of the University of the Free State.

Signature

Date

Dedication

I dedicate this dissertation to my father Rabolou Gabriel Mokhahlane, who passed away in November 2008. Thank you for always encouraging me to further my studies and set a good academic example to our family. You are truly missed.

Acknowledgments

This research project emanated from Eskom's Sustainability and Innovation Department and their financial support throughout this project is acknowledged with sincere gratitude.

This study has become a great journey of success with the selfless efforts and contributions of countless men and women. The following people deserve a special mention:

- My mentor Prof. Gideon Steyl, whose academic and technical guidance throughout this project was splendid. You believe in me from day one. Thank you.
- Dr. Danie Vermeulen for reviewing my work and always opening his door to me, many thanks.
- Mrs. Lorinda Rust and Mrs. Dora Du Plessis, for my research travels and all the materials you arranged for me that made my life a lot easier.
- To all the staff at the Institute for Groundwater Studies; Teboho Shakhane you were at my side, from sampling stage to the data analysis, thanks a lot my brother. Mrs. Lora Marie and all the special ladies in the laboratory thanks for all the assistance and to Dr Moderick Gomo your advice throughout is much appreciated.
- To the hardworking group at Simlab especially my friend Mr Charlton Deon Leeu, I am grateful for all your help. Thanks to Mr Barnes van Vuuren for all your supervision and allowing me to use your facilities.
- The goodhearted people of Soil Science Department. Ms Yvonne Dessels, your willingness to help at all times was cherished. My brother Edwin your tireless help with sample preparations motivated me.
- To the meticulous group of people at the Geology Department. Prof. Chris Gauert, Dr. Frederick Roelofse, Ms. Huibrie Pretorius, Mr. Choane you guys were amazing.
- To the wonderful people at Eskom's Analytical Chemistry and Microbiology. A special thanks to Mr Gerhard Gericke, you are my inspiration, Mrs Jenny

Reeves, thanks for all your support, Ms Linda Makhubela, your help was always comforting, Ms Kelly Whitehead, for always giving IT assistance, you rock, and Ms Lineo Tlali, your unending help was truly refreshing. You are an angel.

- To all the individuals at Eskom who assisted me. Mr Xolani Ngubeni, my brother your swiftness in providing me with results was a light to me. Ms Shinelka Sign, your assistance was great and truly appreciated.

I would like to take this opportunity to thank my family. My mum, Mabatho Mokhahlane you are the best mother in the whole world and first lady of my life. Your love towards me was an inspiration that propelled me even when the odds seemed to be against me. Thank you. My sisters, Mpho and Reitumetse you guys are my best friends and biggest supporters, thanks for believing in me.

The biggest shout of praise is to my God and Saviour Jesus Christ. I am nothing without You but with You by my side I can achieve all things. Thank You for loving me and guiding me into all truth, You have always been at my side throughout this whole journey. My life is not my own, to You it belongs, all I have is from You and I know You are taking me from glory to glory. I live only for your glory Lord.

Thank You Jesus Christ, my Lord and Saviour.

Table of Contents

Declaration	i
Dedication	ii
Acknowledgments	iii
Table of Contents	v
List of Figures	ix
List of Tables	xii
List of Equations	xiii
List of Abbreviations	xv
List of Quantities and Units	xvi
1 Introduction	1
1.1 Background	1
1.2 Aim of study	3
1.2.1 Specific objectives	3
1.2.2 Study approach and thesis outline	4
1.3 Summary	4
2 Literature review	6
2.1 Fly ash	6
2.1.1 Introduction	6
2.1.2 Physical Properties of fly ash	7
2.1.3 Chemical properties and classification of fly ash	7
2.1.4 Mineralogy of fly ash	9
2.1.5 Hydration of fly ash and secondary minerals	10
2.1.6 Environmental impact of fly ash disposal methods	12
2.1.7 Dynamics of fly ash leaching	14

2.1.8	Utilization of fly ash.....	16
2.1.9	Fly ash application as a liner material: Previous studies	21
2.2	Contaminant transport.....	23
2.2.1	Introduction.....	23
2.2.2	Transport in porous media.....	23
2.2.3	Hydraulic conductivity.....	26
2.2.4	Advection.....	29
2.2.5	Diffusion.....	30
2.2.6	Dispersion.....	31
2.3	Landfill liner designs.....	33
2.4	Environmental regulations.....	37
2.5	Summary.....	39
3	Methods and Materials.....	41
3.1	Materials.....	41
3.2	Sampling and storage	42
3.3	Mixture preparations	42
3.4	Engineering methods	43
3.4.1	Maximum dry density and optimum moisture content.....	43
3.4.2	Unconfined compression strength (UCS)	48
3.4.3	Indirect tensile strength (ITS).....	50
3.4.4	Atterberg limits.....	52
3.5	Geochemical methods	54
3.5.1	X-ray Diffraction (XRD).....	54
3.5.2	X-ray fluorescence (XRF)	55
3.5.3	Scanning electron microscopy (SEM).....	56
3.5.4	Quantitative evaluation of minerals by scanning electron microscopy (QEMSCAN).....	57

3.6	Cation exchange capacity (CEC)	59
3.6.1	Sample Preparation	59
3.7	Texture analysis	60
3.7.1	Procedure	60
3.8	Hydraulic conductivity	60
3.8.1	Experimental procedure.....	60
3.8.2	Preparation and packing of the column	61
3.8.3	Wetting and drying cycles.....	63
3.9	Multi-layer liner system	64
3.9.1	Daily percolation tests.....	69
3.9.2	Continuous percolation test	71
3.10	Summary	72
4	Results and Discussions	74
4.1	Introduction	74
4.2	Engineering performance	74
4.2.1	Moisture content – dry density relationship.....	74
4.2.2	Unconfined compression strength (UCS) and indirect tensile strength (ITS)	76
4.2.3	Atterberg limits.....	78
4.3	Hydraulic conductivity	81
4.3.1	Effects of leaching with brine water on hydraulic conductivity	83
4.3.2	Wet/dry cycles	85
4.4	Leachate analysis	86
4.5	Physical, chemical and mineralogical compositions.....	92
4.5.1	Morphology analysis by Scanning Electron Microscope (SEM).....	93
4.5.2	Chemical composition by X-ray Fluorescence (XRF)	95
4.5.3	Mineralogical composition by X-ray Diffraction (XRD)	97

4.5.4	Quantitative analysis by QEMSCAN.....	101
4.5.5	Texture analysis	102
4.5.6	Cation exchange capacity.....	103
4.6	Performance of multi-layer liner system	105
4.7	General discussion.....	109
4.8	Summary.....	111
5	Conclusion and Recommendations.....	113
5.1	Conclusion	113
5.2	Recommendations	114
	References.....	116
	Abstract.....	123
	Opsomming.....	125
	Appendices	127

List of Figures

Figure 2-1 Flow diagram for processes at a coal fired power station that lead to a variety of residue products, adapted from (Gitari, 2006)	6
Figure 2-2 Aqueous inflows and outflows in dry and wet ash deposits, adapted from (Hansen et al., 2002).....	12
Figure 2-3 Pathways for pollution transport in ash impoundments, modified from (Fatoba, 2007).....	14
Figure 2-4 Darcy's experimental set-up, adapted from (Freeze and Cherry, 1979) .	24
Figure 2-5 6 macroscopic and microscopic concepts of flow in porous media, adapted from (Freeze and Cherry, 1979).....	25
Figure 2-6 Possible scenarios of heterogeneity and anisotropic, adapted from (Freeze and Cherry, 1979).....	27
Figure 2-7 Unit volume demonstrating flow through porous media (conservation of mass), adapted from (Freeze and Cherry, 1979)	28
Figure 2-8 Dynamics of microscopic dispersion in porous media, adapted from (Daniel, 1993).....	32
Figure 2-9 Liner design systems, adapted from (Hughes et al., 2013).....	35
Figure 3-1 Mould with collar and base plates, adapted from (TMH1-A7, 1986)	45
Figure 3-2 Mould under a tamper during compaction.....	46
Figure 3-3 Example of a graph of moisture-density relationship, adapted from (TMH1-A7, 1986)	48
Figure 3-4 Specimens being prepared for rapid curing. The plastic bags create a constant humid environment around the specimens as they were cured for 48 hours in the oven at 60 °C.....	49
Figure 3-5 Specimens in a water bath at 25 °C.....	49
Figure 3-6 Unconfined compression strength test on a fly ash admix sample.....	50
Figure 3-7 Sample splits in half during an indirect tensile strength test.....	51
Figure 3-8 Fly ash sample in a casagrande cup used for liquid limit determinations, <i>left</i> shows sample after being transferred to the cup, <i>right</i> shows the sample after having divide into two portions before tap action.....	52

Figure 3-9 Sample preparation for XRD, <i>left</i> is a sample being crushed, <i>right</i> is sample being pressed into a sample holder before being entered into the Diffractometer.....	55
Figure 3-10 Sample after being carbon coated	57
Figure 3-11 Preparation of block samples, left sample from permeameter is being cut, right is square blocks of samples.....	59
Figure 3-12 Experimental set up for hydraulic conductivity determinations.....	61
Figure 3-13 Sample mixing, (left) gypsum and lime just added to fly ash, (right) homogeneous mixture of fly ash, gypsum and lime after vigorous mixing.....	62
Figure 3-14 Compaction of samples into a column	62
Figure 3-15 Drying of LSM 7 in an oven at set 60 °C, desiccator inserted in oven to encourage drying	64
Figure 3-16 Compaction procedure using rammer inside permeameter cell.....	66
Figure 3-17 Geotextile being placed on top of compacted layer, also a small piece of geotextile is placed at an outflow point to prevent clogging of the pipe.....	66
Figure 3-18 Gravel layer inside permeameter cell.....	67
Figure 3-19 Tutuka fly ash being added on top of the multi-layer liner system.....	68
Figure 3-20 Configuration of layers within a multi-layer liner system	69
Figure 3-21 Permeameter enclosing multi-layer liner system, <i>left</i> quarter compaction, <i>right</i> full compaction	70
Figure 3-22 Adhesive plastic covering collecting bottle to avoid losses due to gravity	70
Figure 3-23 Continuous percolation test on a permeameter containing a multi-layer liner system. Brine water coming out of Outflow point 1 is being received in a container and circulated back into the constant head compartment.....	72
Figure 4-1 A plot of UCS (4 hours and 7 days curing) and ITS values in KPa	76
Figure 4-2 White patches of unreacted lime in LSM 9 after ITS crushing.....	78
Figure 4-3 Dura-Pozz fly ash collapses in a water bath during curing.....	78
Figure 4-4 Specimens in troughs after oven drying. Specimen 1 in the picture is LSM 7, 2 is LS 2, 3 is clay which has undergone ductile deformation upon drying and 4 is soil-clay mixture that has contracted lineally. This can be seen by the departure from the trough walls (red arrow). 3 and 4 were included for demonstration purposes only.	80

Figure 4-5 Specimen LS2 being leached under a constant head test, dark colour of lignosulphonate dominant in the leachate.	81
Figure 4-6 Hydraulic conductivity (m/s) values plotted over the seven day period for samples LSM 1 – LSM 5	82
Figure 4-7 Hydraulic conductivity (m/s) values plotted over the seven day period for samples LSM 6 – LSM 9 all with 3% gypsum.....	83
Figure 4-8 Brine water and demineralized water used to outline the changes in hydraulic conductivity with time on specimen LSM 7. A table of the data points is included in the right corner of the graph.	84
Figure 4-9 Parametric measurements for LSM 10 (Tutuka fly ash) with time.....	87
Figure 4-10 Parametric measurements for LSM 1 (Dura-Pozz fly ash) with time.....	89
Figure 4-11 Parametric measurements for specimen LSM 7 with time	90
Figure 4-12 SEM-EDS micrograph of Dura-Pozz fly ash (1A & 1B) and Tutuka fly ash (2A & 2B) and sample LSM 7 (3A & 3B)	94
Figure 4-13 Diffractogram of sample LSM 1 showing mineral formations	98
Figure 4-14 Diffractogram of sample LSM 7 showing mineral formations	99
Figure 4-15 QEMSCAN false colour images of vertical and horizontal block samples of LSM 7 (top) and a powdered sample of LSM 1 (bottom).....	101
Figure 4-16 Exchangeable cation determined during CEC determinations	104
Figure 4-17 Cation exchange capacity determined as (Na) (cmol/Kg)	105
Figure 4-18 Graphical representation of multi-layer liner system at full compaction (MLF).....	106
Figure 4-19 Graphical representation multi-layer liner system at a quarter compaction.....	107

List of Tables

Table 2-1 Chemical constituents in South African fly ash (Kruger, 2003).....	7
Table 2-2 Chemical requirements for classification of fly ash (ASTM-C618, 1993)....	8
Table 2-3 Thermal changes in major inorganic phases during coal combustion, modified from (Mattigod et al., 1990).....	10
Table 2-4 Ranges of values of hydraulic conductivity, adapted from (Daniel, 1993)	26
Table 2-5 Waste disposal criteria and risk rating according to Government Gazette notices 432 and 433 of 2011	39
Table 3-1 Mix preparation and sample labels.....	43
Table 3-2 Summary of polishing process	58
Table 4-1 Optimum moisture content and maximum dry densities of specimens.....	74
Table 4-2 Atterberg limits of specimens	79
Table 4-3 Ratios of hydraulic conductivity after each wet/dry cycle to background K	86
Table 4-4 SEM-EDS spot analysis of LSM 1, LSM 7 and LSM 10 in compound %..	95
Table 4-5 XRF analysis results for major elements in %(wt/wt)	96
Table 4-6 XRF results for trace elements (in part per million)	97
Table 4-7 Mineralogical analyses results from XRD.....	100
Table 4-8 QEMSCAN results showing qualitative results of mineral phases.....	102
Table 4-9 Soil texture results showing different texture as % wt/wt.....	103
Table 4-10 Water balance of MLF after cycles of 20L brine injections	108
Table 4-11 Water balance of MLQ after cycles of 20L brine injections	108
Table 4-12 Water balance of 30 day continuous brine circulation	109
Table 4-13 Risk profile of leachate from LSM7 according to Government Gazette notice 34415 of 1 July 2011	111

List of Equations

2.1 Hydration of lime	11
2.2 Dissociation of lime	11
2.3 Formation of calcium silicate gel	11
2.4 Formation of calcium aluminate gel.....	11
2.5 Formation of ettringite	11
2.6 Pyrite oxidation.....	17
2.7 Wet limestone FGD	18
2.8 Oxidation of NO.....	19
2.9 Reduction of NO.....	19
2.10 Formation of gypsum.....	19
2.11 Darcy law for one dimensional flow	23
2.12 Darcy equation	23
2.13 Differential Darcy equation	24
2.14 Darcy's equation: alternative	24
2.15 Darcy's equation compacted	24
2.16 Actual velocity of water through porous media	25
2.17 Mass as a function of density and volume.....	28
2.18 Continuity equation for flow in porous media.....	28
2.19 Continuity equation for incompressible fluids	28
2.20 Substitution of Darcy into continuity equation.....	29
2.21 Steady state flow equation through a homogeneous-isotropic medium	29
2.22 Laplace's equation	29
2.23 Seepage velocity	29
2.24 Advective mass flux.....	30
2.25 Transit time	30
2.26 Fick's first law in one dimension	30
2.27 Coefficient of longitudinal mechanical dispersion.....	32
2.28 Mechanical dispersive flux	33
3.1 Moisture content.....	47
3.2 Dry density	47

3.3 Calculation of UCS	50
3.4 Calculation of indirect tensile strength test	51
3.5 Moisture content for liquid limit	53
3.6 Liquid limit calculation using one-point method	53
3.7 Plastic limit	53
3.8 Plasticity index	54
3.9 Linear shrinkage.....	54
3.10 Darcy equation for constant head test.....	61
3.11 Water balance on multi-layer liner system.....	71

List of Abbreviations

m	metre(s)
cm	centimetre(s)
kg	kilogram(s)
kPa	kiloPascals
g	gram(s)
FA	Fly ash
FGD	Flue gas desulphurization
AMD	Acid mine drainage
XRF	X-ray Fluorescence
XRD	X-ray Diffraction
PI	Plasticity index
ICP-MS	Inductively Coupled Plasma Mass Spectrometry
RO	Reverse osmosis
QEMSCAN	Quantitative evaluation of minerals by scanning electron microscopy
CEC	Cation exchange capacity

List of Quantities and Units

Area (A)	m^2
Length	m or cm
Concentration	mg/l
Hydraulic conductivity	m/s or m/d
Electrical conductivity (EC)	$\mu S/cm$ or mS/m

1 Introduction

1.1 Background

Groundwater as a natural resource can be impacted by anthropogenic activities and landfills in particular pose a threat due to possible toxic leachate which has the potential to percolate into the subsurface (Christensen et al., 1992). The addition of inorganic and organic matter by man to the saturated zone constitutes groundwater contamination since this ultimately changes the composition of the aquifer (Freeze and Cherry, 1979). An aquifer is a hydrogeological stratum of permeable rock or unconsolidated material that has the ability to store water in the pore spaces and can also transport water through the interconnected spaces (Kruseman and Ridder, 2000). The capability of an aquifer to act as a vehicle for water flow enables contaminants in the saturated zone to be mobilised. Since groundwater forms part of the water cycle any contamination to it will ultimately impact the environment as a whole.

Leachate is a liquid that is derived from contact with waste as it percolates through a man-made structure. It becomes augmented in soluble and insoluble organic and inorganic material in the waste (Christensen et al., 1992). This liquid phase of waste management facilities is usually managed by liner systems that are designed to contain all liquid phases percolating through waste. A liner is a layer of low permeability that underlies waste in an attempt to contain leachate. Landfill design undertakes to position landfills in semi impermeable soils such as clays or to engineer low hydraulic conductivity liners that will impede leachate movement (DWAF, 1998a) nowadays however, liners consist of more sophisticated designs with leachate collection pipes and geosynthetic material making up complex multi-layer liner systems. But the main purpose of a liner still remains to form a barrier for leachate containment.

A detailed understanding of contaminant movement through both the vadose zone and the phreatic zone is essential when designing liners and similar structures meant to inhibit pollutants from contaminating groundwater. Daniel,(1993) determined that the passage of effluents through earth material is controlled by advection, diffusion,

mechanical dispersion and to a lesser extent coupled flow processes such as osmosis and ultrafiltration. Advection is the main mechanism for solutes transport and it is a result of hydraulic gradient. This movement occurs at an equal rate to the seepage velocity of the transporting fluid. Advection is easily addressed by most liner systems by simply restricting the seepage velocity. Contaminants can however still be transported by diffusion which does not require velocity but rather a gradient in the concentration of the contaminant species. When designing a liner system it is essential to consider all the transport processes as it will have to comprehend with all the mechanisms of contaminant transport.

Governments across the world have drawn up legislation that regulates landfills to contain and control potential contaminants from such facilities in an attempt to reduce environmental pollution (Daniel, 1993). Leachate from landfills remains a concern to groundwater contamination and the South Africa Government has put in place regulations that attempt to safeguard groundwater and the environment by assigning a liner system for collection and removal of leachate from landfills (DWAF, 1998a). South African regulating bodies namely the Department of Water Affairs (DWA) and the Department of Environmental Affairs (DEA) are in the forefront of protecting groundwater as a resource. The National Environmental Management Waste Act of 2008 (NEMWA) which is managed by (DEA) and the National Water Act of 1998 (NWA) are two of the most important legislations pertaining to waste management and safe guarding of water resources (DWAF, 1998a). These legislations make provisions for classification, risk profiling and containment structure for various waste that is being stockpiled in South Africa.

Energy demands in the world have driven construction of various power stations for electricity production (Ahmaruzzaman, 2009). Coal fired power stations have predominantly been used and this has resulted in large amounts of fly ash being produced annually (Cokca and Yilmaz, 2003). In South Africa 36.2 million tonnes of fly ash were produced in 2011 alone while only 5.5 % of it was recycled leaving 34.2 million tonnes to be disposed in ash dumps and dams (Eskom, 2011). As industrialization increases in South Africa, energy demands will also be on the rise to meet the production loads. South Africa generates 90% of its electricity from coal (Roberts, 2008), with the associated fly ash production increasing to match the upsurge.

Large areas of land are required for fly ash dumping (112 Km² in India alone) which consecutively increases the cost of disposal (Ahmaruzzaman, 2009). Fly ash holds pozzolanic and self-toughening properties and has conventionally been used in various industries including concrete (Nochaiya et al., 2009, Wang et al., 2006), embankment fill (Raymond, 1961, Santos et al., 2011), and soil stabilization (McCarthy et al., 2011). Clay especially in the form of bentonite has traditionally been the preferred liner material because of its low hydraulic conductivity. However development of discontinuities upon successive wetting and drying cycles and the fact that bentonite is not available everywhere presents a challenge for power stations to find substitutes for liner material (Christensen et al., 1992). Fly ash has been successfully investigated as a possible liner material (Sivapullaiah and Baig, 2011, Nhan et al., 1996, Palmer et al., 2000) that can replace clay in liner systems.

1.2 Aim of study

The aim of this study is to enhance the engineering and geohydrological properties of fly ash in order to assess its compatibility to act as a liner material that can inhibit contaminant transport in ash dumps. The liner material will be composed of fly ash as the major product and small quantities of additives added to it for material performance enhancement.

1.2.1 Specific objectives

- To investigate reusing waste in the form of fly ash as a liner material for ash dumps at power stations.
- To analyse the geochemical and mineralogical properties of fly ash liner material.
- To improve engineering and geohydrological properties of fly ash in order to be utilised as liner material by cost effective means.
- To evaluate the chemistry of leachate derived from fly ash liner material.
- To assess the performance of a multi liner system composed primarily of fly ash in containing leachate.

1.2.2 Study approach and thesis outline

The outline of the thesis is structured around the specific objectives which are as follows:

- Chapter 1 provides the background to the study and thus introduce the aim of the study with its objectives. This forms the foundation to the thesis and gives the outline of the rest of the chapters.
- Chapter 2 is the literature review of the study. Case studies of previous work on fly ash and relevant applications to liners are presented. The concepts of contaminant transport are discussed in detail and the chapter also highlights the South African legislation in relation to landfills and liner systems.
- Chapter 3 provides the sampling practices, experimental methodology and analytical techniques used in this study.
- Chapter 4 presents the results of the study. All the geochemical, engineering and geohydrological results are included as well as the characterization of leachates and specimens, with emphasis on patterns and risk profiles. Also included are the hydraulic conductivity results and the performance of the multi-layered liner system in containing leachate.
- Chapter 5 provides the conclusion of the study. Recommendations are also given based on the findings of the study.

1.3 Summary

Coal fired power stations produce massive volumes of fly ash every year and landfilling is currently the most applied method of disposing waste. Government legislation in most countries strives for landfills to be lined with impermeable material to inhibit migration of contaminants from percolating into underlying bedrock and aquifers. The challenge is to find cheaper methods of lining. Fly ash is already abundant in landfills but exists in a state that is not environmentally friendly. The task in this dissertation is to use the same fly ash stacked in landfills so as to reduce its high quantities, by treating it and improving its engineering and geohydrological properties to a level where it can be used for the same ash dumps.

Utilisation of fly ash as a liner material in ash dumps solves a number of problems for thermal power stations managers. It reduces the amount of fly ash in landfills and

also saves on costs of having to purchase and transport clay or geosynthetic liners from sources outside the power plants which increase the costs of landfilling. The obvious cost saving advantages of using fly ash as a liner material may be attractive but the possible toxic leaching of some trace elements from any reuse of fly ash remains a problem, and must be adequately addressed for fly ash to qualify as a prospective liner material. Leaching tests coupled with geochemical analysis are therefore explored in the following chapters to ascertain the risk profile of using fly ash for lining ash dumps. The next chapter provides a detailed literature review of fly ash, its properties and its role in applicable case studies. Contaminant transportation mechanisms are also explored as well as a review of the South African environmental regulation that relates to landfills and liners.

2 Literature review

2.1 Fly ash

2.1.1 Introduction

The processes in coal fired power stations generate large quantities of combustion residue, Figure 2-1. These include fly ash, bottom ash, boiler slag and the flue gas. Bottom ash and boiler slag get deposited at the base of the boiler and are made up of coarse particles (19 – 75mm) (Gitari, 2006). Fly ash is a fine powdered substance made out of round-shaped particles that ascends with flue gases. It is removed from the exhaust systems by electronic precipitators. SO_2 (which is a gas responsible for acid rain) is a constituent of the flue gases emitted by the boiler and is removed by flue gas desulphurization (FGD) prior to atmospheric release. FGD products are a result of a chemical reaction between sulphur gases and a sorbent, usually lime or limestone, which is typically in a form of calcium salts slurries. When flue gas passes through the calcium salts slurry the SO_2 reacts and forms hydrated calcium sulphate (Gitari, 2006).

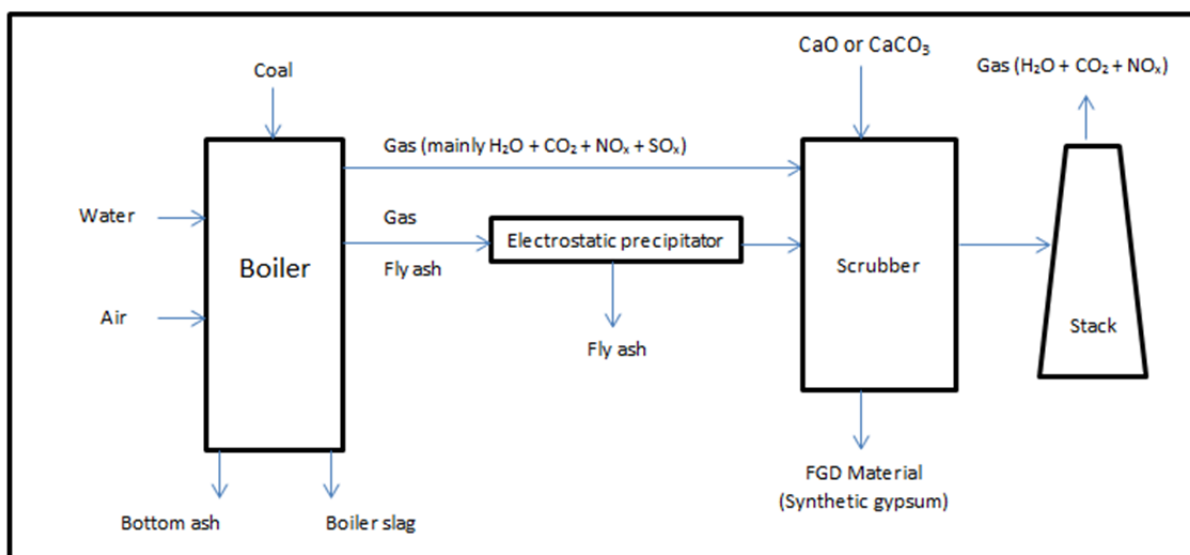


Figure 2-1 Flow diagram for processes at a coal fired power station that lead to a variety of residue products, adapted from (Gitari, 2006)

Fly ash is composed of organic and inorganic material that is amalgamated during the burning of coal (Bin-Shafique et al., 2003). The chemical composition of fly ash is therefore heavily dependent on the composition of burned coal, see Table 2-1, but all fly ash has a characteristic aluminium silicate glassy component to it (Kruger, 2003). In order to successfully apply fly ash in various industries a proper understanding of its properties is essential. The following sections explore the geochemistry, mineralogy and reactions that fly ash undertakes.

Table 2-1 Chemical constituents in South African fly ash (Kruger, 2003)

Constituent	Range (wt %)	Degree of influence of coal source on constituent variation
SiO₂	45 – 55	Strong
Al₂O₃	28 – 35	Strong
Fe₂O₃	3.0 - 5.0	Medium
TiO₂	1.5 - 2.0	Not determined
P₂O₅	0,5 -1,5	Not determined
CaO	4 – 12	Strong
MgO	1.5 - 2.0	Strong
Na₂O	0.1 – 0.8	Negligible
K₂O	0.5 - 1.0	Strong
SO₃	0.3 – 0.8	Negligible
Loss on ignition	0.5 - 2.0	Negligible

2.1.2 Physical Properties of fly ash

Fly ash is formed as a result of the amalgamation of organic and inorganic particles from scorched coal. The particles join together and coagulate while in suspension with flue gases and hence the shape of most fly ash particles is generally orbicular (cenospheres and pleropheres) and ultra-fine at 0.074 – 0.005mm (Bin-Shafique et al., 2003). The surface area of fly ash is an important physical feature because it is where advection and ionic exchange takes place (Miller et al., 1992). According to (Ahmaruzzaman, 2009) the specific surface area of fly ash is usually in the range of 170 to 1000 m²/kg with specific gravity in the series of 2.1 to 3.0.

2.1.3 Chemical properties and classification of fly ash

Fly ash is classified according to total aggregates and this chemical classification brings about two classes of fly ash namely Class F and Class C. Classification of fly ash according to the American Society for Testing Materials (ASTM-C618, 1993) dictates that fly ash comprising of more than 70 wt% SiO₂ + Al₂O₃ + Fe₂O₃ and also

having low levels of CaO be classified as Class F and fly ash holding ranges of between 50 wt% and 70 wt% $\text{SiO}_2 + \text{Al}_2\text{O}_3 + \text{Fe}_2\text{O}_3$ with high values of CaO be classified as Class C fly ash, see Table 2-2.

Table 2-2 Chemical requirements for classification of fly ash (ASTM-C618, 1993)

	Class	
	F	C
$\text{SiO}_2 + \text{Al}_2\text{O}_3 + \text{Fe}_2\text{O}_3$, min, %	70	50
Sulphur trioxide (SO_3), max, %	5.0	5.0
Moisture content, max, %	3.0	3.0
Loss on ignition	6.3	6.0

The lime content of fly ash is important as it plays a role in the hydration reactions that the pozzolanic material undergoes. A pozzolan is comprised of siliceous and/or aluminous siliceous substances that do not form cementitious compounds (Blissett and Rowson, 2012). Class F fly ash which has pozzolanic properties is a residue of the incineration of highly ranked anthracite and bituminous coals and needs the addition of lime in order to exhibit cementitious properties in the presence of water. Class C fly ash, which is derived from burning of lower order lignite and sub-bituminous coals, reacts with water producing cementitious compounds without the addition of an activator and is therefore not a true pozzolan (Blissett and Rowson, 2012). The range of lime in class F is 1% to 12% while the range for the self-cementing Class C fly ash is above 20%. This high lime content is the reason it is able to self-harden in the presence of water (Ahmaruzzaman, 2009).

Colour can also be used to classify fly ash: high levels of organic material or poor ignition in fly ash produce dark grey fly ash. Fly ash with high amounts of calcium is usually depicted by a light grey colour (Bin-Shafique et al., 2003).

South Africa burns low grade coal for energy production leaving vast amounts of ash as residue (Fatoba, 2007). Chemical properties of fly ash are reliant on the coal bed make-up from which the coal burned was derived, the burning process in the boiler and methods of disposal and treatment (Ahmaruzzaman, 2009). Major (> 1%) and minor (0.1 – 1%) elements in fly ash are usually metal oxides of Si, Ca, Fe, C, K, Mg, Na, Ti, P (Izquierdo and Querol, 2011). Trace elements (<0.1%) commonly

found in fly ash include Cr(III), Cr(VI) Se, Pb, Cd, Co, B, Cu, As, Mo etc. but as previously stated the chemical composition of fly ash is not consistent and will vary from sample to sample (Vassilev and Vassileva, 2006).

2.1.4 Mineralogy of fly ash

The mineral composition in fly ash is dominated by an amorphous phase, crystalline phase and to a lesser extent unburned coal minerals (Muriithi, 2009). The glass phase forms due to the hurried cooling that minerals undergo in the boiler systems and comprises of aluminosilicate for fly ash with a calcium content of less than 10%. Fly ash with calcium content of more than 15% has an amorphous phase that is made up of calcium aluminosilicates but also crystalline calcium structures of C_3A , C_4A_3S , and CS formats (Blissett and Rowson, 2012). The solidification process when is done at a slower rate results in the formation of crystals with the chemical composition that is dependent on the mineral phases present in the coal burned. The mineralogy and crystal configuration, however of the newly formed fly ash will be mostly dependent on the boiler conditions (Bin-Shafique et al., 2003).

Quartz minerals present in coal are generally unaltered as the temperature range in the furnace (1400 – 1500°C) is below melting point and will consequently be present in fly ash in crystalline form (Hower, 2012). Mullite which is also a crystalline mineral is common with most fly ashes and it is usually associated with the decomposition of the polymorphs: silliminite / kyanite / andalusite. Mullite and other crystalline silicates solidifies from the aluminium-silicate melt and contains the elementary composition of two stoichiometric arrangements $3(Al_2O_3) \cdot 2(SiO_2)$ or $2(Al_2O_3) \cdot 3(SiO_2)$ (Hower, 2012). Spinel is a category of minerals which have an isometric crystal structure, and the group usually has a general composition of $X^{2+}Y_2^{3+}O_4^{2-}$ such as Chromite $FeCr_2O_4$ (Nesse, 1999). Magnetite which is a member of the spinel group is common with most fly ashes resulting from high-Fe source coals (Hower, 2012). Hematite which is not regarded as a spinel (Fe_2O_3) is found in fly ashes and forms from alterations of iron sulphates minerals such as pyrite and siderite which are present in coal (Table 2-3).

Table 2-3 Thermal changes in major inorganic phases during coal combustion, modified from (Mattigod et al., 1990).

Minerals in coal	Transformation products in fly ash
Phyllosilicates (clay minerals: e.g. kaolinite)	Glass, mullite ($Al_6Si_2O_{13}$), quartz
Quartz	Glass, quartz
Pyrite (FeS_2), siderite ($FeCO_3$), iron sulfates	Hematite (Fe_2O_3), magnetite (Fe_3O_4)
Calcite ($CaCO_3$)	Lime (CaO)
Dolomite [$CaMg(CO_3)_2$]	Lime (CaO), periclase (MgO)
Gypsum ($CaSO_4 \cdot 2H_2O$)	Anhydrite ($CaSO_4$)
Ankerite [$CaMg_xFe_{(1-x)}(CO_3)_2$]	Calcium ferrite ($CaFe_2O_4$), periclase (MgO)

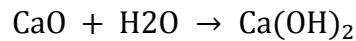
Lime and sulphates are present in fly ash especially if the coal is enriched in calcium bearing minerals. Gypsum will consequently lose water and be altered to anhydrite with limestone/dolomite impurities in the coal being transformed to lime. The alterations in the boiler also give way to the liberation of inorganic elements (Fatoba, 2007). These elements are concentrated on the surface of fly ash particles upon rapid cooling in the boiler and are readily removed from the particles surface by water since they are fixated on the outer layers (Gitari, 2006). This volatilization of trace elements and subsequent deposition on fly ash surface particles presents an environmental challenge as they are easily pulled out by water and can percolate into the groundwater.

The hydration and leaching behaviour of fly ash is dependent on the mineral phases present in fly ash. These include the non-crystalline amorphous phase, all the crystalline phases, the chemical make-up of the different phases and the size distribution of fly ash particles (Bin-Shafique et al., 2003).

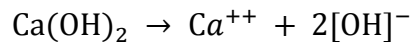
2.1.5 Hydration of fly ash and secondary minerals

Hydration is the process of adding water to other constituents and forming new compounds (Kruger, 2003). The hydration reaction in fly ash involves the pozzolans (AlO_3 , SiO_2 , Fe_2O_3) reacting with lime (CaO) in the presence of water and producing cementitious compounds. The cementitious substances are hydrated calcium silicate gel or calcium aluminate gel that are capable of infusing inert substances together (Bin-Shafique et al., 2003). The following presents the pozzolanic reactions that take place in fly ash (Bin-Shafique et al., 2003):

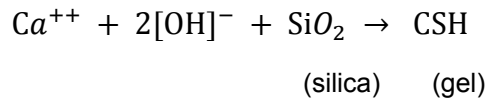
2.1 Hydration of lime



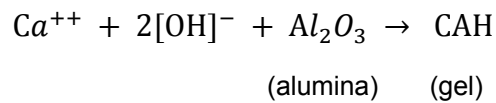
2.2 Dissociation of lime



2.3 Formation of calcium silicate gel



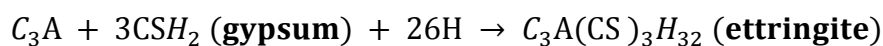
2.4 Formation of calcium aluminate gel



Class C fly ash contains high levels of lime (calcium oxide) and will therefore undergo the pozzolanic reactions. South African fly ash is classified as class F and needs additional lime in order for it to undertake hydration reactions that produces binding material.

Secondary minerals are common in fly ash as a result of hydration reactions with primary minerals. Ettringite which is a water bearing calcium aluminium sulphate, forms as a secondary mineral in fly ash containing sulphate and calcium aluminate (Tishmack et al., 1999). Formation of ettringite is as follows (Kruger, 2003):

2.5 Formation of ettringite



Where: C = CaO, H = H₂O, A = Al₂O₃, and S = SO₃

Tishmack et al., 1999 used three different high calcium fly ashes mixed with Portland cement for 28 days curing at 100% humidity. Portlandite, ettringite and monosulfate were all identified by X-ray diffraction (XRD) analysis of samples at room temperature. Unhydrated fly ash had no secondary minerals but only primary minerals that are synonymous with most fly ashes, Table 2-3.

2.1.6 Environmental impact of fly ash disposal methods

Eskom, the major electricity producer in South Africa is currently using the wet and dry ash disposal techniques, see Figure 2-2. When fly ash is dry-dumped it is first stabilised by adding around 10% effluent water in order to suppress dust development during conveyance and dumping (Hansen et al., 2002). Fly ash is then transported on conveyer belts from the power station to the landfilling site where it is dumped periodically irrigated with effluent water for dust suppression (Muriithi, 2009). The wet ash disposal method requires 10:1 to 20:1 ratios of liquid to solid combined in wet slurry and is then channelled via a pipe to the ash dam. The ash particles will generally sink to the bottom displacing the effluent water that is recycled back to the power station and reprocessed (Hansen et al., 2002).

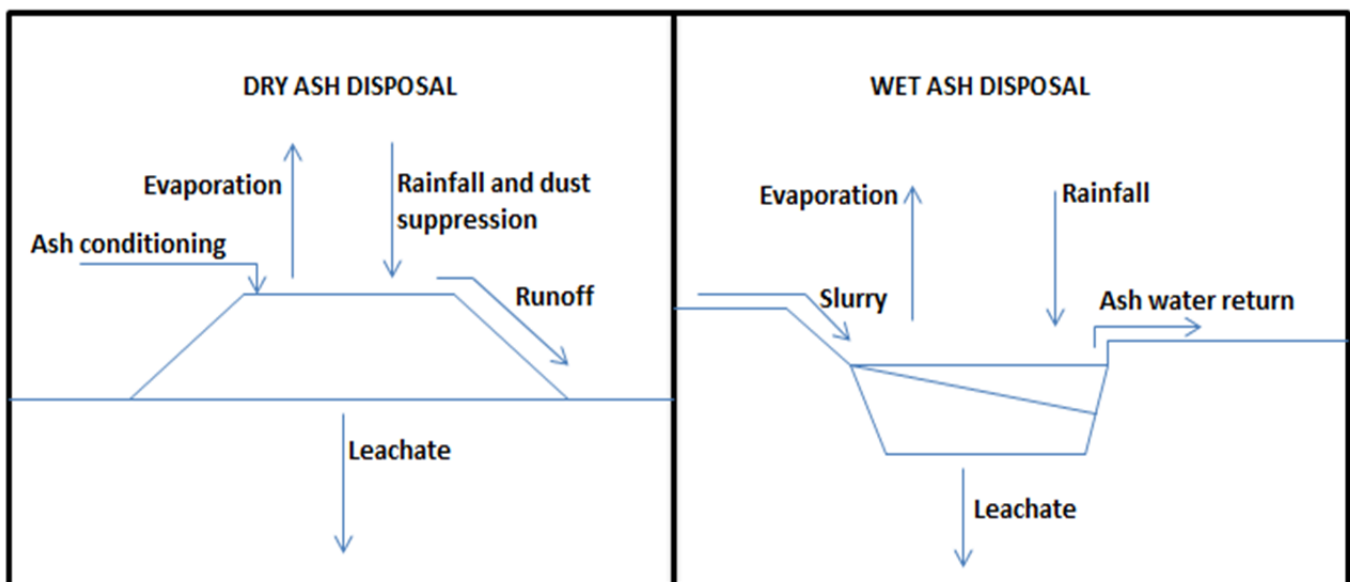


Figure 2-2 Aqueous inflows and outflows in dry and wet ash deposits, adapted from (Hansen et al., 2002).

An environmental impact assessment is the process of assessing the influence and effects a project may have on the environment (Affairs, 2010). Disposal of fly ash can impact negatively on the environmental performance of power stations. The environmental impacts of ash disposal can affect air, groundwater, surface water bodies and soil (Muriithi, 2009). According to Fatoba, (2007) fly ash is to be regarded as hazardous to the environment due to the likely discharge of toxic elements from its matrix during weathering. These toxic elements have the potential to be airborne especially in dry landfills where they can cause air pollution or be deposited into nearby surface water bodies, Figure 2-3.

Dry ash dumps are occasionally sprayed with effluent water to suppress dust development which subsequently helps to compact the ash. Compaction and development of a pozzolanic crust also assists in restricting leaching as a wetting front should move through a mass of waterless ash before it reaches the subsurface groundwater where contamination can occur (Hansen et al., 2002). Groundwater pollution as a result of dry ash dumps would consequently be from on-going seepage at the foot of the landfill when the wetting front spreads to the bottom. Cover systems for dry ash landfills made up of a layer of soil with appropriate vegetation are common rehabilitation measures taken to restrict leaching and dust development (Muriithi, 2009). Daniel, (1993) proposes that a cover system should be engineered to consist of a surface layer, a protection layer, a drainage layer, a barrier layer and also a gas collection layer. These multi-layer liner cover systems are meant to ensure minimum infiltration into the buried waste hence preventing leachate progression.

The risk of groundwater contamination remains one of the biggest challenges of ash disposal impoundments. In wet ash disposal, enormous volumes of water consisting of soluble elements dissolved from the ash slurries remain confined in ash dams over extended periods (Muriithi, 2009). If a lining system is absent underneath the ash dam or there is no underlying low permeability layer, such as clay, groundwater is at risk of contamination by downward infiltration of the leachate, Figure 2-2. The wet ash disposal system also limits the cementation reaction from taking place leading to high permeability (Hansen et al., 2002). Groundwater contamination can be a result of continuous seepage of ash pore water from the bottom of the ash dam. On the other hand if heavy rainfall was to occur resulting in flooding of the ash dam, the flushing out of stored salts would also lead to groundwater pollution (Hansen et al., 2002). Polluted groundwater can discharge contaminated water as base flow back to the surface water bodies. A summary of pollutant pathways is depicted in Figure 2-3.

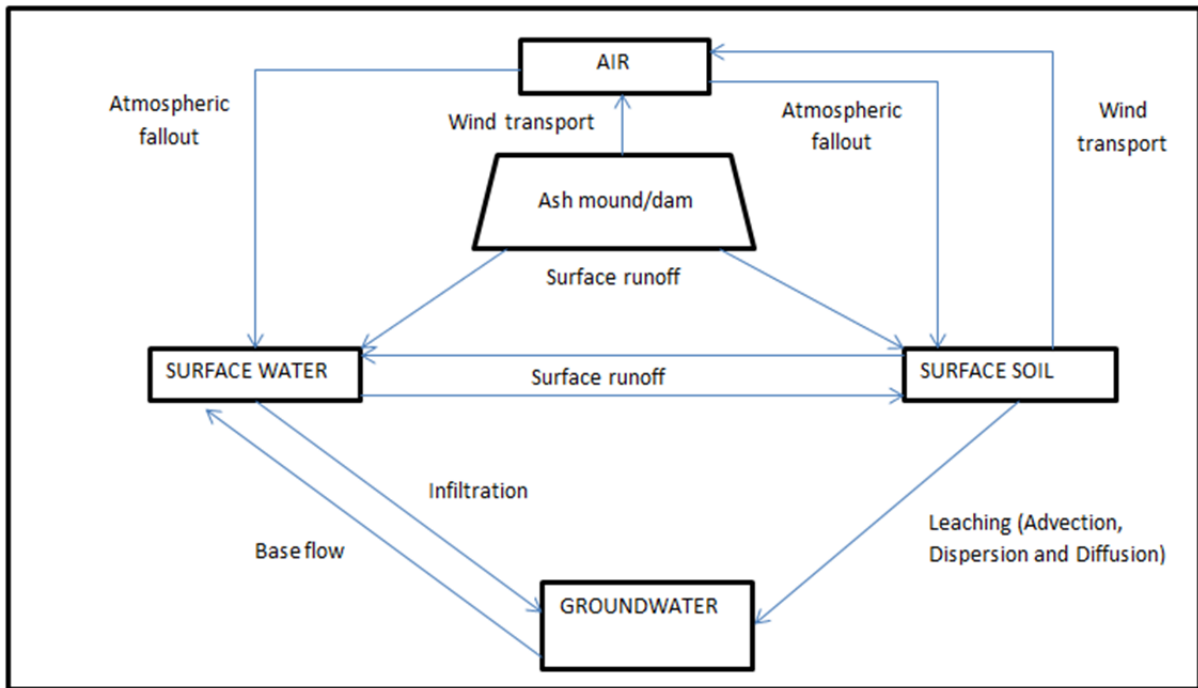


Figure 2-3 Pathways for pollution transport in ash impoundments, modified from (Fatoba, 2007).

2.1.7 Dynamics of fly ash leaching

Coal combustion in boilers at power stations constitutes mineral alteration and heterogeneity in fly ash particles (Iyer, 2002). Heterogeneity of fly ash particles means that there is a mineral and chemical variation between the core and surface of the particle. According to Izquierdo and Querol, (2011) the process of coal combustion brings about changes in mineral phases through decomposition, volatilisation, fusion, agglomeration and condensation. Fly ash rises with flue gas in the boiler under extreme temperatures but as the temperature drops volatile elements from the flue gas become deposited on the surface of fly ash particles during condensation (Kukier et al., 2003). These volatile elements including As, B, Hg, Cl, Cr, Se, which mix with S and Ca to form compounds with a wide range of solubilities (Izquierdo and Querol, 2011). Iyer, (2002) suggests that even though the surface of fly ash particles is very small, only microns in thickness, it contains a substantial amount of readily leachable elements. Elements in the core of fly ash particles, such as Al and Fe, are effectively shielded from extract solutions and are not readily available for leaching, however their subsequent release is governed by diffusion and dissolution kinetic rates of the surface layers (Kukier et al., 2003). Elements in the surface of fly ash are more susceptible to leaching in an aqueous environment (Izquierdo and Querol, 2011).

The aqueous environments of wet and dry fly ash disposal methods are all subjected to environmental settings including humidity, solar heating, frost, and radiation. These environmental factors bring about weathering in fly ash which causes changes in chemical behaviour and mechanical properties. As an aqueous solution passes through such waste bodies it will interact with the porous media under diffusion, advection and dispersivity forces, Section 2.1.9. Ash-water interactions will be subjected to the various geochemical factors that occur during the weathering of fly ash. Gitare, (2006) proposes that the thermodynamics of dissolution and/or precipitation, adsorption/desorption and redox conditions are essential to the understanding of leaching chemistry. According to Bin-Shafique, (2003) factors that affect leaching in fly ash are solubility of metals, adsorption of metals, chemistry of pore water and chemistry of the solid phase.

Water moves through interconnected void spaces in porous media and a chemical potential exists between the pore water and fluid surrounding the porous matrix (Bin-Shafique et al., 2003). Geochemical factors of dissolution/precipitation and/or adsorption/desorption will determine elements mobility between fly ash particles and pore water. Mobility and solubility of most elements are sensitive to pH changes therefore controlling leaching actions of waste disposal bodies (Izquierdo and Querol, 2011). The proportion of acidic and alkaline fractions in combustion wastes controls the overall pH of the soluble portion of the waste. For instance according to Fatoba, (2007) leachate derived from alkaline wastes, such as fly ash, exhibit a high pH due to the dissolution of alkali metal oxides and hydrolysis of alkali earth metals. The calcium content of fly ash has also been found to increase the pH of the pore water-ash interactions (Izquierdo and Querol, 2011).

Calcium and sulphate ions are the most readily released elements from the surface of fly ash particles and consequently influences the extraction solution pH. Izquierdo and Querol, (2011) suggest that calcium contributes to the alkalinity of the leachate as dissolution of free lime dominates leaching from strongly alkaline ashes, pH 11 - 13. Acidic leachate results from acidic fly ashes with low MgO and CaO content but high sulphate content. The acidity of the leachate will occur once the sulphate ions go into solution and form sulphuric acid. Gitare, (2006) suggested that Ca/S ratios of less than 2.5 produce acidic leachate while Ca/S of more than 2.5 produce alkaline extracts. A moderate alkaline leachate is due to low-Ca levels balanced with Ca/S

ratios typical of anhydrite dissolution with pH values of 8-9 (Izquierdo and Querol, 2011). The pH of leachate from ash dumps is not fixed and will be subject to change as dissolution of calcium and sulphate elements continue and precipitation of secondary minerals occur during weathering conditions. The alkaline nature of fly ash reduces the discharge of some of the environmentally concerning elements such as Cd, Co, Hg, Ni, Pb, Sn, or Zn. However at the same time releasing oxy-anionic species As, B, Cr, Mo, Sb, Se, V and W. Secondary minerals like ettringite present in most fly ashes can via precipitation take out contaminant elements like As, B, Cr, Sb, Se and V (Izquierdo and Querol, 2011).

Leaching tests are designed to assess and predict the potential of a solid phase to discharge contaminants to the environment (Bin-Shafique et al., 2003). A number of standard leaching procedures are available across the world but they can be classified into two general groups: water extractions and acid extractions (Gitari, 2006). Water extractions are usually conducted using deionized water to extract water soluble elements allowing for quantification the leachable elements present in the material. Acid extraction are conducted using either weak or strong acids and hence impose much harsher conditions on the material and extract greater proportions of ions thus offering an estimate of the total extractable leachable elements and is a suitable method for long term contaminant predictions. The leaching trends observed by (Izquierdo and Querol, 2011) show that some elements have high concentrations in early leachates with subsequent leachates containing decreasing concentrations until steady state concentrations are reached. Continuous leaching can also have a different trend for other elements which start with very low concentrations that will increase during successive leaching as the pH is lowered.

2.1.8 Utilization of fly ash

750 Mt of fly ash is annually produced from coal centred power generation facilities across the world but less than 50% is reused (Izquierdo and Querol, 2011). Fly ash has physical, chemical and mineralogical properties that make it attractive for many industrial applications. Ahmaruzzaman, (2009) provides a detailed review of the utilization of fly ash in various industries including its use in concrete construction work, as a road sub-base, in mine backfill, synthesis of zeolites, removal of toxic

metals from wastewater, and also as adsorbents for cleaning flue gas. A brief review of fly ash utilisation related to this study is provided below.

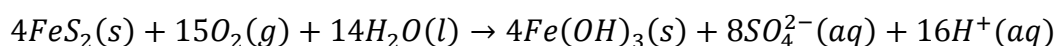
1.1.1.1. Synthesis of zeolites

Zeolites are aluminosilicate silicate minerals with alkali or alkaline earth metals forming part of their chemical composition that have wide applications as ion exchange, gas adsorption and water adsorption (Ahmaruzzaman, 2009). The zeolite structural framework comprises of a tetrahedral $[\text{SiO}_4]^{4-}$ but Al can substitute Si in the crystal lattice and form $[\text{AlO}_4]^{5-}$ with a resultant negative charge (Ahmaruzzaman, 2009). Since the structure of zeolites is very porous this negative charge can attract cations as the solution passes through and hence an increased cation exchange capacity (CEC). Zeolites are formed naturally from volcanic rocks and clay minerals but can be synthesized from an extensive range of materials with Al and Si as starting blocks (Ahmaruzzaman, 2009). Dominant species in fly ash are usually SiO_2 (40 – 65 wt%) and Al_2O_3 (40 – 65wt%) depending on the composition of the coal (Kikuchi, 1999). Fly ash through hydrothermal treatment (Querol et al., 1997) provides suitable starting material for the formation of zeolites, with its large surface area and aluminosilicate amorphous phase. For example (Tanaka et al., 2007) used hydrothermal treatment of fly ash with NaOH solution by microwave to produce a single-phase Na-A zeolite with CEC of 508 cmol/kg.

1.1.1.2. Neutralization of acid mine drainage

Acid mine drainage is low pH water that usually outflows from coal and precious metals mines, due to sulphite oxidation. Pyrite (FeS_2) is a sulphite mineral that undergoes oxidation when exposed to water and oxygen is commonly associated with acid mine drainage problems in South Africa. Pyrite oxidation takes place as observed in equation 2.6, producing acidic solutions and lowering the pH to less than 4.5 (Gitari, 2006).

2.6 Pyrite oxidation



Fly ash is an alkaline substance that has been used to neutralize and improve AMD (Gitari et al., 2008, Perez-Lopez et al., 2007, Madzivire et al., 2010). Batch reactions of AMD with a pH < 3 and fly ash in water were used by (Gitari et al., 2008) in ratios

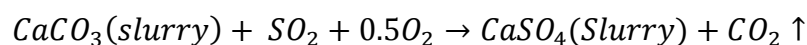
of 1:3 and 1:1.5, FA:AMD. The fly ash was from a South African power station and the AMD was acquired from a coal washing facility in Mpumalanga. The reactions water pH after 24 hours equilibration time had increased to a pH of > 8 meeting the South African water quality standards for irrigation set by DWAF. The pH increase was attributed to the dissolution of CaO and MgO from fly ash.

Madzivire et al., (2010) used fly ash to remove sulphates from mine water in Mpumalanga. This was done by precipitating sulphates from solution as gypsum and ettringite crystals. Treatment of circumneutral mine water with fly ash at pH > 11 resulted in removal of > 60% of sulphates, which was followed by the seeding of gypsum crystals. Addition of Al(OH)₃ precipitated ettringite successfully removing the sulphates from liquid phase.

1.1.1.3. Adsorbents for decontamination of flue gas

Flue gas desulphurization (FGD), depicted in Figure 2-1, is a process used for reducing SO_x emissions to the atmosphere. This is usually achieved by using the wet type limestone scrubbing procedure because it is easy to operate and yields high concentrations of DeSO_x flue gas (Ahmaruzzaman, 2009). Kikuchi, (1999) suggests that this process has shortcomings as it consumes a lot of water and also requires a wastewater treatment plant. The wet type limestone FGD also emits greenhouse gas CO₂ according to the following equation (Kikuchi, 1999):

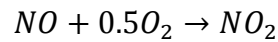
2.7 Wet limestone FGD



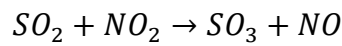
The dry type FGD has no need for a wastewater treatment plant but requires a huge amount of absorbent to effectively DeSO_x the flue gas due to the high ratio of calcium to sulphur (Kikuchi, 1999). This makes fly ash ideal for use in the dry type FGD process. Dry FGD is achieved by mixing equal proportions of fly ash and slaked lime in a powder mixer (Kikuchi, 1999). The mixture is then taken to a kneader that contains sufficient amount of water, and after kneading the mixture is pressed into pellets and then steam cured in a belt type unit. In the curing stage the material develops large pore spaces favourable for increased absorption. The last stage of preparation of the pellets involves drying them in hot air and then storing them in adsorbent tanks or silos. The calcium in the pellets absorbs SO to fix it as gypsum. The pellets have a great affinity for SO₂ in the presence of NO, O₂ and H₂O present

in flue gas to produce gypsum according to the following reaction from (Kikuchi, 1999):

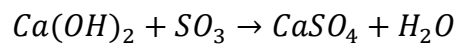
2.8 Oxidation of NO



2.9 Reduction of NO



2.10 Formation of gypsum



The spent absorbent material is discharged from the FGD and can be recycled back as raw material to make fresh absorbent pellets or be consumed in other industries such as being used as deodorant for refrigerators (Kikuchi, 1999). (Davini, 1996) also investigated the effects of using fly ash for FGD and obtained similar results. It was found that by mixing fly ash with $Ca(OH)_2$ in sufficient water, a pozzolanic substance was acquired which absorbed SO_2 better than $Ca(OH)_2$ alone. Mixes of fly ash and lime provide cheap SO_2 control mechanisms.

1.1.1.4. Treatment of wastewater

The on-going industrialisation has seen water quality being reduced by increased heavy metals discharge into these vulnerable resources. Heavy metals even when at low concentrations pose many health and environmental problems. The ingestion of Cd has been found to disturb various enzymes and can cause renal failure, Pb is extremely toxic to the body and can cripple the central nervous system (Gupta and Torres, 1998). Cr(VI) is a carcinogen that is associated with leaching in ash dumps (Roberts, 2008). Long term exposure to Hg can lead to permanent brain damage. There are various ways to remove heavy metals in wastewater including precipitation, ion exchange, membrane filtration and adsorption (Gupta and Torres, 1998). Ahmaruzzaman, (2009) suggests that of all these practices adsorption technique is the most simple and more effective at removing heavy metals from wastewater.

Endorsed adsorbents are usually alumina, silica, ferric oxide and activated carbon and fly ash is composed of all of these elements at varying amounts of each other (Gupta and Torres, 1998). Fly ash also has other physical properties such as

porosity, particle size distribution and surface area making it an attractive adsorbent for contaminant heavy metals in wastewaters (Ahmaruzzaman, 2009). Wastewaters containing toxic metals usually have low pH and the alkaline nature of fly ash helps neutralize these waters. Bayat, (2002) used two different Turkish fly ashes to successfully remove Cr(VI) and Cd(II) from aqueous solution. After a contact time of two hours, the fly ashes were discovered to have a higher affinity for Cd(II) than for Cr(VI) but however the adsorption capacity of both fly ashes were three time less than that of activated carbon for the removal of Cr(VI) (Bayat, 2002).

Hg removal from aqueous solution was investigated by (Rio and Delebarre, 2003) using silico-aluminous and sulfo-calcic fly ashes. After contact time of three days, adsorption equilibrium was reached as sulfo-calcic fly ash was seen to be more effective in removing Hg. Sulfo-calcic fly ash had a higher adsorption capacity at 5.0 mg g⁻¹ than silico-aluminous fly ash at 3.2 mg g⁻¹. Adsorption capacity of fly ash can also be enhanced by mixing it with other materials. Co-adsorption of Humic acid and fly ash give better heavy metal removal efficiency than when fly ash is used by itself (Wang et al., 2008). Fly ash alone successfully adsorbed 18 mg g⁻¹ of Pb²⁺ and 7 mg g⁻¹ of Cu²⁺ ions from solution but co-adsorption of humic acid and fly ash increased the adsorption to 37 mg g⁻¹ of Pb²⁺ and 28 mg g⁻¹ of Cu²⁺. Humic acid provides extra sites for ion exchange with heavy metals.

Inorganic elements have also been successfully removed from wastewater by fly ash (Ahmaruzzaman, 2009). Two grams of fly ash from Matla Power Station in Mpumalanga, South Africa, was used to investigate phosphate ion adsorption in 20mg L⁻¹ aqueous solutions (Agyei et al., 2000). Phosphate ions were successfully adsorbed by fly ash with contact time proving to be a critical factor. Batabyal et al, (1995) successfully removed 2,4 – dimethyl phenol from solution using fly ash. Temperature plays an important role in the rate of adsorption as 2,4 – dimethyl phenol adsorbs to fly ash at high temperatures by both diffusion and kinetic resistance, while at low temperatures adsorption is controlled by diffusion only (Batabyal et al., 1995).

1.1.1.5. Addition to cement

In concrete mixtures cement is the highest amount of the material added. Cost saving measures on high cement costs has seen fly ash partly replacing cement in

concrete blends. Kruger, (2003) investigated Portland cement(PC)/fly ash(FA) blends using various fly ashes from South Africa. PC/FA concrete had better workability than PC concrete due to the reduced water content in PC/FA, for 30-50% FA substitution a 20-25 L m⁻³ water reduction was obtained. Setting time also improved by 15 minutes when 15% PC replaced FA and by 30 – 60 minutes when 30% of PC was replaced by FA. Ahmaruzzaman, (2009) found that fly ash is most suited for mass concrete uses like dam constructions and in large volume placements to limit expansion caused by heat of hydration reducing cracking/shrinkage at early ages.

Durability of concrete depends partially on the permeability of the material as (Kruger, 2003) concluded that partial replacement of PC with FA decreases both the permeability and water adsorption in the concrete. The low permeability is attributed to the round shape of fly ash particles which brings about improved dense packing and pozzolanic reactions (Ahmaruzzaman, 2009). Corrosion caused by chloride penetration from steel reinforcement remains a concern in construction work but FA concrete has a better resistance to chloride penetration than PC concrete (Kruger, 2003). Corrosion resistance by fly ash is as a result of the conversion of Ca(OH)₂ in cement into a more stable cementitious compound of calcium silicate hydrate (CSH), see section 2.1.5. While Ca(OH)₂ is soluble in water CSH is less soluble hence reducing leaching of Ca(OH)₂ from concrete (Ahmaruzzaman, 2009). CSH is also a gel that binds inactive material together and reaction products have a tendency to fill capillary voids in concrete blends thereafter reducing permeability (Ahmaruzzaman, 2009). Kruger, (2003) found that a mixture of 70%PC:30%FA had 40% more strength than PC concrete after one year.

2.1.9 Fly ash application as a liner material: Previous studies

Low hydraulic conductivity is an essential component of waste disposal liner material with at least 10⁻⁹ m/s (Daniel, 1993). Fly ash on its own can increase in strength when exposed to moisture but the hydraulic conductivity it achieves may be lower than regulatory ranges for liner material. Sivapullaiah, (2011) investigated the permeability and compressive strength of class F fly ashes with additives lime and gypsum. Lime was added in a set of increments of 1%, 2.5%, 5%, 7.5% and 10% with gypsum varied at 1% and 3% per set of lime increments. The results showed

that addition of gypsum reduced the hydraulic conductivity more for samples with high lime contents than for samples with lower lime percentages. Unconfined compression strength was higher for samples with lower lime than with high lime contents. This was attributed to the fact that excess lime in fly ash does not enter into pozzolanic reactions. Leaching tests also indicated that mobility of trace elements in fly ash was greatly reduced by additions of lime hence augmenting stabilised fly ash as a liner material (Sivapullaiah and Baig, 2011).

Bentonite clay which is the favoured liner material can also be mixed with fly ash. Nhan, (1996) combined 70% fly ash, 20% lime dust and 10% calcium-bentonite with water in the construction of a liner material for synthetic municipal solid waste. The liner material was found to have hydraulic conductivity of $4.3 \pm 1.6 \times 10^{-8}$ m/s. Heavy metals in the waste were successfully removed through precipitation reactions with the liner material (Nhan et al., 1996). Shredded rubber tyres and bentonite were mixed with fly ash (Cokca and Yilmaz, 2003) and evaluated for hydraulic conductivity, leachate analysis, unconfined compression, split tensile strength, one-dimensional consolidation, swell and freeze/thaw cycle tests. Rubber was incorporated into the material to improve the flexibility of the material, but the hydraulic conductivity however increased as rubber percentages were increased.

Field and laboratory scale hydraulic conductivity tests on class F fly ash were conducted by (Palmer et al., 2000). Flexible-wall permeameters were used in the laboratory to determine the hydraulic conductivity of class F fly ash that had been combined with various materials (sand, class C fly ash, bottom ash). The results showed that the mixtures can be compacted to achieve the desired hydraulic conductivity needed for a landfill liner if compacted at optimum moisture content. Laboratory and field scale hydraulic conductivity determinations of fly ash depend on transport mechanisms in the material. Contaminant transport principles are outlined in the next section.

2.2 Contaminant transport

2.2.1 Introduction

The pathway of pollutants from the ground surface to the saturated zone occurs via the vadose zone prior to them reaching groundwater. Contaminants have to pass through soil, sedimentary formations, fractured rock, synthetic channels and other pathways before being introduced to aquifers (Palmer, 1996). Contaminants can migrate through porous media and even impermeable material due to secondary porosity features such as fractures. It is therefore essential to understand the transport mechanism through porous media in order to halt contaminant transport.

2.2.2 Transport in porous media

In 1856, Henry Darcy published a report on laboratory experiments conducted on water flow through different sands. These experiments were done using apparatus similar to the one depicted in Figure 2-4. He filled a cylinder with sand and inserted two manometers at a constant distance, l , apart. Water was then injected and allowed to flow through the cylinder of cross sectional area A until all pore spaces were completely filled to such an extent that inflow Q was equal to outflow Q (Freeze and Cherry, 1979). If elevation of the fluid in the manometer column is taken from an arbitrary datum, the fluid levels are h_1 and h_2 . The separation distance between the manometers is Δl . The flux can be written as:

2.11 Darcy law for one dimensional flow

$$v = \frac{Q}{A}$$

Where v is the specific discharge and has dimensions of velocity [L/T] and Q is the volumetric flow rate [L³/T] and A has dimensions [L²]. From the laboratory experiments Darcy concluded that the rate of flow through a porous medium is directly proportional to the loss of hydraulic head ($v \propto \Delta h$) and inversely proportional to the length of flow pathway ($v \propto 1/\Delta l$). Darcy's law can therefore be rewritten as:

2.12 Darcy equation

$$v = -k \frac{\Delta h}{\Delta l}$$

2.13 Differential Darcy equation

$$v = -k \frac{dh}{dl}$$

K is the constant of proportionality known as the hydraulic conductivity and it has dimensions of velocity [L/T]. The hydraulic gradient, i , is a dimensionless quantity that is defined by dh/dl .

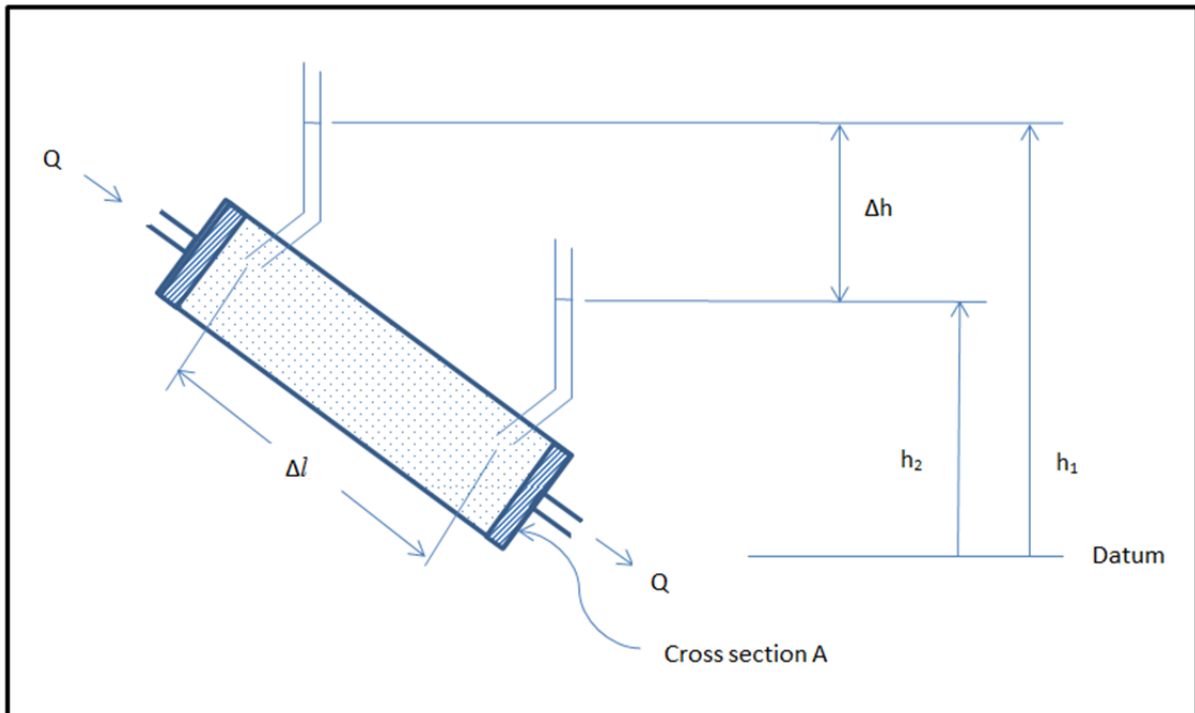


Figure 2-4 Darcy's experimental set-up, adapted from (Freeze and Cherry, 1979)

Substitution of equation 2.11 into equation 2.13 yields:

2.14 Darcy's equation: alternative

$$Q = -k \frac{dh}{dl} A$$

Or alternatively Darcy's equation can be rewritten as:

2.15 Darcy's equation compacted

$$Q = -kiA$$

The above equations are adapted from (Freeze and Cherry, 1979, Kruseman and Ridder, 2000, Schwartz and Zhang, 2003) and are stated to be valid for groundwater flow through porous media in all directions in space. The specific discharge depicted in equation 2.11 makes the assumption that flow is occurring through the entire column whilst it is actually occurring in interconnected pore spaces. Specific discharge or Darcy velocity is therefore a macroscopic concept and can easily be measured (Kruseman and Ridder, 2000). In groundwater contamination scenarios which involve solute transport, real flow velocities are investigated. These involve actual pathways where water molecules migrate through as they meander along porous media Figure 2-5. One of these microscopic concepts is advection and will be addressed in section 2.2.4.

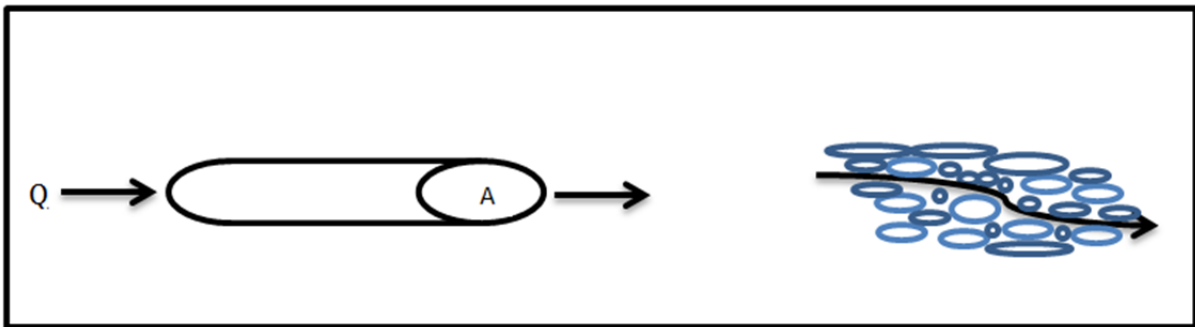


Figure 2-5 6 macroscopic and microscopic concepts of flow in porous media, adapted from (Freeze and Cherry, 1979)

When considering real velocity the porosity of the medium is taken into account and the real velocity is given by equation 2.16 (Kruseman and Ridder, 2000):

2.16 Actual velocity of water through porous media

$$v_s = \frac{Q}{nA}$$

Where v_s is defined as the seepage velocity and n is the porosity. Porosity of a material is the ratio of the volume of voids to the total volume of the material. All earth material usually contain primary porosity from its formation due to the matrix or can obtain secondary porosity due to secondary solution or fracturing (Freeze and Cherry, 1979). Porosity can be inter-related with hydraulic conductivity, for example, in well-sorted deposits or fractured rocks, those rocks with elevated n values usually have high K values but, however in clay-rich formations high porosities are experienced with very low K values (Freeze and Cherry, 1979).

2.2.3 Hydraulic conductivity

As previously stated the hydraulic conductivity (K) is the constant of proportionality in Darcy's law as demonstrated in equation 2.12. Kruseman and Ridder, (2000) define hydraulic conductivity as the volume of solution that will pass through a porous medium in unit time under a hydraulic gradient through a cross section area measured at right angle to the direction of flow. Hydraulic conductivity is therefore the measure of the ease with which water can percolate through earth material and it is also known as the coefficient of permeability (Freeze and Cherry, 1979). The hydraulic gradient defined as i in equation 2.15, is therefore the rate of change in the total hydraulic head per unit distance of flow in a specific direction. K values of some earth material are depicted in Table 2-4.

Table 2-4 Ranges of values of hydraulic conductivity, adapted from (Daniel, 1993)

Geological material		K (m/s)
Igneous/metamorphic rocks	Fractured	$10^{-10} - 10^{-13}$
	Weathered	$10^{-4} - 10^{-8}$
Sedimentary rocks	Limestone/dolomite	$10^{-6} - 10^{-9}$
	Sandstone/siltstone	$10^{-4} - 10^{-10}$
	Shale	$10^{-9} - 10^{-13}$
	Coal	$10^{-6} - 10^{-11}$
Unconsolidated sediments	Gravel	$10^{-1} - 10^{-4}$
	Silt	$10^{-6} - 10^{-10}$
	Marine clay	$10^{-9} - 10^{-12}$
	Clay/silt compacted	$10^{-6} - 10^{-9}$
	Sand - clean	$10^{-2} - 10^{-6}$
	Sand - silty	$10^{-3} - 10^{-7}$

There is a general assumption made in most hydraulic equations that aquifers and aquitards are homogeneous and isotropic (Kruseman and Ridder, 2000). These hypotheses portray hydraulic conductivity as being uniform in all directions throughout a geological formation. However, an earth material that varies in grain size and shape can exist throughout a geological formation leading to heterogeneity in hydraulic conductivity. Variations in the direction of measurement of hydraulic conductivity for an arbitrary point give rise to a property known as anisotropic. For example if at a specific point the K value when measured from the vertical direction is different from when measured from the horizontal then the material is termed as anisotropic (Freeze and Cherry, 1979). In earth material K value is affected by

heterogeneity and anisotropy of geological formations **Error! Reference source not found.**

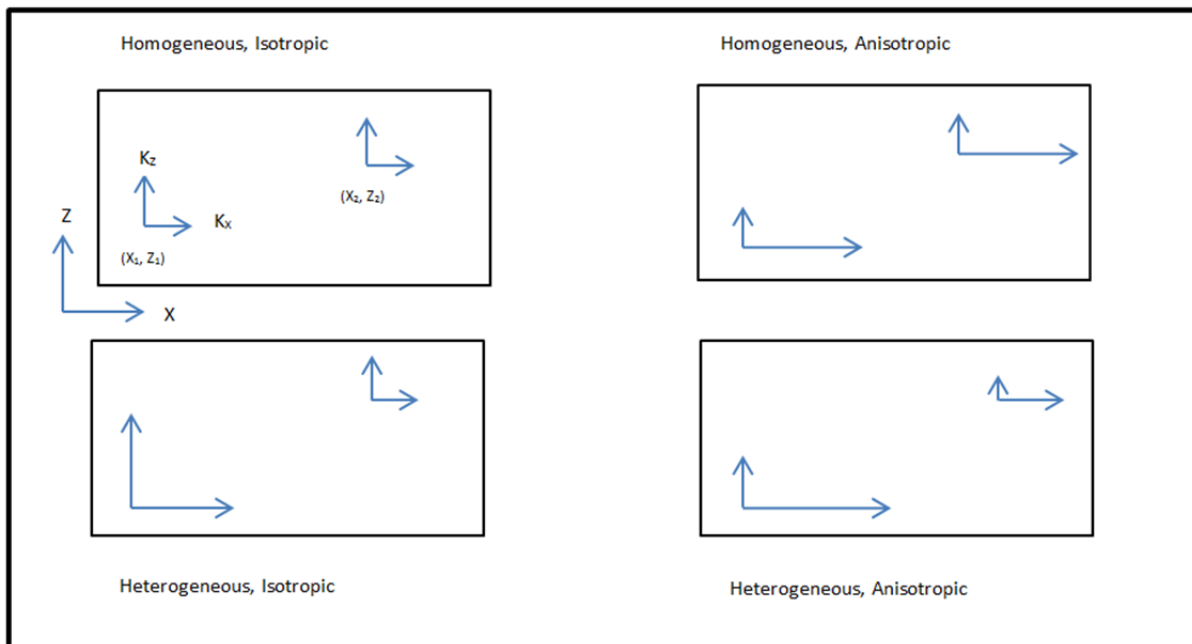


Figure 2-6 Possible scenarios of heterogeneity and anisotropy, adapted from (Freeze and Cherry, 1979)

The principal directions of anisotropy are defined as directions in space that match to the angle θ at which K attains its highest and lowest values, where θ is the angle between the horizontal and the direction of measurement of K (Freeze and Cherry, 1979). A coordinate system of directions xyz can be established to correspond with the principal directions of anisotropy so that the hydraulic conductivity values are quantified as K_x , K_y and K_z . In an isotropic medium at any point (x, y, z) we will obtain $K_x = K_y = K_z$ and if homogeneity is also experienced throughout the material then K would be constant at any place in the material (Daniel, 1993). An anisotropic formation will therefore have $K_x \neq K_y \neq K_z$. Freeze and Cherry, (1979) demonstrated steady-state flow of a unit volume of porous media as shown in Figure 2-7. The requirement of the law of conservation for steady-state flow through a saturated porous medium is that the rate of fluid mass inflowing into the unit volume be equal to the rate of fluid mass outflowing out of the unit volume.

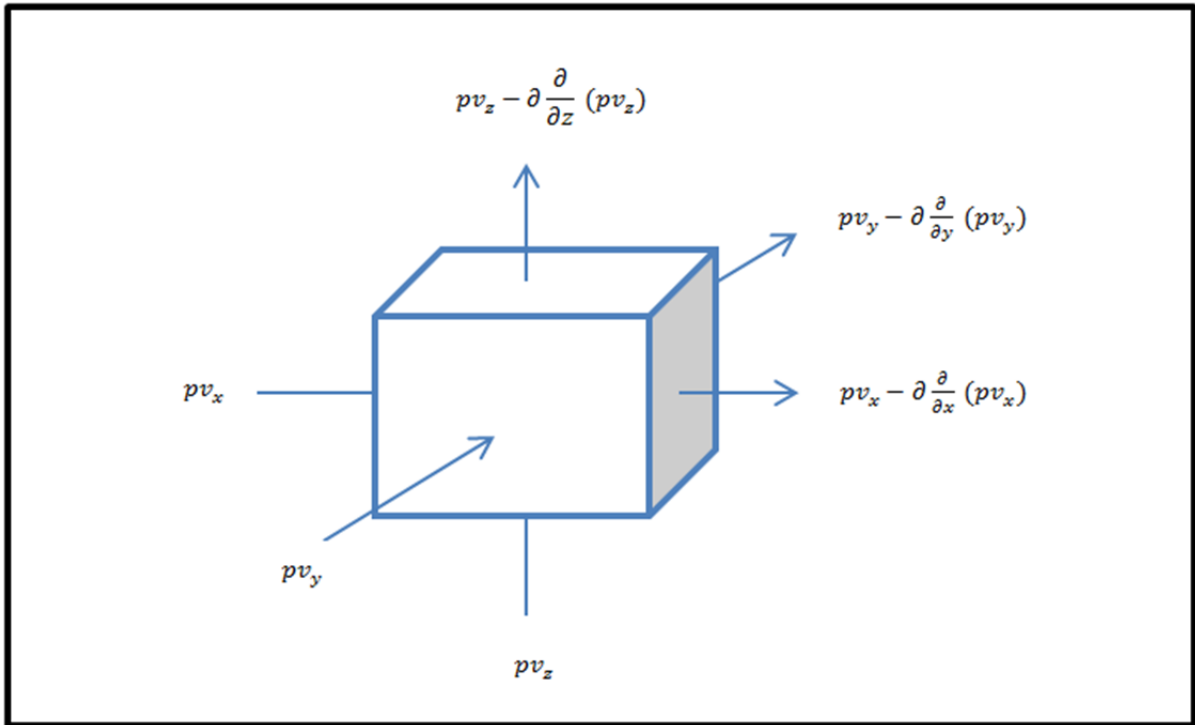


Figure 2-7 Unit volume demonstrating flow through porous media (conservation of mass), adapted from (Freeze and Cherry, 1979)

Since mass can be expressed as:

2.17 Mass as a function of density and volume

$$M = pv$$

Where M is the mass rate of flow and p is the density and v the volume. From the equation of continuity the law of conservation of mass can now be expressed in mathematical notation as equation 2.18 from (Freeze and Cherry, 1979):

2.18 Continuity equation for flow in porous media

$$-\frac{\partial(pv_x)}{\partial x} - \frac{\partial(pv_y)}{\partial y} - \frac{\partial(pv_z)}{\partial z} = 0$$

For an incompressible fluid, $p(x,y,z) = \text{constant}$, and hence the function p can be divided out of equation 2.18 and simplified to:

2.19 Continuity equation for incompressible fluids

$$-\frac{\partial(v_x)}{\partial x} - \frac{\partial(v_y)}{\partial y} - \frac{\partial(v_z)}{\partial z} = 0$$

If we replace v_x , v_y and v_z with Darcy's law, see equation 2.13, we obtain:

2.20 Substitution of Darcy into continuity equation

$$\frac{\partial}{\partial x} \left(K_x \frac{\partial h}{\partial x} \right) + \frac{\partial}{\partial y} \left(K_y \frac{\partial h}{\partial y} \right) + \frac{\partial}{\partial z} \left(K_z \frac{\partial h}{\partial z} \right) = 0$$

As previously stated, for isotropic medium, $K_x = K_y = K_z$ and if the formation is also homogeneous then $K(x, y, z)$ is constant. This means equation 2.20 can be simplified to:

2.21 Steady state flow equation through a homogeneous-isotropic medium

$$\frac{\partial^2 h}{\partial x^2} + \frac{\partial^2 h}{\partial y^2} + \frac{\partial^2 h}{\partial z^2} = 0$$

Equation 2.21 is a second order partial differential equation known as Laplace's equation:

2.22 Laplace's equation

$$\nabla^2 h = 0$$

All the above equations are derived from (Freeze and Cherry, 1979). Homogeneous and isotropic are commonly assumed conditions in groundwater applications (Daniel, 1993) and therefore the solution for equation 2.21 defines the value of the hydraulic head at any point in three-dimensional flow field (Freeze and Cherry, 1979).

2.2.4 Advection

Contaminants can be transported through porous media by a variety of processes. When solutes are transported along with the flowing fluid due to a gradient in the total hydraulic head then the process is termed advection (Daniel, 1993). Advection will therefore move nonreactive solutes at an average rate equal to the seepage velocity of the transporting fluid by the following equation:

2.23 Seepage velocity

$$v_s = \frac{v}{n}$$

Equation 2.23 is a rearrangement of equation 2.16 with v as the quantity of flow per unit area per unit time (Daniel, 1993). The flux (v) is the volumetric flow of water through the total cross-sectional area and it assumes that the whole area is conducting flow, while in actual effect only the interconnected pore spaces are

responsible for advection (Daniel, 1993). Therefore, porosity is introduced in equation 2.23 to suitably define the actual velocity through the voids as seepage velocity. In porous media it is sometimes not all the void spaces that conduct flow as some voids are non-interconnected and hence dead end voids for flow (Fetter, 1993). These non-conducting voids are therefore resolved from advection transport by substituting effective porosity, n_e , for porosity in equation 2.23. Daniel, (1993) defines effective porosity, n_e , as the volume of the voids that contribute to flow divided by the volume of both pores and solids (total volume). In hydraulic equations where $n_e < n$ then n_e should be substituted instead of n .

The amount of solute being transported depends on the concentration in the transporting fluid and the quantity of the flowing fluid (Fetter, 1993). One dimensional advective mass flux, F_x , for a specific nonreactive solute is equal to the amount of fluid flow times the concentration, C , as shown by:

2.24 Advective mass flux

$$F_x = vn_e C$$

Seepage velocity can also be used to estimate the time, t , it takes a nonreactive solute to move through an aquifer of thickness L (Daniel, 1993).

2.25 Transit time

$$t = \frac{L}{v_s} = \frac{nL}{Ki}$$

2.2.5 Diffusion

Diffusion is the process that is responsible for the transportation of solutes from an area of high concentration into an area of low concentration (Fetter, 1993). Fluid flow is not a prerequisite of diffusion since migration of solutes requires only a concentration gradient. The equation for diffusion is defined by Fick's first law which shows that the mass of the solute in the diffusing fluid is proportional to the concentration gradient (Fetter, 1993).

2.26 Fick's first law in one dimension

$$F = -D_a \frac{\partial C}{\partial x}$$

Where F is the mass flux and D_d is the diffusion coefficient and $\partial C/\partial x$ is the concentration coefficient. The negative sign is representative of migration from areas of higher concentration of the solute to those of lower concentration.

2.2.6 Dispersion

Dispersion is a phenomenon that occurs during solute transport where variations in seepage velocity that takes place during flow in porous medium causes the solute to spread (Daniel, 1993). According to Fetter, (1993) three factors contribute to this behaviour which is illustrated in Figure 2-8. The first factor is that movement of fluid inside void spaces is characterized by higher velocity at the middle pore and lower velocity at the boundaries Figure 2-8a. Similar properties transpire during fluid flow in pipes, rivers and stream channels (Daniel, 1993). The second factor is that there are variations in pore size distribution leading to velocity disparities in flowing fluid across a pore channel Figure 2-8b. The third factor is that the winding movement of fluids in porous media result in unpredictable travel time for solutes over the same distance Figure 2-8c.

Variations in seepage velocity in aquifers causes dilution of solutes as mixing of contaminated water and uncontaminated water occurs along the pathways (Fetter, 1993). This simply means if you inject a tracer (e.g NaCl) of known concentration at a borehole and pump out water at an abstraction well 10 metres away, upon arrival of the tracer the concentration will not be the same as the injected concentration. This is due to variations in seepage velocity that leads to mixing. This mixing behaviour is called **mechanical dispersion**. If mixing takes place parallel to the direction of flow it is called **longitudinal dispersion** and if it occurs perpendicular to flow route it is termed **transverse dispersion** (Fetter, 1993).

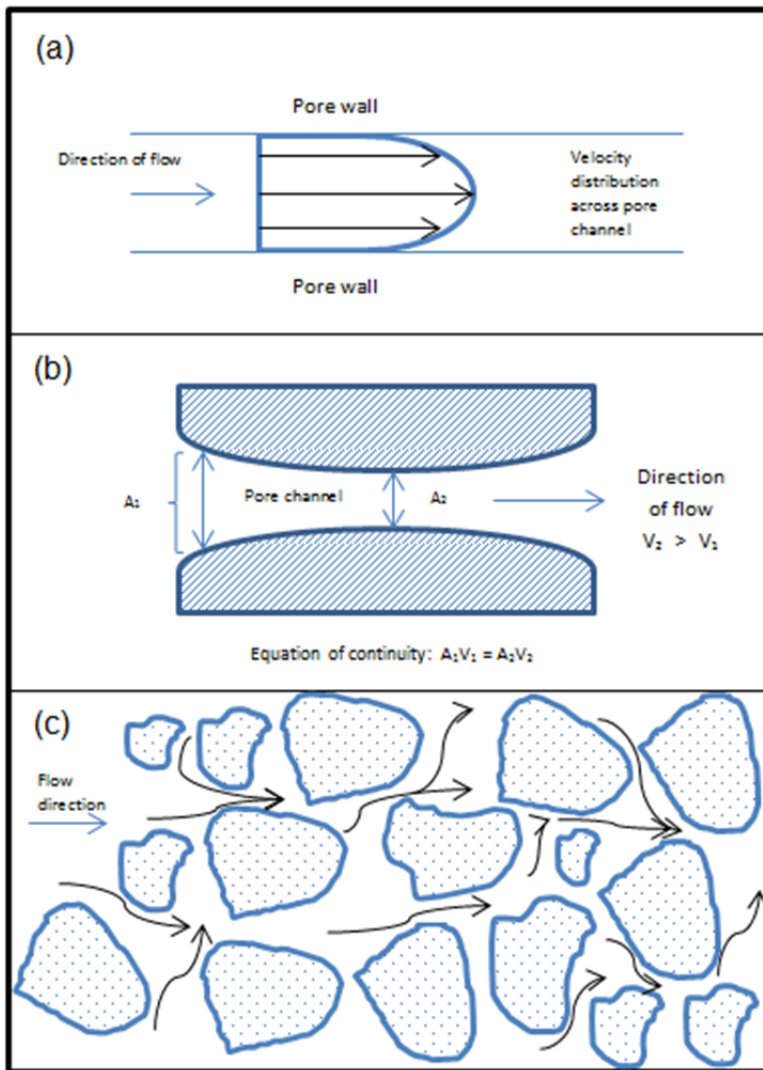


Figure 2-8 Dynamics of microscopic dispersion in porous media, adapted from (Daniel, 1993)

Since variations in seepage velocity are responsible for mechanical dispersion, the coefficient of mechanical dispersion is attained as a function of seepage velocity (Daniel, 1993):

2.27 Coefficient of longitudinal mechanical dispersion

$$D_m = \alpha_l v_s^\beta$$

Where α_l is the longitudinal dispersivity on the porous medium in the direction of flow and β is the experimentally set constant between 1 and 2 (Daniel, 1993). The mechanical dispersion flux, J_m , is assumed to be defined Fick's law and for one dimensional flow is expressed as:

2.28 Mechanical dispersive flux

$$J_m = -D_m n \frac{\partial C}{\partial x}$$

Fly ash dumps/dams are examples of porous media and hence affected by transport mechanisms (advection, diffusion and dispersion) as illustrated previously in Figure 2-3.

2.3 Landfill liner designs

Landfills are containment facilities where all undesirable and unusable waste is deposited (Daniel, 1993). Modern landfills are now composed of sophisticated engineering systems designed to reduce the impact of waste on the environment and human welfare (Hughes et al., 2013). The containment structure is usually a liner system underlying waste and sometimes a cover system overlying the waste. Liner systems are generally used to accumulate and remove leachate from landfills. The cover system is usually added to reduce infiltration of water into the waste (Daniel, 1993). Engineered liners usually have systems in place to drain leachate from waste and to remove it to treatment facilities. These structures provide an interface between waste and the environment and hence assist in quarantining landfill contents (Hughes et al., 2013). For coal fired power stations the wet and dry dumping systems are used to contain fly ash as discussed in section 2.1.6.

The type of liner material utilised should be compatible with the category of waste it is meant to contain. Regulations from governments usually dictate the type of liner that should be used in accordance with the risk profile the waste poses. Before deciding which liner system to use it is essential to get a proper understanding of the different types of liner components:

- **Clay liner** is generally the preferred earth material used in lining systems. Clay is usually compacted to preferred standards to reduce the hydraulic conductivity. It also poses cation exchange capabilities that make it favourable to be used as a liner material. Clay performance is however affected by wetting/drying cycles and freeze/ thaw cycles that lead to cracks and hence high K values (Hughes et al., 2013, Sivapullaiah and Baig, 2011).

- **Geosynthetic clay liners (GCL)** are more modern types of liner material that is composed of a clay liner infused between two geotextile layers. The thickness of these type of liners is very small (mm) making them less labour intensive and freeze/thaw cycles negligibly affect them (Hughes et al., 2013).
- **Geotextiles** are usually woven or unwoven mats that are used as filtering medium. They are effective at draining out leachate from particulates and often overlay leachate collection layers. They can also trap piercing particles in the waste thereby protecting geomembranes from puncture holes (Hughes et al., 2013).
- **Geomembranes** are very low permeability synthetic membrane liners (Daniel, 1993). They can be made up of a number of plastic based products including; high density polyethylene (HDPE), chlorinated polyethylene (CPE), chlorosulphonate polyethylene (CSPE) and polyvinyl chloride (PVC) (Daniel, 1993).
- **Geonets** are high permeability liquid conveyer structures which are usually made out of a plastic net structure with wide gaps to allow water through. They usually are inserted to replace sand and gravel in liner systems but are however subject to clogging by minute particles (Hughes et al., 2013).
- **Leachate collection systems** are usually made up of high permeability material like sand/gravel with leachate collection pipes inserted into them to remove leachate from the liner system.

There are generally three types of liner systems depicted in Figure 2-9 single liner, composite liner and double liner systems.

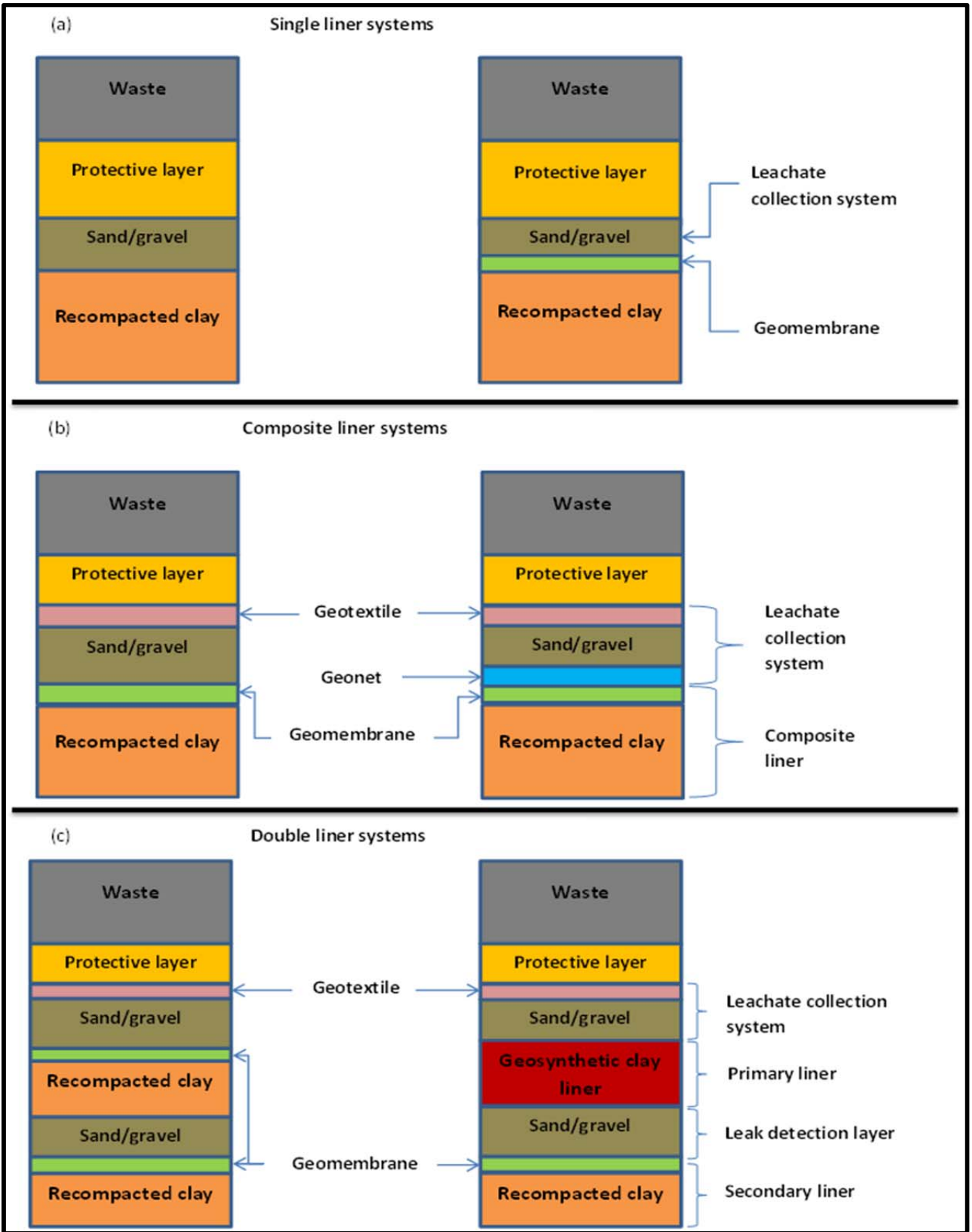


Figure 2-9 Liner design systems, adapted from (Hughes et al., 2013)

Single liner systems are usually composed of either a clay liner, geosynthetic clay liner (GCL), or a geomembrane Figure 2-9a. This type of liner system is usually designed for general waste that is not classified as hazardous and is therefore usually used to line demolition and construction debris (Hughes et al., 2013). The protective layer incorporated in this liner system is utilised to protect the geomembrane or clay from particles that can potentially puncture them. The type of waste that can be disposed of within this type of liner system in South Africa is prescribed by the minimum requirements for waste disposal by landfill (DWAF, 1998b).

Composite liner systems are normally made up of a grouping of a geomembrane with a clay liner Figure 2-9b. This combination of two low permeability materials is more effective at restricting leachate from seeping into the subsoil than a single liner system (Hughes et al., 2013). A geotextiles and geonet can be incorporated into this liner system for better leachate control. The type of waste deposited in this kind of system is usually an interface between the general waste disposed in single liners and hazardous waste deposited in double liners systems.

Double liner systems have a design made up of either a combination of two single liners, or two composite liners, or a single and a composite liner in one system Figure 2-9c. This system can be divided into two liner systems, with the uppermost liner acting as a primary liner and the lower liner acting as a leakage detector. The primary liner is usually thicker and has a leachate collection system. The secondary liner also has a similar leachate collection system but it is usually called a leak detection system since it plays the role of patrolling the primary liner. A leak detection system usually have high hydraulic conductivity ($\geq 1\text{cm/s}$) and should be able to identify a leak inside 24 hours (Daniel, 1993).

Hazardous waste is generally prescribed to be disposed of in double liner systems (Hughes et al., 2013). Legislation is largely the driving force behind developments in liner systems and the classification of waste according to regulatory standards will ultimately determine the kind of liner system to be utilised for dumping of waste in landfills.

2.4 Environmental regulations

The minimum requirements for waste disposal by landfill (DWAF, 1998b) are generally the prescribed guidelines that the South African Government recommend for waste management. Section 8.4.3 in the minimum requirements outlines some of the requirements that a liner layer should meet in order for it to qualify and hence be incorporated in liner systems. These guidelines include:

- The Plasticity Index (PI) of any soil used should be ≥ 10 but not so high that it effects unnecessary desiccation cracking.
- Clay must be compacted to a minimum dry density of 95% Standard Proctor maximum dry density at Proctor optimum water content or Proctor optimum + 2%.
- Full particle size analysis
- Double hydrometer test
- Atterberg limits
- Shear strength tests
- Permeability determinations

There are three types of landfill systems stipulated in the minimum requirements for waste disposal by landfill (DWAF, 1998b) Class **G:B⁺** landfills, Class **H:h** landfills and Class **H:H** landfills. All these landfill types have a specific liner system attached to them which is graphically demonstrated in Appendix 8.2 of minimum requirements for waste disposal by landfill (DWAF, 1998b). Class **G:B⁺** landfills are generally based on a single liner system while both Class **H:h** landfills and Class **H:H** landfills have a double liner system. The maximum outflow rates permitted in the clay liner measured in metres per year are as follows:

- Class **G:B⁺** landfills: 0.3 m/y ($1 * 10^{-8}$ m/s)
- Class **H:h** landfills: 0.1 m/y ($3 * 10^{-9}$ m/s)
- Class **H:H** landfills: 0.03 m/y ($1 * 10^{-9}$ m/s)

These outflow rates correspond to international standards, as the hydraulic conductivity value for liners of hazardous waste is set at $1 * 10^{-9}$ m/s by the EPA (Daniel, 1993).

The South African Government has put in place a number of laws to protect the environment from waste pollution and in particular landfills. The Minister of Water Affairs is the custodian of all water resources including groundwater. Through the National Water Act (1998) essential protective measures have been put in place to safeguard our water resources. The National Water Act highlights the protection, use, development, conservation, management and control of water resources as key points that ensure the sustainability of water resources for people, animals and the aquatic environment for the current generation and also future generations. The reserve which is determined by the minister is defined as the quantity and quality of available water resources which is emphasised in chapter 3, part 3 of the National Water Act (1998). It is divided into basic human need reserve and ecological reserve. In considering waste facility the reserve becomes important as migration of pollutants from such facility can alter the quality of the reserve.

Part 4 (Chapter 3) of the National Water Act (1998) deals with the prevention of pollution to water resources as a result of activities on land. The minister bills the person who owns or uses the land in question with the responsibility to undertake preventive measures to avert pollution of water resources. The National Environmental Management Waste Act (2008) stipulates the necessary prevention measures to be considered for waste management. Since waste differs from one setting to the next it is essential to accurately classify waste at the beginning in order to properly constrain it from contaminating the environment. The minister introduced Government Gazette Notice 433 of 2011 on 1 July 2011 which outlines the procedure for assessing waste in landfills for classification. The notice prescribes leachate concentrations (LC) or total concentrations (TC) as indicators of pollution. Set thresholds for metal ions, inorganic anions, organics and pesticides are included for evaluation of the risk rating of the waste disposal site, Table 2-5.

Table 2-5 Waste disposal criteria and risk rating according to Government Gazette notices 432 and 433 of 2011

Criteria	Waste disposal risk rating	Description of risk associated with disposal to landfill	Landfill disposal requirement
LC > LCT2 or TC > TCT2	Type 0: Very high risk	Considered very high risk waste with a very high potential for contaminant release. Requires very high level of control and on-going management to protect health and the environment.	The disposal of Type 0 waste to landfill is not allowed. The waste must be treated and re-assessed in terms of the standard for Assessment of Waste for Landfill Disposal to determine the level of risk associated with disposing the waste to landfill
LCT1 < LC ≤ LCT2, or TCT1 < TC	Type 1: High risk	Considered high risk waste with high potential for containment release. Requires very high level of control and on-going management to protect health and the environment.	Type 1 waste may only be disposed of at a Class A landfill designed in accordance with paragraph 3(1) and 3(2) of Notice 432 of 2011 (DEA), may be disposed of at a landfill site designed and operated in accordance with the requirements for a Hh / HH landfill as specified in the minimum requirements for waste disposal by landfill (2 nd Ed, DWAF, 1998)
LCT0 < LC ≤ LCT1 and TC ≤ TCT1	Type 2: Moderate risk	Considered moderate risk waste with some potential for contaminant release. Requires proper control and on-going management to protect health and the environment	Type 2 waste may only be disposed of at a Class B landfill designed in accordance with paragraph 3(1) and 3(2) of Notice 432 of 2011 (DEA), may be disposed of at a landfill site designed and operated in accordance with the requirements for a GLB + landfill as specified in the minimum requirements for waste disposal by landfill (2 nd Ed, DWAF, 1998)
LCTi < LC ≤ LCT0 and TC ≤ TCT0	Type 3: Low risk	Low waste with low potential for contaminant release. Requires some level of control and on-going management to protect health and the environment	Type 3 waste may only be disposed of at a Class C landfill designed in accordance with paragraph 3(1) and 3(2) of Notice 432 of 2011 (DEA), may be disposed of at a landfill site designed and operated in accordance with the requirements for a GLB landfill as specified in the minimum requirements for waste disposal by landfill (2 nd Ed, DWAF, 1998)
TC < 20*LCTi, or LC ≤ LCTi and TC ≤ TCTi	Type 4: Inert waste	Very low risk waste. Only basic control and management required	Disposal allowed at a Class D landfill designed in accordance with paragraph 3(1) and 3(2) of Notice 432 of 2011 (DEA), may be disposed of at a landfill site designed and operated in accordance with the requirements for a GSB + landfill as specified in the minimum requirements for waste disposal by landfill (2 nd Ed, DWAF, 1998)

2.5 Summary

Through literature studies fly ash is found to exhibit properties that can render it a possible liner material. These properties include a low hydraulic conductivity that is induced by its pozzolanic reaction mechanism and also its large surface area that can adsorb contaminants through cation exchange and other processes. Given the attractive physical and mineralogical properties of fly ash there is enough basis for research on how it can be used as a liner material. Legislation in South Africa is clear on the requirements and analysis that should be performed on any material for

it to be accepted as a liner material. The minimum requirements for waste disposal by landfill (DWAF, 1998b) as a guideline document has outlined laboratory procedures on how a liner material is to be assessed. These methodologies are considered in this study and additional tests and analysis will also be incorporated to get a more profound evaluation of fly ash and its compatibility in lining ash dumps in electric power stations.

The next chapter presents the materials and methods applied to this study. All these methods were used in order to achieve the objectives of the study.

3 Methods and Materials

This chapter serves to describe the experimental and analytical methods employed to achieve the objectives of this study.

3.1 Materials

The first objective of this study was to reuse waste and since fly ash is regarded as a waste product the intention was to use it as a primary material of a lining system for ash dumps. The other objective was to find cost effective techniques that met the main aim of the study and the cost of materials used was moderate so that in reality if deemed a suitable method for waste management, it would not be too expensive for power stations. The materials used in this study were as follows:

- Dura-Pozz fly ash was supplied by Ash Resources (Pty) Ltd. Dura-Pozz fly ash is fly ash produced from Lethabo Power Station which is situated in the Free State Province between the towns of Sasolburg and Vereeniging in South Africa. Ash Resources (Pty) Ltd is a leading company of fly ash products in South Africa and distributes fly ash under different product names.
- Calcium hydroxide Ca(OH)_2 also known as lime was supplied by Merck, South Africa.
- Calcium sulphate dihydrate $\text{CaSO}_4 \cdot 2\text{H}_2\text{O}$ also known as gypsum was supplied by Merck, South Africa.
- Lignosulphonate was supplied by Sappi. The Sappi Group specializes in paper products and lingosulphonate is a by-product of the paper production process.

The above materials form part of the main products used in this study and any additional materials used will be addressed accordingly. Dura-Pozz fly ash is taken directly from the power station through pipes and bagged without getting in contact with the atmosphere. This creates a high performance substance that is predominantly utilised as a cement extender in South Africa (Ash-Resources, 2013). This particular method of collecting fly ash is however not used by most power stations where traditional disposing still takes place, as discussed in section 2.1.1

and section 2.1.6. Fly ash from a landfill at Tutuka Power Station was therefore incorporated into the study to provide a more practical product.

Fly ash sampled from the landfill at Tutuka power station is however not 100% Fly ash but rather a combination of bottom ash, coarse ash and effluent water that is used for conditioning and dust suppression. Nonetheless fly ash still forms the major component. Tutuka fly ash is therefore more representative of a real life landfill waste body unlike Dura-Pozz fly ash. Tutuka fly ash consequently serves as the waste body in this study and not necessarily as a material for lining, it also provides a point of reference for the methods used in this study.

3.2 Sampling and storage

Fresh samples of fly ash were taken straight from the conveyor belt in the landfill at Tutuka Power Station. The samples were then sealed in plastic bags in order to limit air flow into them as much as possible. The samples were sealed at room temperature, away from direct sunlight.

Brine water was sampled from Lethabo Power Station. This brine water is actually rejected water from the reverse osmosis plant that is responsible for the purification of cooling water. The brine water was collected in plastic bottles and sealed and thereafter stored in a laboratory at room temperature and placed away from direct sunlight.

3.3 Mixture preparations

Two fly ashes were used in this study: Dura-Pozz fly ash from Lethabo Power Station as the dominant substance in a liner material and fly ash from Tutuka Power Station which represents a waste body. The two fly ashes were in most part subjected to the same tests even though they played two different parts in this study. In some of tests however Tutuka fly ash was only treated to optimum conditions that were pre-determined from Dura-Pozz fly ash.

Dura-Pozz fly ash was mixed with varying amounts of lime (1, 3, 6, 10%) on a dry weight percentage basis. Two dry weight percentages of gypsum of (1 and 3%) were then added to the lime mixes accordingly. An addition of high amounts of gypsum

lead to a decrease in durability as more ettringite is formed (Sivapullaiah and Baig, 2011). 3% was therefore the highest amount used in this study. Table 3-1 shows the mix percentages for fly ash with lime and gypsum. These admix concentrations were used throughout the study and the sample names assigned to each admixture are used in the rest of the text to refer to the designated admixture as shown in Table 3-1. LSM 1 for example refers to Dura-Pozz sample with no added additives. Tutuka fly ash was only incorporated into this study to represent waste material and was therefore not stabilised with lime or gypsum. It is important to note that LSM 1 is, Dura-pozz fly ash with no additives and LSM 10 is Tutuka fly ash with no additives.

Table 3-1 Mix preparation and sample labels

Sample name	Sample composition	%Lime added	%Gypsum added
LSM1	Dura-Pozz fly ash	0%	0%
LSM2	Dura-Pozz fly ash	1%	1%
LSM3	Dura-Pozz fly ash	3%	1%
LSM4	Dura-Pozz fly ash	6%	1%
LSM5	Dura-Pozz fly ash	10%	1%
LSM6	Dura-Pozz fly ash	1%	3%
LSM7	Dura-Pozz fly ash	3%	3%
LSM8	Dura-Pozz fly ash	6%	3%
LSM9	Dura-Pozz fly ash	10%	3%
LSM10	Tutuka Fly ash	0%	0%

3.4 Engineering methods

There are several engineering methods used in this study to obtain key engineering properties of fly ash. These tests include the determination of: maximum dry density and optimum moisture content, atterberg limits, unconfined compression strength and indirect tensile strength. All the engineering tests were carried out at an accredited geotechnical engineering laboratory, Simlab (Pty) Ltd. Bloemfontein.

3.4.1 Maximum dry density and optimum moisture content

The standard methods of testing road construction materials (TMH1-A7, 1986) define the maximum dry density as the maximum value that is attainable for density of a material. This occurs when a constant compactive force is employed over a range of moisture contents. Optimum moisture content is the moisture content of a

material where the maximum dry density is achieved. Maximum dry density and optimum moisture content determinations were done according to the standard methods of testing road construction materials, method A7 (TMH1-A7, 1986).

Fly ash and the additives used in this study were all taken directly from their air sealed containers and were judged to have a zero moisture level. If judged to contain moisture, they were air-dried before use. A mass of 35 Kg of each sample was prepared according to Table 3-1, and was mixed thoroughly. The mixed material was then divided to obtain five basins of similar material of about 6 – 7 Kg each. Each sample was then weighed to the nearest 5 g and transferred to the mixing basin. A measured volume of water was put into a spray-can or sprinkler where it was then slowly added to the material while continuously mixing with a trowel. Water was then added until the material had attained its optimum moisture content. The volume of water remaining in the spray-can or sprinkler was then measured to obtain the actual amount added and was then expressed as **percentage of the air dried material**. The moist material was then covered with a damp sack to prevent evaporation and was allowed to stand for 30 minutes so that moisture could be evenly distributed. In other basins water was added and mixed at higher or lower moisture content than the first (usually 1 - 2% difference).

The weight of a clean dry mould was determined to the nearest 5 g and assembled onto a base plate with a spacer plate. The dimensions and set up of a mould are shown in Figure 3-1. To avoid the material from adhering to the surface of the plate during compaction two rounds of 150 mm filter paper were placed onto the space plate and the collar was then fixed to the mould with the spacer plate inside the mould. The effective depth of the mould was 127 ± 1 mm.

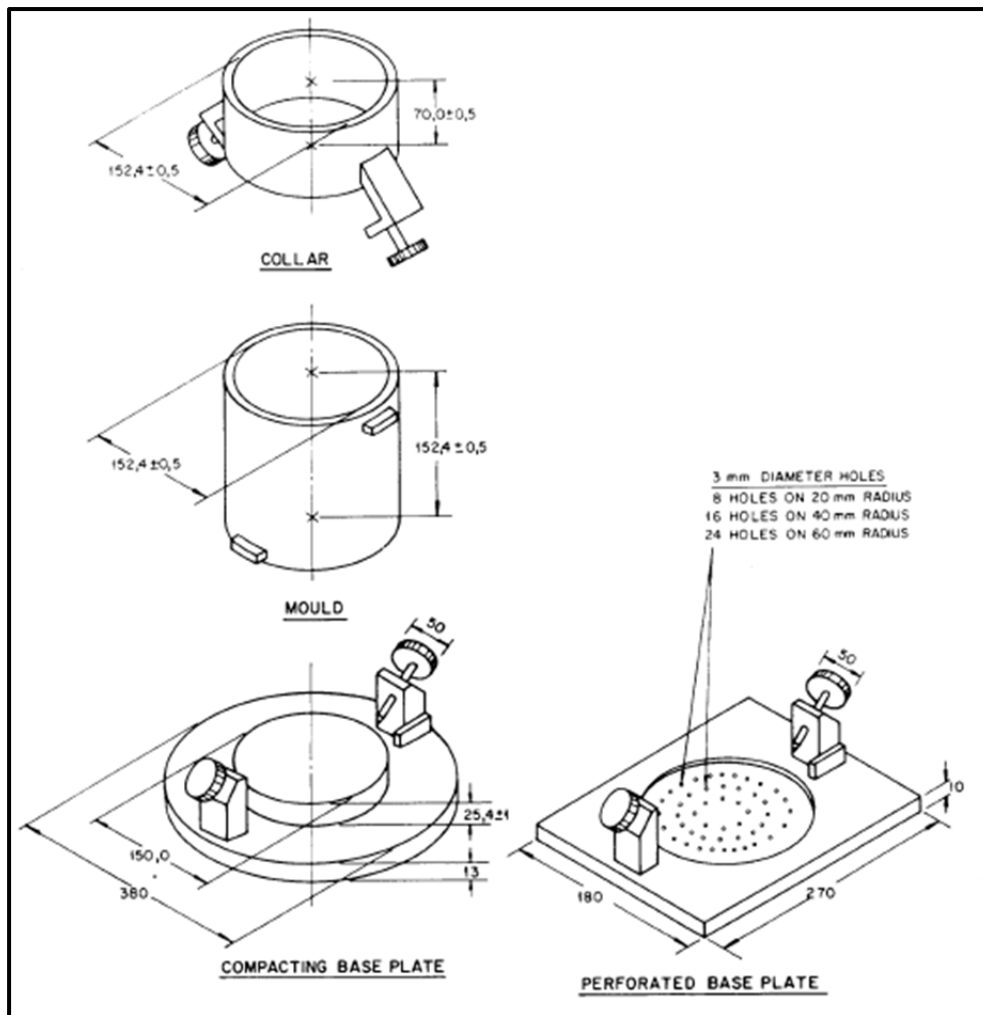


Figure 3-1 Mould with collar and base plates, adapted from (TMH1-A7, 1986)

The moist material was then mixed once more and about 1000 g was weighed out and added to the mould. The surface of the soil was then flattened by lightly pressing down and tamping. The material was thereafter compacted by tamping 55 times with a 4 536 g tamper dropping precisely 457.2 mm Figure 3-2. The blows were spread equally throughout the whole surface in five cycles of 11 with 8 blows to the outside circumference and 3 blows on the centre. After tempering the first layer the depth of the surface of compacted material below the top of the mould was in the range of 96 and 99 mm. Four more layers were then compacted in the same manner and each layer was in the range of 25 – 30 mm thick. After compaction of the 5th layer the material was between 5 – 15 mm on top of the mould without the collar. This excess material was then removed after the collar was dislodged from the mould by a steel straight edge until the material was level with the top of the mould. The mould was

subsequently removed from the base plate along with the compacted material weighed to the nearest 5 g.



Figure 3-2 Mould under a tamper during compaction

A representative sample was taken from the basin after the second layer was compacted and placed into a suitable container for moisture content determination. The sample was in the range of 50 – 100 g and it was weighed to the nearest 0.1 g. The sample was then transferred to an oven set at 105 – 110°C where it was dried to a constant mass. The moisture content was determined to the nearest 0.1%.

The procedure above represents the determination of one point of moisture-density relationship. Additional points were determined using the same procedure whilst varying the water content. A graph of moisture content and dry density produces a breakthrough curve with the highest value of dry density obtained corresponding to the optimum water content. After the first two points the third point was determined according to how the outline of the graph was taking shape. For example if after two points the graph was on a declining trend it simply meant the optimum moisture content was exceeded and the additional points were determined at a lesser water content than the previous points. Moisture content was expressed as a percentage using the following equation:

3.1 Moisture content

$$d = \frac{a - b}{b - c} * 100$$

Where:

d = moisture content expressed as a percentage of the dry soil

a = mass of container and wet material

b = mass of container and dry material

c = mass of container only

The dry density for each point was calculated to the nearest 0.1 Kg/m³ using the following equation:

3.2 Dry density

$$D = \frac{w}{d + 100} * \frac{100}{V} 1000$$

Where: D = dry density in Kg/m³.

W = mass of wet material in gram.

V = volume of mould in ml

Since the volume of the mould does not change then Equation 3.2 can be expressed as:

$$D = \frac{w}{d + 100} * F$$

Where: F is the factor of the mould ($100/V * 1000$). Moisture content was calculated to the nearest first decimal figure and density to the nearest whole number. After all the moisture content points had been calculated and all the dry density points had also been determined the results were plotted graphically. The graph of moisture content versus dry density revealed a curve with the highest value of dry density corresponding to the optimum moisture content Figure 3-3.

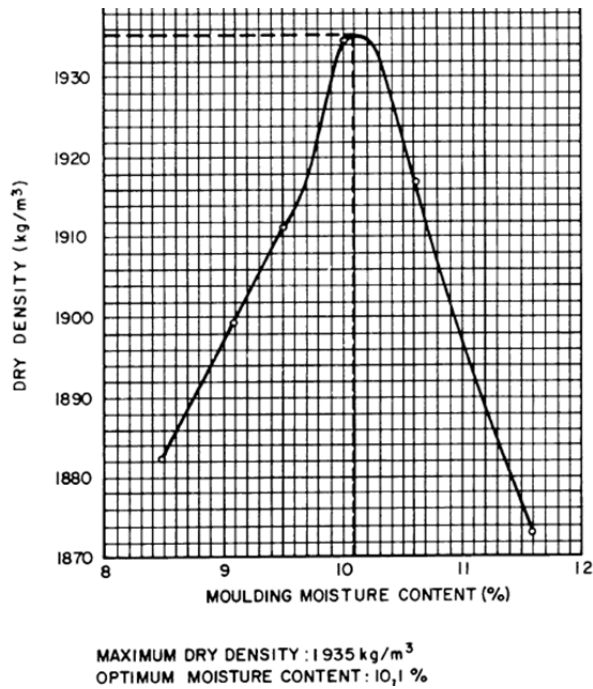


Figure 3-3 Example of a graph of moisture-density relationship, adapted from (TMH1-A7, 1986)

3.4.2 Unconfined compression strength (UCS)

The unconfined compression strength test was done according to the standard methods of testing road construction materials namely, method A14 (TMH1-A14, 1986). Unconfined compression strength (UCS) test of cohesive soil, is defined as the load per unit area at which an unconfined cylindrical specimen (127.0 mm high and 152.4 mm diameter) of soil will fail in a simple compressive test (Karol, 1955). The compressive load was fixed at 140 KPa/s. The samples for the UCS test were prepared and compacted into moulds using the procedure described in section 3.4.1 (TMH1-A7, 1986).

The UCS test could only be performed on soils which had enough cohesive strength to be able to stand on their own without being supported by the mould. The material that was going to be subjected to UCS was compacted at optimum water content according to the procedure described in section 3.4.1. Once the specimens were compacted they were prepared for UCS in accordance with the procedure described in (TMH1-A14, 1986). Moisture content was also determined by taking a representative sample and oven drying as described in section 3.4.1. The compacted specimens were taken out of the moulds and put through a rapid curing process. Instead of putting samples in a curing room for seven days as prescribed by (TMH1-A14, 1986) the specimens were inserted in plastic bags and sealed off as shown in

Figure 3-4. The specimens were then placed in an oven set at 60 °C for 48 hours curing time. This was done so that the samples would undergo curing in the humid environment created within the plastic bags. The specimens were then removed from the oven and inserted into a water bath at temperature 22 – 25 °C Figure 3-5.



Figure 3-4 Specimens being prepared for rapid curing. The plastic bags create a constant humid environment around the specimens as they were cured for 48 hours in the oven at 60 °C



Figure 3-5 Specimens in a water bath at 25 °C

After 4 hours of curing in the water bath the specimens were crushed to total failure using a compression testing machine, Figure 3-6. A second set of specimens were prepared in the same way but were placed in the water bath for 7 days in order to determine if lengthier curing affected the strength of the material.



Figure 3-6 Unconfined compression strength test on a fly ash admix sample

In the compression test machine the load was applied to the flat surfaces of the specimen at a rate of 140 KPa/s which is equivalent to a load of 150 KN/min for 152 mm diameter specimens. The load was recorded to the nearest 1 KN. The UCS was then calculated to the nearest 10KPa as follows:

3.3 Calculation of UCS

$$U = \frac{KN}{\pi r^2} = \frac{KN}{0.01824}$$

Where U is the unconfined compressive strength in KPa, KN is the load required to crush the specimen in kilonewtons and r^2 is the radius of the specimen face in metres.

3.4.3 Indirect tensile strength (ITS)

The indirect tensile strength test was done according to the standard methods of testing road construction materials, method A16T (TMH1-A16T, 1986). The indirect tensile strength (ITS) of stabilised material was determined by measuring the resistance to failure of the cylindrical prepared specimen when a load is applied to the curved sides of the specimen. Samples were prepared in the same way as in the unconfined compression strength test in section 3.4.2, the only difference being that there was no curing of the samples in a water bath. A cylindrical specimen was

loaded diametrically across the circular cross section. The loading causes a tensile deformation perpendicular to the loading direction, which yields a tensile failure, as seen in, Figure 3-7. By recording the ultimate load and by knowing the dimensions of the specimen, the indirect tensile strength of the material was computed.



Figure 3-7 Sample splits in half during an indirect tensile strength test

The load of 40 KN/min was applied during the ITS test until failure and the maximum applied load was then recorded accurately to 0.1KN. The indirect tensile strength (ITS) of each sample was determined to the nearest 1KPa by using the following equation:

3.4 Calculation of indirect tensile strength test

$$T = \frac{2P}{\tau ld}$$

Where:

T = is the indirect tensile strength is KPa

P = maximum applied load (KN)

l = is the length of specimen (m)

d = diameter of specimen (m)

$\tau = 32.89P$ for specimen 152.4 mm in diameter

3.4.4 Atterberg limits

Atterberg limits are limits of uniformity used to categorise fine grained soils. These limits include plastic limit (PL), liquid limit (LL) and plasticity index (PI) of the soil and they depend on the moisture content. The plasticity index of soil is defined as the arithmetical difference between the liquid limit and the plastic limit ($PI = LL - PL$). The plastic limit, liquid limit, plasticity index and linear shrinkage were determined according to the standard methods of testing road construction materials.

1. Liquid limit

Liquid limit was determined according to (TMH1-A2, 1986). 48 g of each sample was weighed out and put into a porcelain dish. Distilled water was added in a stepwise manner whilst mixing with a spatula for a period of 10 minutes. Adequate water was mixed into the sample to form a stiff consistency and approximately three quarters of the wet sample was transferred to a brass bowl of the liquid limit device and then flattened out with a spatula, Figure 3-8. The wet material left over in the porcelain dish was kept for the determination of the plastic limit, section 2. The material was then halved by cutting through the middle with a grooving tool. The device was then tapped at a speed of two taps per second and this rate was applied to the material until the lower parts of the faces of the two split portions had rolled together and made contact across a distance of about 10 mm, Figure 3-8.

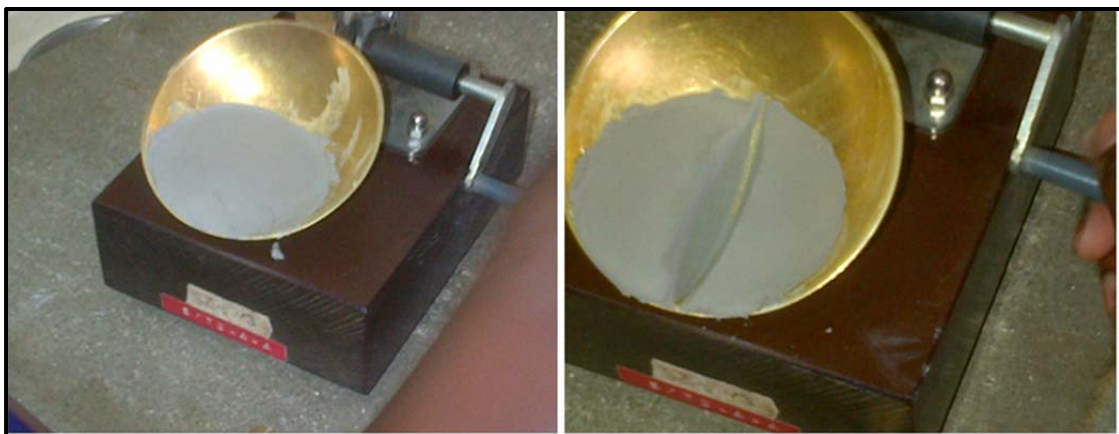


Figure 3-8 Fly ash sample in a casagrande cup used for liquid limit determinations, *left* shows sample after being transferred to the cup, *right* shows the sample after having divide into two portions before tap action

The number of taps required to close the gap across the distance was recorded and a sample of 2 to 3 g was transferred into an empty weighing container for the

determination of the moisture content. The mass of containers containing the samples were recorded and then oven dried at 105 to 110 °C overnight. The containers were taken from the oven and then weighed. The loss in mass was regarded as the mass of water and was expressed as a percentage of the oven dried mass of soil. The moisture content of the sample was calculated using the following:

3.5 Moisture content for liquid limit

$$\text{Moisture content (\%)} = \frac{\text{mass of water}}{\text{mass of oven dried soil}} * 100$$

The one-point method which is described in 5.2 of (TMH1-A2, 1986) was used to determine the liquid limit. The liquid limit (LL) was determined by use of the following formula:

3.6 Liquid limit calculation using one-point method

$$LL = W \left(\frac{N}{25} \right)^{0.12}$$

Where N is the number of taps needed to close the groove at moisture content W .

2. Plastic limit and plasticity index

The plastic limit and plasticity index were determined according to (TMH1-A3, 1986). Wet samples (2 to 3 g) were kept aside from the liquid limit determination, section 1, and were rolled out into ellipsoidal shapes. The samples were rolled until the crumbling of the sample prevented the formation of a thread 3 mm in diameter, which was regarded as a reasonable end point. At this point the samples were judged to have crumbled only on account of lack of plasticity. The crumbled samples were transferred to a weighing container for the determination of moisture content. The containers with the samples were weighed to the nearest 0.01 g and then the samples were oven-dried overnight. The plastic limit was determined by the following equation:

3.7 Plastic limit

$$\text{Plastic limit} = \frac{\text{mass of water}}{\text{mass of oven dried soil}} * 100$$

The plasticity index was obtained by subtracting the liquid limit from the plastic limit, the following equation was used:

3.8 Plasticity index

$$\text{Plasticity index (PI)} = \text{liquid limit (LL)} - \text{plastic limit (PL)}$$

3. Linear shrinkage

Linear shrinkage was conducted according to (TMH1-A4, 1986). A clean, dry linear shrinkage trough was briefly warmed in the oven to prevent early setting of the wax. A thin layer of wax was then smeared on the inside of the trough covering the inside completely. Left over material after the one point method in section 1 was used to fill the trough completely with the sample. The trough with the wet material was transferred to the oven at 105 – 110 °C overnight and was then removed from the oven and allowed to air dry. The trough has a fixed length of 150 mm and any shrinkage in the material was observed by gaps visible from the trough walls. The length of the material was then measured and the linear shrinkage was calculated using the following equation:

3.9 Linear shrinkage

$$LS = LS_N * \frac{0.8}{1 - 0.008N}$$

LS is the linear shrinkage, quantified as a percentage of the original wet length of 150 mm when the moisture content is condensed from the liquid limit to an oven-dry condition. LS_N is the linear shrinkage, quantified as a percentage of the original wet length of 150 mm, when the moisture content equivalent to N taps in the liquid limit test is condensed to an oven-dry condition.

3.5 Geochemical methods

3.5.1 X-ray Diffraction (XRD)

XRD was used for qualitative analysis of mineral phases present in samples obtained from the compacted specimens in the constant head test, section 3.8. Samples for XRD examinations were prepared by drying in the oven at 100°C for 24 hours. Samples were then milled to a fine powder using ceramic pestle and mortar. The fine powder was then pressed into the sample holders, Figure 3-9.

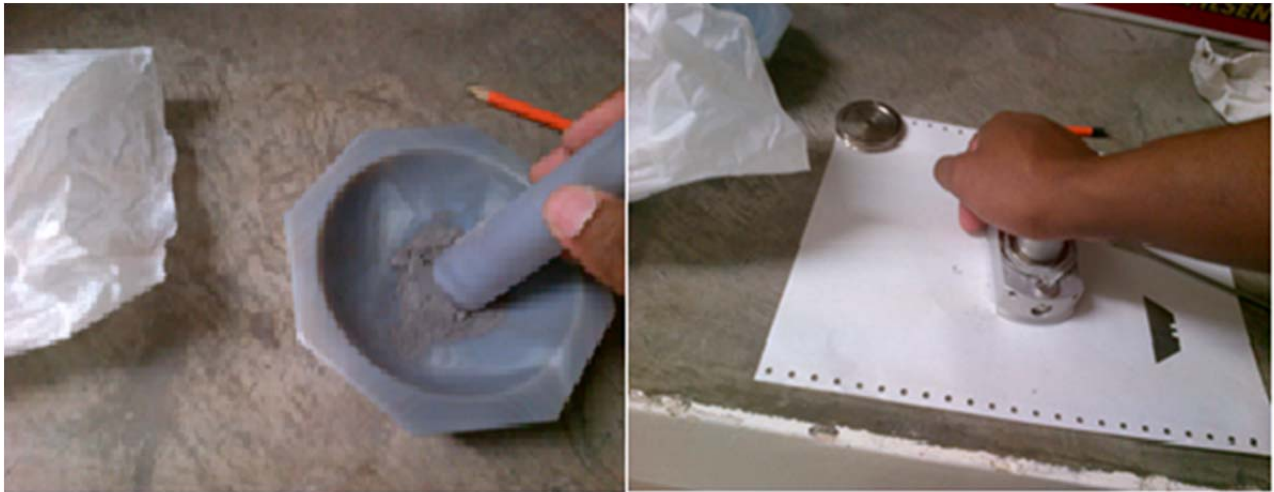


Figure 3-9 Sample preparation for XRD, left is a sample being crushed, right is sample being pressed into a sample holder before being entered into the Diffractometer

The XRD analyses were conducted with the Diffractometer system Panalytical EMPYREAN theta-theta goniometer that uses a Cu anode material (45 Kv, 40mA). Data was collected in the 2 theta range 5 – 70° in 0.017° steps with a scan speed of 15.87 seconds per step.

3.5.2 X-ray fluorescence (XRF)

XRF investigations were conducted to quantify the chemical composition of Dura-Pozz fly ash and Tutuka fly ash.

4. Sample preparation for majors elements

The samples were dried at 105 °C overnight and then passed through a 45 µm sieve before being inserted into a dessicator to remove excess moisture. A mixture of lithium tetraborate 66% + lithium metaborate 34% was used as a fluxing agent and 9 g was mixed with 0.9 g of each sample with a spatula in a crucible. The mixture was put through a fusion program where it was melted at 1050 °C for 420 sec in a fluxer instrument from, Katanax (RJM Systems). The mixing process was then done by the fluxer instrument at an angle of 45° for 480 sec at 80% speed. The mixture contained 0.05 ppm of lithium bromide which prevents the solution from sticking to the platinum crucible inside the fluxer instrument during pouring. The fused mixture was poured into the moulds for 15 sec and then cooled for 10 sec. The fusion discs were thereafter analysed by an Axios max (PANalytical instrument) at Eskom laboratories (Research Development and Innovation Centre).

5. Sample preparation for trace elements

8 g of sample was mixed with 3 g of Hoechst wax micro-powder. Hoechst wax was used to aid samples to form tablets/pellets. The mixture was then pressed into pellets using a hydraulic press at 4000 bars. The pellets were then analysed with the XRF (PANalytical instrument) using Protrace mode, at the Geology Department (University of the Free State).

3.5.3 Scanning electron microscopy (SEM)

Scanning electron microscope uses a focused beam of high energy electrons that interact with the sample producing various signals that can be detected. These signals can be used to obtain different sample characteristics which provide information about the external morphology of materials, distribution of electrically active crystal defects or local chemical composition in the form of an image (Lábár, 2002). Scanning electron microscopy was conducted in order to determine the morphology of samples obtained from the compacted specimens in the constant head test, section 3.8.

6. Energy dispersive spectroscopy (EDS) on the SEM

The energy dispersive spectroscopy is usually part of the scanning electron microscope SEM. As electrons are reflected by the specimen during SEM they produce image disparity with some elements backscattering electrons more than others. The EDS makes it possible for the identification of specific elements and their corresponding fractions usually in atomic weight percentage (Hafner, 2013). The EDS was used for spot quantitative analysis on samples in the SEM.

7. Sample preparation

Samples were lightly crushed into a fine powder using a ceramic pestle and mortar. The fine powder was then sprinkled on glass slates. The samples were then carbon coated with graphite before being placed in the SEM Figure 3-10. Coating with electrically conductive material is common when using SEM since nonconductive material tends to charge and accumulate electrostatic charge at the surface when scanned with an electron beam and this usually causes scanning faults and image imperfections (Lábár, 2002). Samples were coated using a Q150T turbo-molecular pumped carbon coater. The coated samples were then analysed by a SEM machine (Joel JSM – 6610) at the Geology Department (UFS).



Figure 3-10 Sample after being carbon coated

3.5.4 Quantitative evaluation of minerals by scanning electron microscopy (QEMSCAN)

QEMSCAN was performed on powdered samples and on block samples obtained from the compacted specimens in the constant head test, section 3.8.

8. Sample preparation and procedure

A powdered sample was riffled by a Rotary Micro Riffler (Quantachrome Instruments). The riffled sample of 0.16 ± 0.02 g was weighed using a mass balance and then put through the potting process. 30 mm Teflon silicon sample mould was coated with silicone oil and then oven dried at 60 °C for 1 hour. The riffled sample was added to the molten wax and stirred with a bamboo stick. After vigorous stirring the sample was left in the oven at 120 °C for 35 min to equilibrate the temperature of the sample, wax and Teflon mould. The temperature of the oven was then decreased to 60 °C to allow the sample to solidify and was left undisturbed for 90 min. The sample was then taken out of the oven and allowed to cool at room temperature after which it was removed from the sample mould and labeled.

A 30 mm diameter plastic mould was coated with silicone oil and left to dry. In a separate disposable container epoxy resin and hardener were weighed and mixed (ratio of resin/hardener varied depending on the brand of resin). 10 g of resin/hardener mixture was poured into dry plastic moulds and the riffled sample was slowly added and mixed in with a bamboo stick. The mixed sample was placed in a pressure vessel set at 2 bars for 5 to 12 hours (depending on the brand of resin). This was done to minimize the bubble formation that usually occurs with

unpressurised curing. Once curing was completed the sample was then removed from the pressure vessel and removed from the mould for polishing.

The samples were polished using a polishing instrument – Struers TegraPol-21. Polishing was conducted at a force of 10N/60N with a rotation speed of 300rpm. Table 3-2 gives the summary of the polishing procedure. After polishing the sample was then washed with soapy water and air dried to ensure the surface was sufficiently clean.

Table 3-2 Summary of polishing process

Polishing Step No.	Polishing Surface	Polishing Paper	Time (s)	Lubricant
1	Sample back	MD Piano 80	10	Water
2	Sample surface	1200 SiC grit	10	Water
3	Sample surface	2400 SiC grit	10	Water
4	Sample surface	4000 SiC grit	10	Water
5	Sample surface	MD Nap	10	Water

The sample was then transferred to a carbon coating instrument – K950x turbo evaporator. The polished surface of the samples was placed upwards and carbon coated in a vacuum. The sample was then transferred to the QEMSCAN (Zeiss EVO 50 QEMSCAN with four silicon drift detectors) for analysis. This procedure was conducted for all powdered samples.

Some compacted specimens were taken from the permeameter cell and analysed without grinding to powder form and hence analysed as blocks. This was done to determine the in situ mineralogy of samples in the permeameter cells. The blocks were cut and moulded into small square blocks able to fit into sample holders used in the QEMSCAN machine. The block samples underwent the preparation process described above before being analysed by Zeiss EVO 50 QEMSCAN with four silicon drift detectors at Eskom laboratories (Research Development and Innovation Centre).



Figure 3-11 Preparation of block samples, left sample from permeameter is being cut, right is square blocks of samples

3.6 Cation exchange capacity (CEC)

Cation exchange capacity (CEC) analyses were carried out in accordance with method 35 of Handbook of Standard Soil-Testing Methods for Advisory Purposes (Committee, 1990). Samples used for CEC were obtained from the compacted specimens in the constant head test, section 3.8.

3.6.1 Sample Preparation

10 g of sample was weighed and transferred into a filter paper placed in a funnel. The sample was then leached with 1N ammonium acetate solution and 250 ml of leachate was collected and kept for **exchangeable cation analysis**. The sample was then leached with 1N sodium acetate solution until 200 ml of leachate was collected. The leachate was discarded and then the sample was then rinsed with 60% alcohol until about 300 ml of leachate was collected. The collected leachate was discarded. The sample was again leached with 1N ammonium acetate until 250 ml of leachate was collected. The collected leachate was then analysed using Atomic Emission Spectrometer Agilent 4100 Microwave Plasma at the Soil, Crop and Climate Science Department (UFS).

3.7 Texture analysis

Texture analysis of fly ash was carried out in accordance with method 12 of the Handbook of Standard Soil-Testing Methods for Advisory Purposes (Committee, 1990). Texture analyses were done on both Dura-Pozz fly ash and Tutuka fly ash.

3.7.1 Procedure

30 g of sample was weighed and 50 ml of calgon was added where after the mixture was shaken well for 10 min. The silt and clay were separated out by washing through a 0.5 mm sieve. The sand was then dried in the oven at 60 °C for 3 hours and was then passed through .5 mm, .25mm and .107mm sieves. The silt and clay mixture was then poured into a 1L cylinder and water was added to the 1L mark. Following this silt and clay fractions were then read with a hydrometer at the Soil, Crop and Climate Science Department (UFS).

3.8 Hydraulic conductivity

Hydraulic conductivity was discussed in detail in section 2.2.3. The saturated hydraulic conductivity of unconsolidated material can be measured in the laboratory by the constant head permeameter or the falling head permeameter (Freeze and Cherry, 1979). In this study the constant head permeameter was used to determine the hydraulic conductivity of all samples employed.

3.8.1 Experimental procedure

A cylindrical rigid wall permeameter cell of length 11.4 cm and diameter 10.5 cm was used to house the samples for hydraulic conductivity tests using constant head method. A sample was sealed off between two porous plates in a cylindrical permeameter cell. A constant head was maintained across the sample by placing a container of water above the permeameter and allowing water to flow down into the permeameter cell, Figure 3-12. The volume of fluid seeping through the sample was recorded with time. The Darcy equation was rearranged and used in the following form to calculate the hydraulic conductivity:

3.10 Darcy equation for constant head test

$$K = \frac{QL}{AH}$$

Where K is the hydraulic conductivity, Q is the volumetric discharge through the system, H is the constant head differential across the sample and L is the length of the column where the compacted specimen is contained (Freeze and Cherry, 1979).

Deionized water was used for down-flow percolation through the specimen in the constant head test. Water discharged from the column was collected in a sample bottle and the volume was recorded with time. The sample bottle was sealed and then taken to the Institute for Groundwater Studies for chemical analysis.

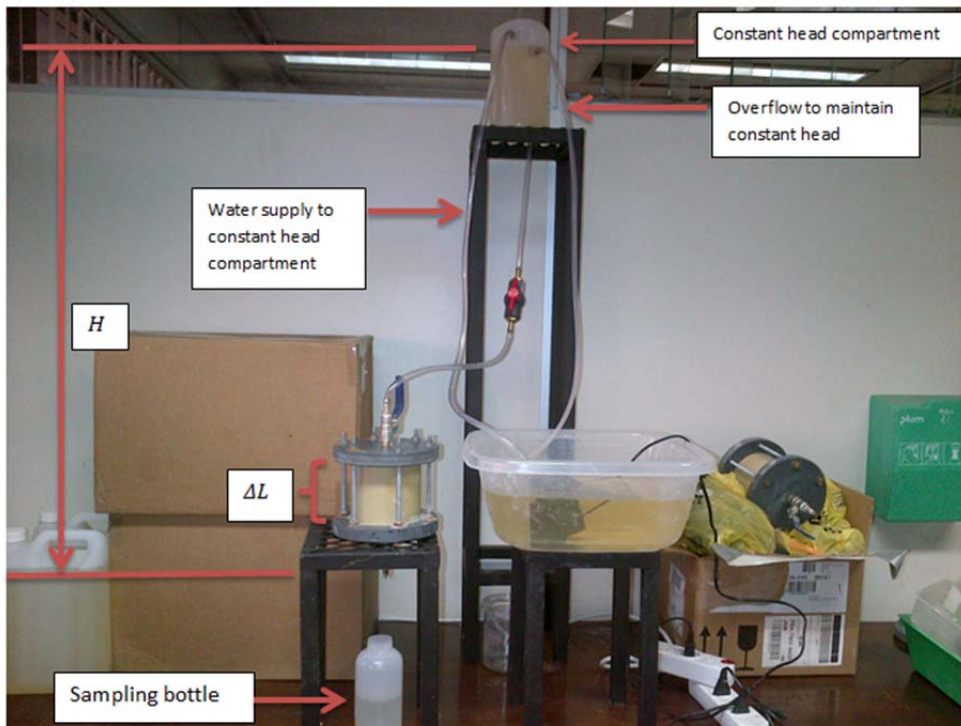


Figure 3-12 Experimental set up for hydraulic conductivity determinations

3.8.2 Preparation and packing of the column

Samples were dry mixed according to the ratios prescribed in Table 3-1. Mixing of the samples was done by hand until a homogeneous mixture was obtained and water was added according to each sample's optimum moisture content, Figure 3-13 shows a mixed homogeneous sample. Samples were then compacted at their optimum moisture contents, see section 3.4.1.



Figure 3-13 Sample mixing, (left) gypsum and lime just added to fly ash, (right) homogeneous mixture of fly ash, gypsum and lime after vigorous mixing

A rammer with a total weight of 1421.4g was used for compact samples into the columns. The rammer had a movable gliding weight of 765.3 g and was allowed to fall down a guide rod 30 cm into the compacting disc of diameter 10.4 cm. It was essential not to compact straight onto the surface of the sample but to use a compaction disc to avoid preferential pathways developing in the material during compaction. A compacting disc was placed on top of the unconsolidated material and the rammer fell onto it pressing it down with the material Figure 3-14.



Figure 3-14 Compaction of samples into a column

The compacting process was conducted in such a manner that 3 blows were made in the centre and 7 blows at the circumference moving in a clockwise direction with every blow while completing a cycle hence covering the whole spherical area (A). This process was repeated three times per compacting cycle, the sample was thus compacted 30 times ((3 centre * 7 edges) * 3 times). 200 g of sample was added after each successive compaction process and the rammer and compacting disc were removed and reinserted accordingly. The column was filled with the compacted sample to about 95% the length of the column, as a small space was needed to fit the porous plate onto the column. The length (L) of approximately 11 cm of the column was filled with compacted specimen. The mass of the column with the sample was recorded.

The constant head test was then prepared by first inserting a whatman No. 42 filter paper at the bottom of the column to prevent particulates from blocking the piping system. A second filter paper was attached at the top of the column to allow for even distribution of input water. The porous plates were then inserted on the top and bottom parts of the column and screwed tightly in place. The permeameter cell was then transferred to the constant head test, where water was permitted to flow through the compacted sample as head (H) of 74 cm was being maintained. The test was carried out for 7 days without any disruptions and all the water outflowing from the bottom of the permeameter cell was collected in sample bottles. The volume of water collected each day was recorded with time (Q). The sample bottles containing discharged water were then sealed and sent to an accredited laboratory for analysis.

3.8.3 Wetting and drying cycles

One feature that a liner material of a dry ash landfill will have to contend with is wetting and drying cycles. LSM 7 was subjected to wet/dry cycles to determine the effect on hydraulic conductivity. A similar test was performed by Palmer et al., (2000) on compacted fly ash specimens. Specimens were first subjected to hydraulic conductivity testing for seven days using the same procedure as described in section 3.8. The hydraulic conductivity that was determined on the seventh day was recorded and used as a background to determine the effects dry/wet cycles will have on the hydraulic conductivity of the specimens. The rigid permeameter cells containing the specimens were then unfastened from the porous plates and placed

into an oven set at 60 °C for 24 hours. A desiccator was also placed in the oven to assist with drying Figure 3-15. The dried specimens were then taken from the oven and subjected to hydraulic conductivity testing as before. Measurements were taken after steady state flow was reached (6 hours). The test was done in triplicate.

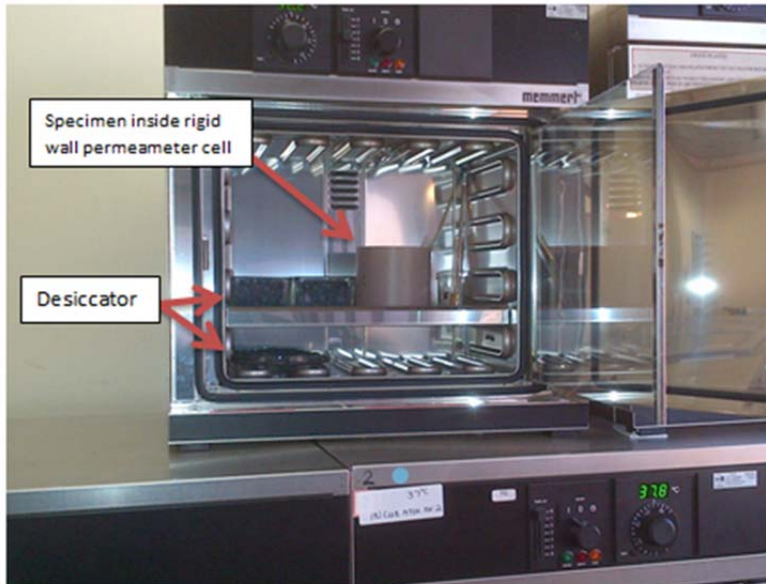


Figure 3-15 Drying of LSM 7 in an oven at set 60 °C, desiccator inserted in oven to encourage drying

3.9 Multi-layer liner system

A rigid wall permeameter cell of 31.1 cm in length and a diameter 29.5 was used to contain the multi-layer liner system. The inside of the permeameter cell was marked accordingly using a marker on the two outflow positions. The lowermost outflow position was 7.5 cm from the base of the permeameter cell and the upper outflow position was 24.5 cm from the base. For consistency, the thicknesses of all the layers were marked on the inside of the permeameter cell with a marker. The layers were stacked on top of each other starting from the bottom of the permeameter cell moving up, and were distributed as follows:

- The first layer was 7.5 cm thick from the bottom of the permeameter cell.
- The second layer was 1.5 cm thick and corresponded with the position of the lowermost outflow point
- The third layer was 15 cm thick

- The fourth layer was 1.5 cm thick and corresponded with the position of the upper outflow point
- The fifth layer was 6 cm thick and ended at the top of the permeameter cell.

The multi-layer liner system was stacked from the bottom moving up with different materials. A level 4 geotextile (supplied by Keytech Engineered fabrics (Pty) Ltd) was cut to size of the inner diameter of the permeameter cell (30 cm) and fitted to the bottom of the permeameter cell, on top of the bottom porous plate. A mixture of (Dura-Pozz fly ash 94% + lime 3% + gypsum 3% (wt %)) was dry mixed thoroughly by hand until a homogeneous mixture was obtained, see Figure 3-13. Depending on the mass of the mixture, the amount of water needed to bring the mixture to optimum water content was added to the mixture via a spray can.

2000 g of the wet mixture was transferred to the permeameter cell and placed on top of the geotextile where the mixture was levelled out. A compacting disc of diameter 29 cm was inserted into the permeameter cell on top on the levelled mixture. A rammer was then placed on top of the compaction disc and compaction was carried out with the rammer Figure 3-16. The same rammer described in section 3.8.2 was used. The compaction routine was as follows: 3 blows to the centre followed by a circular movement of blows on two circles drawn on the compaction disc. The first circle was 7 cm from the centre and the number of blows that completed a clockwise cycle was 8. The second circle was at 3 cm from the edge (circumference) of the compacting disc and the number of blows that completed a clockwise cycle was 15. 26 blows were made in total per round of compaction and this was repeated so that 52 blows were directed per 2000 g of sample compacted.

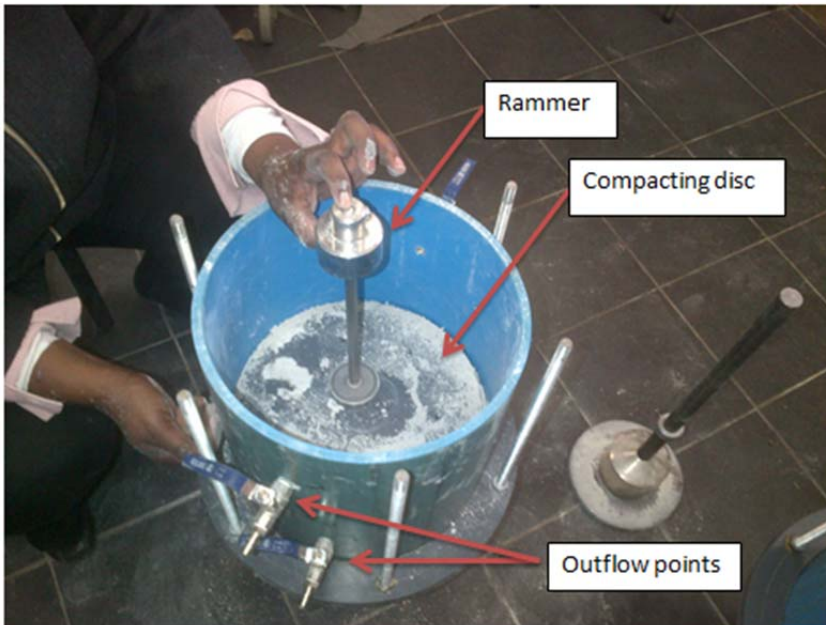


Figure 3-16 Compaction procedure using rammer inside permeameter cell

After each successive compaction the compacting disc was removed along with the rammer and an additional 2000 g of mixture was added to the permeameter cell. The same compacting procedure was followed until the layer was 7.5 cm thick after the last compaction. The same size geotextile was once again inserted on top of the compacted layer and river pebble gravel of 1.2 Kg was placed on top of it. The same compaction process was done on the gravel layer. The layer of gravel corresponded with the lowermost position of the outflow point and a small piece of geotextile was fixed at the opening of the outflow point to prevent clogging, Figure 3-17.



Figure 3-17 Geotextile being placed on top of compacted layer, also a small piece of geotextile is placed at an outflow point to prevent clogging of the pipe

Geotextile was placed on top of the gravel layer so that the gravel was sandwiched between two geotextile layers. The lower geotextile layer served to protect the layer underneath from puncture by piercing particles from the gravel while the upper geotextile layer aided in providing a consistent surface for the layer above it. Furthermore the geotextiles still served out their primary purpose of making sure that only liquids passed through thereby acting as filtering media. A mass of 2000 g of the same mixture of fly ash, lime and gypsum was placed on top of the geotextile and the same compaction procedure was conducted until the upper marked position was reached. Another gravel layer sandwiched by two geotextiles was repeated again on top of this layer corresponding to the upper outflow point, Figure 3-18.



Figure 3-18 Gravel layer inside permeameter cell

Untreated fly ash from Tutuka Power Station was then placed on top of the upper geotextile. The compaction on the Tutuka fly ash was performed differently as the rammer was only allowed to fall 3 cm, a tenth of the distance for the other layers. This was done because Tutuka fly ash was added to simulate ash in a landfill, where it is dumped by a conveyor belt and no formal compaction procedures are carried out. On ash dumps trucks driving over the ash and water sprayed for dust suppression are the only two significant processes that contribute to ash compaction in any form.



Figure 3-19 Tutuka fly ash being added on top of the multi- layer liner system

The test was conducted twice, but by using different compaction rates for the fly ash admixture layers and gravel layers. In the first compaction rate which was conducted in a permeameter cell, the rammer was allowed to fall 30 cm as described above, and this will be referred to as **full compaction**. In another permeameter cell the rammer was only allowed to fall 7.5 cm during compaction and this will be referred to as the **quarter compaction**. The layer with the Tutuka fly ash was compacted in the same way for both permeameter cells (as described above). The stacking of the layers within the multi-layer liner system is depicted in Figure 3-20.

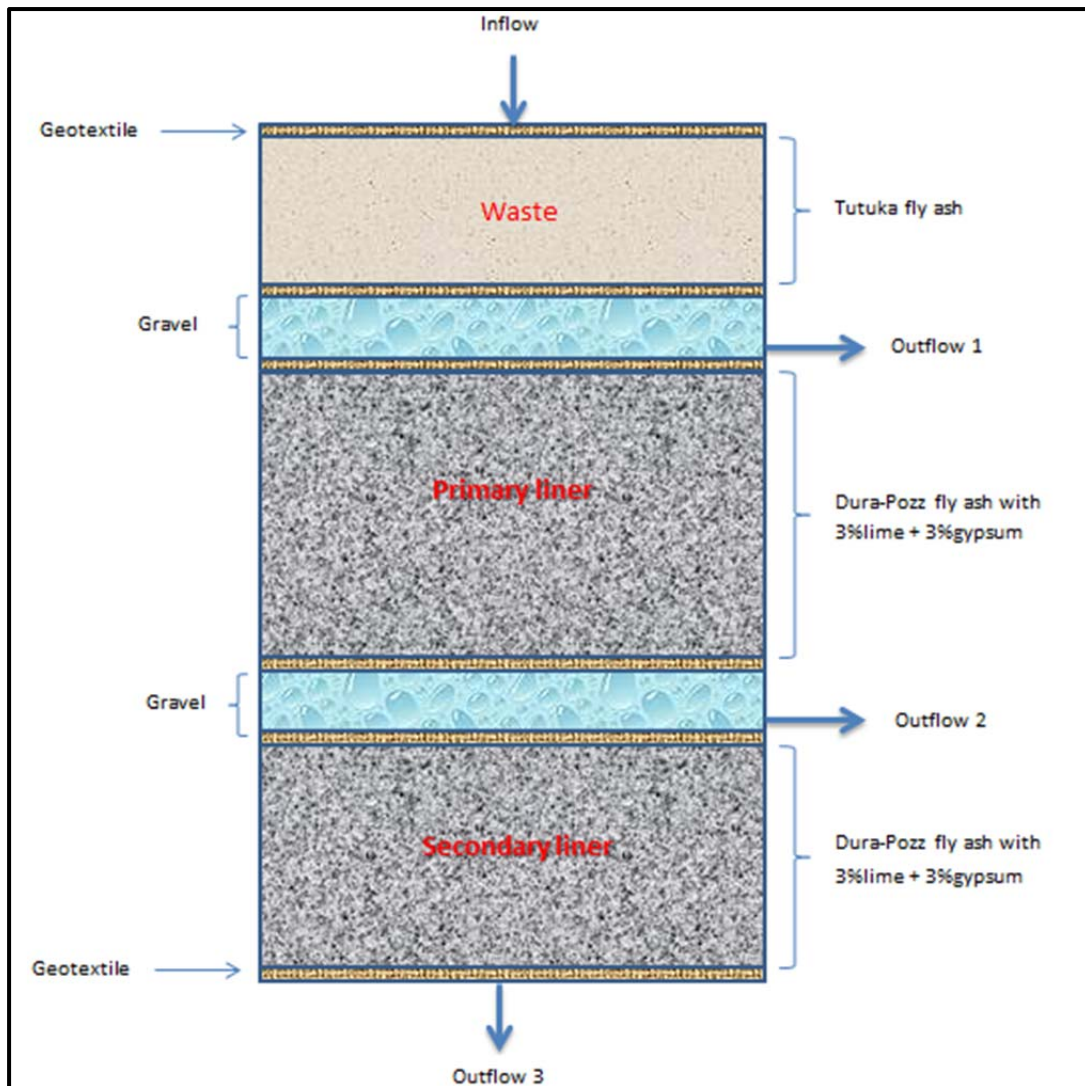


Figure 3-20 Configuration of layers within a multi-layer liner system

3.9.1 Daily percolation tests

Daily percolation tests were conducted on both the full compaction and the quarter compaction multi-layer liner systems. A volume of 20 L of brine water was allowed to flow into the multi-layer liner system without disruption using the apparatus of a constant head, section 3.8. Brine water was allowed to enter the multi-layer systems through the inflow point in the porous plate on top of the system. All the outflow points were opened during the course of the experiment. Collection containers were placed on all the outflow points accordingly to receive water outflowing from each outflow station.



Figure 3-21 Permeameter enclosing multi-layer liner system, *left* quarter compaction, *right* full compaction

After all the 20 L of brine water had run into the permeameter the system was left undisturbed for 1 hour and then the volume of water collected at each outflow point was then recorded. The collection containers were then removed and replaced with dry clean bottles that were left to collect overnight. Care was taken not to lose any water via evaporation and adhesive plastic was wrapped around the top openings of the bottles with an opening to allow collection. It also contained another small hole to release pressure and avoid vacuum built up (Figure 3-22).



Figure 3-22 Adhesive plastic covering collecting bottle to avoid losses due to gravity

Water collected overnight was recorded and the total water collected per overflow point was adjusted accordingly. A water balance was then determined and the process was repeated for seven days using the following equation:

3.11 Water balance on multi-layer liner system

$$\text{Holding capacity} = \sum \text{inflow} - \sum \text{outflow}$$

The volume of brine water injected daily was recorded, as well as the volume collected at every outflow station. The difference in volume was therefore regarded as the holding capacity of the system.

3.9.2 Continuous percolation test

The continuous percolation test was carried out on both the full compaction and the quarter compaction multi-layer liner systems. A constant head of 74 cm was used to drive flow through the system. 10 L of brine water was percolated continuously in a loop through the permeameter. Water flowing out of outflow 1 was directed back into the system by a water pump that pumped the water back to the constant head compartment. The other outflow points were kept open and water sample bottles were placed accordingly to collect water from each outflow point. The container collecting water from outflow 1 was covered with aluminium foil together with the top of the constant head reservoir to restrict water loss via evaporation. The test was carried out non-stop for 30 days and a water balance was then determined.

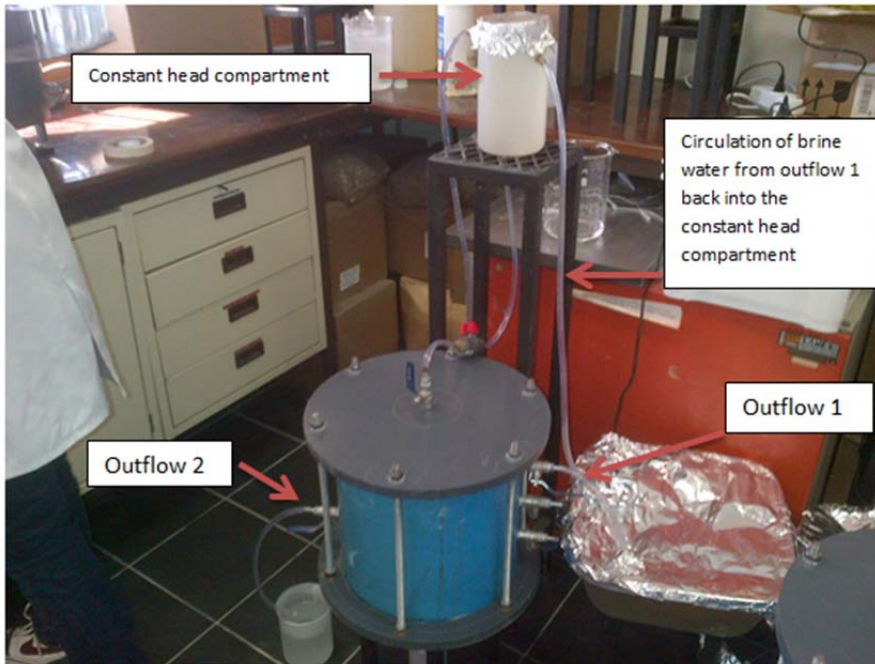


Figure 3-23 Continuous percolation test on a permeameter containing a multi-layer liner system. Brine water coming out of Outflow point 1 is being received in a container and circulated back into the constant head compartment.

3.10 Summary

This study set out to investigate an inexpensive liner that could be used to line ash dumps at coal power stations. The materials used in this study are low-cost resources that are readily available to power stations. Fly ash for instance is produced in millions of tons in every power station and gypsum will be available in huge amounts from the Flue gas desulphurization process that is planned for the new power stations (Kusile and Medupi power stations) (Eskom, 2012). The methods used to meet the objectives of this study are in most part prescribed by the minimum requirements for disposal of hazardous waste by landfill. However additional methods such as geochemical analysis (XRF, XRD, SEM, QEMSCAN) and cation exchange capacity were incorporated to fully address the objectives of this study. Perhaps the most important property of any liner material is its low permeability and hence hydraulic conductivity investigations were conducted on each sample, and including wet/dry cycles. The multi-layer liner system which simulates a double liner system was constructed in the laboratory for performance monitoring.

The next chapter presents the results obtained from the methods described in this chapter. It also includes interpretation of results and a general discussion.

4 Results and Discussions

4.1 Introduction

This chapter presents engineering results as well as Atterberg limits of the samples. Physical, chemical and mineralogical composition of fly ash and its admixtures are presented through various analytical techniques including XRD, XRF, SEM, and QEMSCAN. Soil texture analysis and cation exchange capacity are also included with hydraulic conductivity test results.

4.2 Engineering performance

4.2.1 Moisture content – dry density relationship

The procedure used to determine the maximum dry density and optimum moisture content was described in section 3.4.1. The moisture content-dry density relationship of specimens were plotted out in graphs which then made it possible to determine the optimum moisture content where the maximum dry density of the specimen was acquired. The results are summarised in Table 4-1.

Table 4-1 Optimum moisture content and maximum dry densities of specimens

Specimen name	Fly ash	Lime (wt %)	Gypsum (wt %)	Optimum (wt %)	moisture content	maximum dry density (Kg/m ³)
LSM1	Dura-Pozz fill fly ash	0%	0%		28.4	1355
LSM2	Dura-Pozz fill fly ash	1%	1%		12.6	1428
LSM3	Dura-Pozz fill fly ash	3%	1%		10.7	1488
LSM4	Dura-Pozz fill fly ash	6%	1%		11.9	1474
LSM5	Dura-Pozz fill fly ash	10%	1%		12.0	1474
LSM6	Dura-Pozz fill fly ash	1%	3%		13.8	1396
LSM7	Dura-Pozz fill fly ash	3%	3%		10.7	1464
LSM8	Dura-Pozz fill fly ash	6%	3%		10.9	1460
LSM9	Dura-Pozz fill fly ash	10%	3%		10.8	1458
LSM 10	Tutuka fly ash	0%	0%		21.4	1278

Samples LSM 1 and LSM 10 are fly ash specimens without any additives and represents Dura-Pozz fly ash and Tutuka fly ash respectively. These two specimens have a higher optimum moisture contents compared to the other specimens. LSM 1 has the highest optimum moisture content of 28.4 (wt %) followed by LSM 10 with (21.4 wt %). For the exception of LSM 10, the optimum moisture content of LSM 1 is more than two times higher than the highest percentage of the other specimens. Even though LSM 1 and LSM 10 have higher optimum moisture content their maximum dry densities are the lowest of all the specimens. It can be concluded that the addition of lime and gypsum in other specimens increased their maximum dry density at lower optimum moisture content percentages. There is a small difference in values obtained for the maximum dry density for specimens LSM 2 to LSM 9 which range from 1396 – 1488 Kg/m³. The optimum moisture content percentages for LSM 2 to LSM 9 are the range of 10.7 – 13.8 (wt %) with LSM 6 having the highest value of 13.8 (w %). Furthermore, LSM 6 has the lowest maximum dry density of these specimens and is the only specimen with a higher gypsum percentage (3%) than lime (1%) which may suggest that gypsum plays a more significant role than lime in terms of moisture content-dry density relationship.

Soils with a low water content are generally difficult to compact but if the water content is gradually increased the water will lubricate the soil grains and assists the compaction process (Chu, 2010). The elevated optimum moisture content percentages of LSM 1 and LSM 10 indicates that fly ash on its own needs to absorb a lot more water for it to overcome repellent forces such as friction between the grains. According to Sivapullaiah and Baig, (2009) the addition of lime imparts plasticity to a naturally non-plastic fly ash material. Gypsum ($\text{CaSO}_4 \cdot 2\text{H}_2\text{O}$) having water in its crystal lattice possibly also acts as a lubricating agent and with frictional forces being subdued, grains are easily compacted together with little water needed. This lubricating effect by the addition of lime and gypsum is observed by higher maximum dry densities at lower optimum moisture content percentages in specimens LSM 2 to LSM 9.

4.2.2 Unconfined compression strength (UCS) and indirect tensile strength (ITS)

The procedures used for the determinations of the UCS and ITS of the specimens were described in sections 3.4.2 and 3.4.3 respectively. For every specimen the UCS and ITS test was done in duplicate and the arithmetic mean calculated. The value of the arithmetic mean was used as the value per UCS and ITS for each specimen and the calculations are included in appendix A-1. The results from the UCS and ITS determinations are graphically displayed in **Error! Reference source not found.**

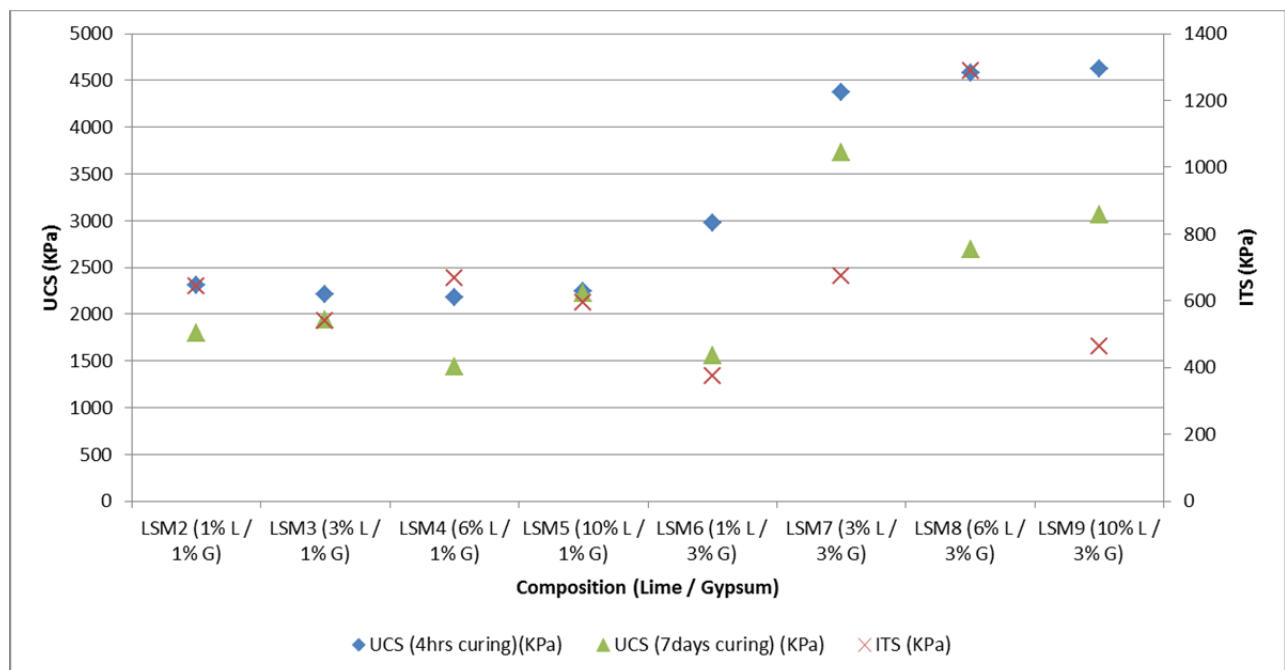


Figure 4-1 A plot of UCS (4 hours and 7 days curing) and ITS values in KPa

Error! Reference source not found. shows UCS results of same composition specimens but with different curing periods (4 hours and 7 days respectively). The UCS measurements are represented in the left column while ITS values are represented in the right column. The addition of 1% gypsum to fly ash does not seem to have such a significant impact on the UCS and ITS properties even if different percentages of lime are used. Once the percentage of gypsum in the sample is increased an increase in UCS behaviour can be observed. However there is a drop in higher UCS values from specimens cured for 4 hours to lower values for specimens cured for 7 days. In one sample, LSM 7, the drop is not so significant when compared to the other specimens having 3% gypsum. No significant strength increases were observed for the other component mixtures and thus the 3% gypsum

and 3% lime additive mixture represents the most optimal composition from an additive and costing perspective.

LSM 7 has the second highest ITS (after LSM 8) but this increasing trend in strength does not appear to be continued with higher percentages of lime addition, LSM 9 therefore dropped to the second lowest ITS value when compared to the rest of the specimens. Upon careful inspection of crushed LSM 9 and LSM 5 specimens, a great deal of white spots was observed. Since the same amount of gypsum was added into specimens LSM 2 – LSM 5 and also LSM 6 – LSM 9 it was accepted that these white spots represents unreacted lime since both LSM 9 and LSM 5 have the highest amount of lime, 10 (wt %), added to the fly ash, Figure 4-2. This is possibly due to excess lime not being successfully converted into pozzolanic compounds (Sivapullaiah and Baig, 2011). If excess lime does not increase the concentration of pozzolanic compounds then an addition of lime beyond 6 % is aimless for a fly ash liner material, as this reduces strength as seen with LSM 9. This indicates that strength is more dependent on the gypsum than on the lime content. UCS test could not be performed on specimen LSM 1 (Dura-Pozz fly ash with no additives) and LSM 10 (Tutuka fly ash with no additives) as the specimens collapsed during the water bath curing stage (Figure 4-3). These specimens were relatively soft (formed a slurry) indicating that the addition of lime and gypsum increases the strength of fly ash.



Figure 4-2 White patches of unreacted lime in LSM 9 after ITS crushing



Figure 4-3 Dura-Pozz fly ash collapses in a water bath during curing

4.2.3 Atterberg limits

A low permeability coupled with high strength is ideal components for a liner but what is also critical is for a liner material to have a certain amount of flexibility in order to prevent it from cracking due to differential settlements in the base soils

beneath the liner (Cokca and Yilmaz, 2003). The minimum requirements for waste disposal by landfill (DWAF, 1998b) as a guideline document recommends that a liner material should have a plasticity index of at least 10. The Atterberg limit tests conducted were the liquid limit, plastic limit and linear shrinkage and were determined using the procedure outlined in sections 1, 2 and 3 respectively. The data obtained from the tests is summarised below in Table 4-2.

Table 4-2 Atterberg limits of specimens

Sample name	Sample composition	% Lime	% Gypsum	% Lignosulphonate	Plasticity index	Liquid limit	linear shrinkage
LSM1	Dura-Pozz fly ash	0%	0%	0%	NP	-	0
LSM2	Dura-Pozz fly ash	1%	1%	0%	NP	-	0
LSM3	Dura-Pozz fly ash	3%	1%	0%	NP	-	0
LSM4	Dura-Pozz fly ash	6%	1%	0%	NP	-	0
LSM5	Dura-Pozz fly ash	10%	1%	0%	NP	-	0
LSM6	Dura-Pozz fly ash	1%	3%	0%	NP	-	0
LSM7	Dura-Pozz fly ash	3%	3%	0%	NP	-	0
LSM8	Dura-Pozz fly ash	6%	3%	0%	NP	-	0
LSM9	Dura-Pozz fly ash	10%	3%	0%	NP	-	0
LS1	Dura-Pozz fly ash	3%	3%	1%	11	19	0
LS2	Dura-Pozz fly ash	3%	3%	2%	12	21	0
LS3	Dura-Pozz fly ash (After 4 days Leaching)	3%	3%	2%	NP	-	0

NP = non plastic, - = not determined

An addition of lime and gypsum does not seem to have any impact on the plasticity index of non-plastic Dura-Pozz fly ash as seen in LSM 1 to LSM 9 (Table 4-2). The liquid limit of the non-plastic specimens could not be determined as described in section 3.3 of (TMH1-A2, 1986). There was no linear shrinkage observed in any specimens.

Lignosulphonate is a by-product of the papermaking industry and has been used successfully to add plasticity to concrete (Reknes, 2004). Lignosulphonate was introduced in this section of the study to see the effect it has on the plasticity index of fly ash. LSM 7 which contains 3% lime and 3 % gypsum (wt %) was concluded to be the optimum mixture ratio in terms combined UCS and ITS performance, from section 4.2.2. The admixture percentages for LSM 7 were then duplicated and 1 % and 2 % (wt %) of lignosulphonate was added to this admixture which then produced samples LS 1 and LS 2 respectively. Normal household sugar (1% (wt%)) was added these mixtures to lessen the viscosity of the lignosulphonate. The Atterberg

limits of these new specimens were determined using the same procedure used for the rest of the other specimens.

LS 1 and LS 2 had a plasticity index (PI) of 11 and 12 respectively. These values of PI are above the limit set by the minimum requirements for waste disposal by landfill (DWAF, 1998b) which states that the plasticity index (PI) of a liner material should be 10 or above but not be so high that excessive desiccation cracks are encouraged. The addition of lignosulphonate was therefore restricted to only 2 wt% on specimen LS 2. The liquid limit was determined and appeared to increase with an increase in lignosulphonate percentage. Even though plasticity was imparted on Dura-Pozz fly ash the material still did not show any linear shrinkage. It is possible that cementitious compounds in fly ash bind particles tight together even when plasticity is induced and hence no linear expansion or contraction was observed (Figure 4-4). This property of zero linear expansion is an attractive feature for a liner material as no cracking would be expected to occur upon drying and wetting cycles. Cokca and Yilmaz, (2003) suggested that bentonite is not a consistent liner material due to the development of shrinkage cracks upon drying.



Figure 4-4 Specimens in troughs after oven drying. Specimen 1 in the picture is LSM 7, 2 is LS 2, 3 is clay which has undergone ductile deformation upon drying and 4 is soil-clay mixture that has contracted lineally. This can be seen by the departure from the trough walls (red arrow). 3 and 4 were included for demonstration purposes only.

An addition of lignosulphonate successfully increased the plasticity of Dura-pozz fly ash, but upon leaching specimens LS 2 for 4 days using the apparatus of a constant head test, the material reverted back to non-plastic, LS 3 in Table 4-2. This was

evident from the leachate collected in the sample bottle as a dark colour emerged Figure 4-5. Even though lignosulphonate induced plasticity it was not retained with leaching and was therefore not considered a suitable component of a fly ash liner material.



Figure 4-5 Specimen LS2 being leached under a constant head test, dark colour of lignosulphonate dominant in the leachate.

4.3 Hydraulic conductivity

Hydraulic conductivities of specimens were determined using a constant head test as described in section 3.8. Hydraulic conductivity was determined daily using equation 3.10 and the test was carried out for seven days. The calculations for hydraulic conductivities of each specimen are presented in Appendix A-2 and are graphically displayed here in Figure 4-6 and Figure 4-7. The changes in hydraulic conductivity with time for specimens containing 1% gypsum are displayed in Figure 4-6 together with the specimen containing only Dura-Pozz fly ash (LSM 1).

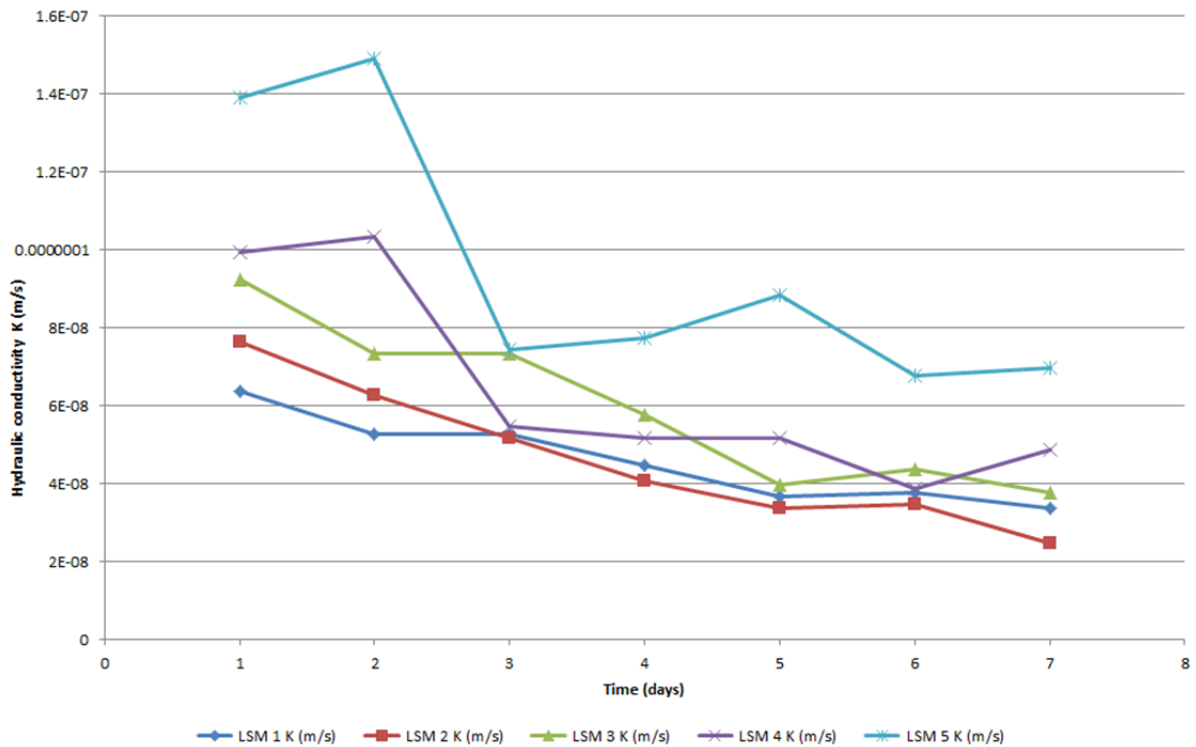


Figure 4-6 Hydraulic conductivity (m/s) values plotted over the seven day period for samples LSM 1 – LSM 5

There is a general decreasing trend in hydraulic conductivity with time for all specimens. This decreasing trend was also observed by Sivapullaiah and Baig, (2011) on fly ash admixtures with varying percentages of lime and gypsum. They attributed this to the formation of a cementitious hydrated calcium silicate gel or calcium aluminate gel which binds particles together, improving the strength and reducing the pore spaces. Low hydraulic conductivity values were therefore observed with time. LSM 5 (10% lime + 1% gypsum) has the highest value of hydraulic conductivity of all the specimens after 7 days. Lime in LSM 5 was observed unreacted in crushed specimens from the ITS test (Figure 4-2). Lime being a soluble compound if unreacted can easily be removed by demineralized water leaving behind pore spaces. If not filled, these void spaces can possibly add more to the total porosity of the specimen, increasing the permeability. This further shows that elevated levels of calcium do not improve the properties of a fly ash as a liner material.

The changes in hydraulic conductivity with time for specimens containing 3% gypsum are displayed in Figure 4-7. These specimens also have a reducing trend in hydraulic conductivity with time. LSM 7 had to lowest value (8.95×10^{-9} m/s) of

hydraulic conductivity after 7 days. The other specimens also have relatively low values of hydraulic conductivity after 7 days with 1.89×10^{-8} m/s, 9.94×10^{-9} and 1.29×10^{-8} for specimens LSM 6, LSM 8 and LSM 9 respectively.

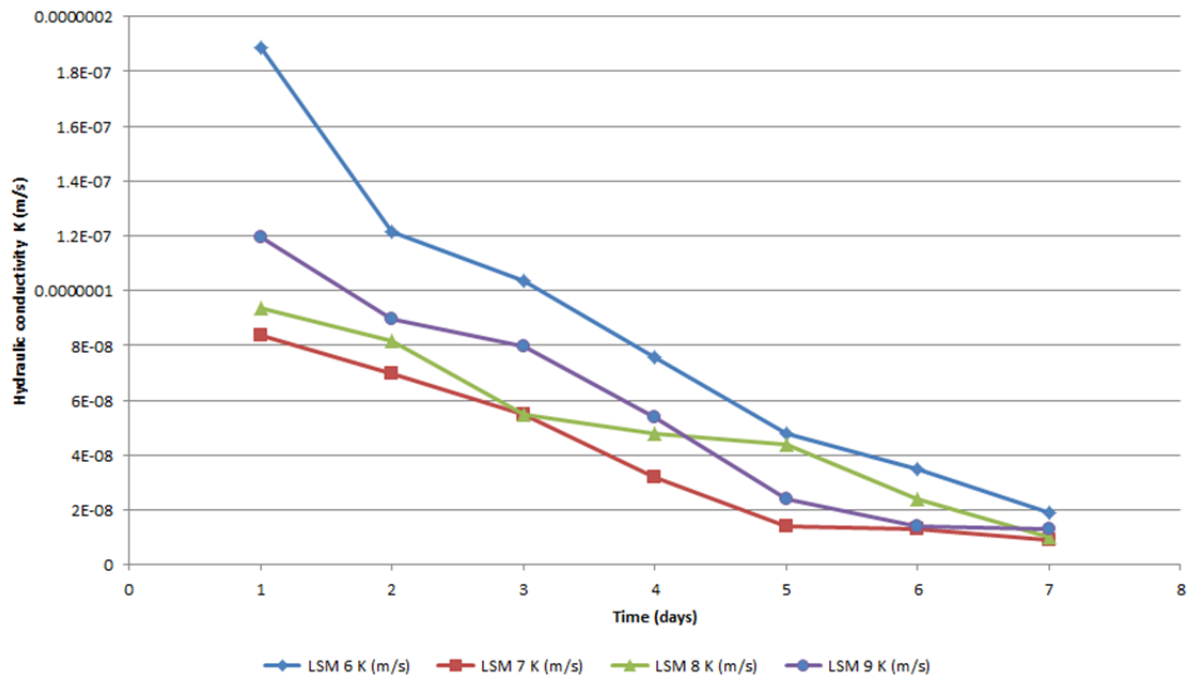


Figure 4-7 Hydraulic conductivity (m/s) values plotted over the seven day period for samples LSM 6 – LSM 9 all with 3% gypsum

The average hydraulic conductivity after 7 days of specimens containing 1% gypsum (LSM 2 to LSM 5) was 4.52×10^{-8} m/s and that of specimens containing 3% gypsum (LSM 6 to LSM 9) was 1.27×10^{-8} m/s. This shows that gypsum plays a more profound role in reducing hydraulic conductivity as samples with 3% gypsum have on average lower hydraulic conductivity values after 7 days than those with only 1% gypsum. An addition of lime in the range 1% to 10% with 1% gypsum had little effect on the hydraulic conductivity as observed in Figure 4-6. LSM 1 (Dura-Pozz fly ash with no additives) had the second lowest hydraulic conductivity after 7 days. The addition of more lime proved to have the opposite effect as hydraulic conductivity of LSM 5 was higher than any other specimen. LSM 7 which contains 3% gypsum and 3% lime additive mixture represents the most optimal composition for low hydraulic conductivity specimen as compared with the other admixtures.

4.3.1 Effects of leaching with brine water on hydraulic conductivity

The minimum requirements for waste disposal by landfill (DWAF, 1998b) in section 8.4.3 suggests that the hydraulic conductivity of a liner material should be tested with

a solution that is representative of the leachate that the liner will be exposed to in its application settings. Brine water was used to represent the leachate from ash dumps. This brine water was sampled out of the rejected water stream from the reverse osmosis plant in the power station and is therefore enriched with toxic salts. The chemical composition of brine water was determined by an accredited laboratory and the results are included in appendix A-3. From section 4.3, LSM 7 composition (Dura-Pozz fly ash with 3% lime / 3% gypsum) was considered the most optimum composition for a low hydraulic material and it was selected to test if brine water can influence the hydraulic conductivity with time. The hydraulic conductivity was determined using a constant head test as described in section 3.8, using both brine water and deionized water for 60 days without disruptions. The calculations of hydraulic conductivity with time are included as appendix A-4 and are presented graphically below in Figure 4-8.

The values of hydraulic conductivity on day 1 were extremely high as compared to the other time points. These values were unable to be captured together with the other data points in the same size grid without losing grid quality, as seen in the illustration in Figure 4-8. These data points were therefore excluded from the graph but a table of all the data points is included in Figure 4-8.

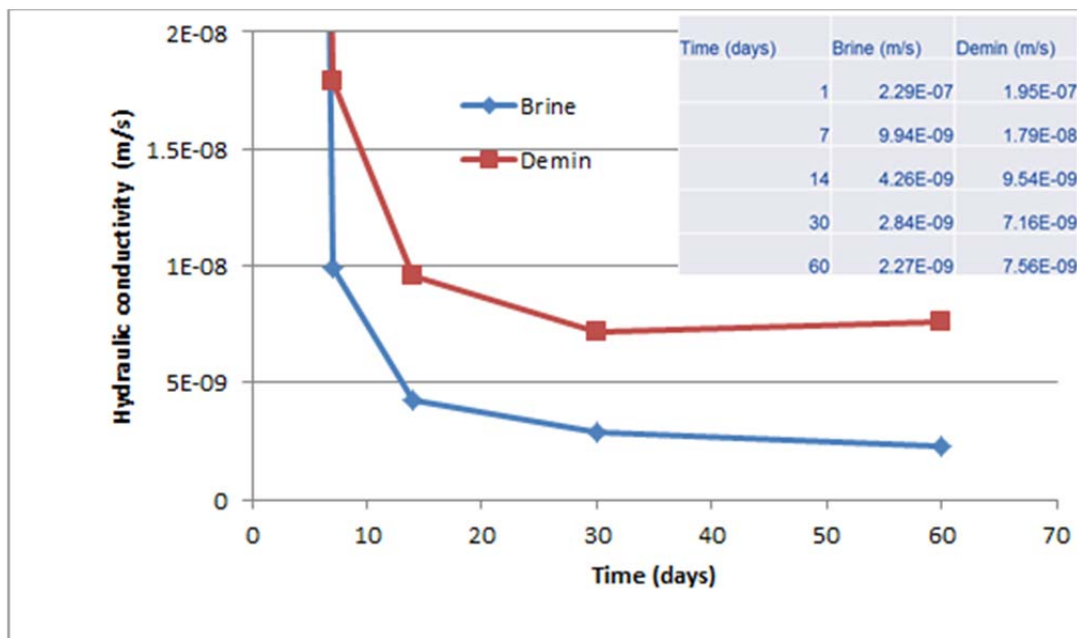


Figure 4-8 Brine water and demineralized water used to outline the changes in hydraulic conductivity with time on specimen LSM 7. A table of the data points is included in the right corner of the graph.

There was a decreasing trend in hydraulic conductivity for both brine and demineralized water solutions. The brine water had an even lower hydraulic conductivity with a value of 2.27×10^{-9} m/s after 60 days. Even though demineralized water had an overall decreasing effect on the hydraulic conductivity with time the hydraulic conductivity value on day 60 (7.56×10^{-9} m/s) is slightly higher than on day 30 (7.71×10^{-9} m/s). Brine water is effluent water rich in salts, specimen LSM 7 has a much more lower hydraulic conductivity with time when leached with brine water. This could be due to brine/fly ash interactions leading to formation of secondary minerals that would block the pore voids thereby reducing the volume of flow paths. Sivapullaiah and Baig, (2011) found secondary mineral ettringite in fly ash stabilised with lime and gypsum. If the pore spaces are clogged up with secondary minerals less water can flow through them and hence a reduction in hydraulic conductivity will be observed. Leaching with demineralised water would have less of this effect because demineralised water contains no minerals by definition, and hence the only secondary mineral phases that could develop would be from interactions between fly ash and the additives added. The hydraulic conductivity value obtained after 60 days with the brine leaching (2.27×10^{-9} m/s) is lower than the value prescribed of a H\h liner material (3×10^{-9} m/s) by the minimum requirements for waste disposal by landfill (DWAF, 1998b).

4.3.2 Wet/dry cycles

The wet/dry cycles were performed on three LSM 7 specimens to determine the effect on hydraulic conductivity using the procedure described in section 3.8.3. Hydraulic conductivity was determined after the specimens were subjected to 7 days of constant head testing and those values of K were used as background to check the performance of the specimen with regards to hydraulic conductivity after every cycle of drying and wetting. Five cycles were carried out in each of the three specimens and a ratio of the newly determined hydraulic conductivity (K_n) value to that of background K_0 values were determined. The results are summarized in Table 4-3 below.

Table 4-3 Ratios of hydraulic conductivity after each wet/dry cycle to background K

Number of Cycles (n)	K_n/K_0	K_n/K_0	K_n/K_0
1	2.4	2.6	1.4
2	2.9	2.3	1.5
3	1.1	1.8	1.3
4	1.0	1.3	1.1
5	0.9	0.9	1.0

The ratios that were more than 1 indicate wet/dry cycles where the hydraulic conductivity was higher than the background K_0 value whereas the ratios that were less than 1 indicate wet/dry cycles where the hydraulic conductivity was less than the background K_0 value. There was an increasing trend in hydraulic conductivity during the initial cycles followed by a decreasing trend in hydraulic conductivity towards the latter cycles. The highest ratio was 2.9 meaning the hydraulic conductivity increased to 2.9 times the background K_0 value however in some instances the hydraulic conductivity was less than the background k_0 value. Overall there was only a slight variation in hydraulic conductivity observed in all specimens (less than 3 times the background value). Palmer et al., (2000) also observed slight changes (2 to 3 times the value of background) in hydraulic conductivity during wet/dry cycles and also in freeze/thaw cycles. These small changes in hydraulic conductivity with wet/dry cycles relates to the results obtained from linear shrinkage in section 4.2.3, where zero linear shrinkage was observed in all fly ash admixture specimens after drying in the oven. The cementitious characteristic of fly ash possibly minimised cracking that is usually caused by drying and hence little change in hydraulic conductivity was observed (Palmer et al., 2000). No visible cracks were observed on the surface of the specimens.

4.4 Leachate analysis

Leachate collected from the constant head test was subjected to chemical analyses using Inductively Coupled Plasma Mass Spectrometry (ICP-MS). Samples which had their leachate analysed were LSM 1, LSM 10 and LSM 7. The full chemical analysis data is included in Appendix A-5. The leaching behaviour of selected elements is graphically presented in Figure 4-9, Figure 4-10 and Figure 4-11, and shows

leachate concentrations with time from specimens LSM10, LSM 1 and LSM 7 respectively.

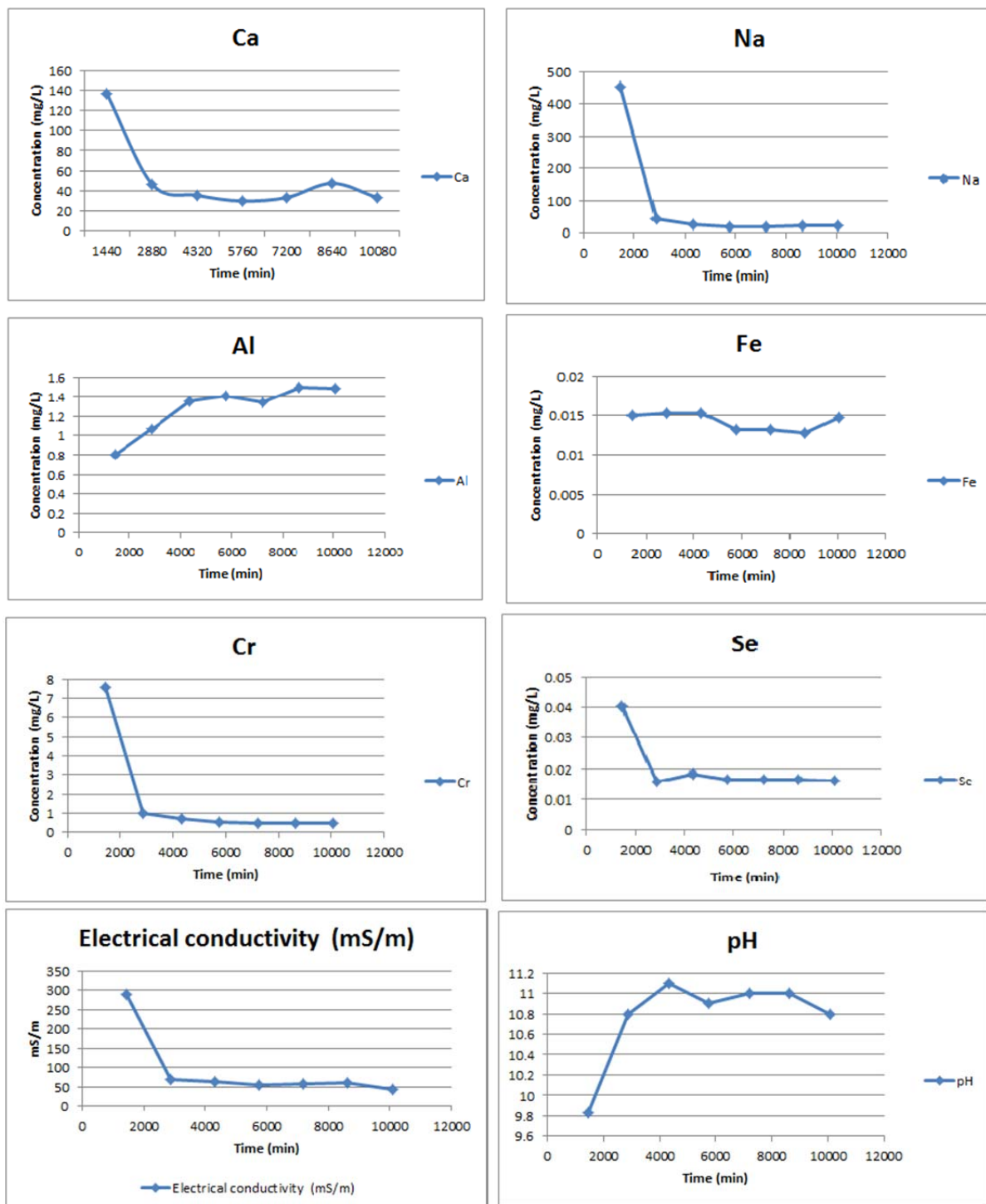


Figure 4-9 Parametric measurements for LSM 10 (Tutuka fly ash) with time

The leaching behaviour of calcium from LSM 10 (Tutuka fly ash) with time shows a sudden decrease from a moderate concentration to a fairly low constant concentration, Figure 4-9. These low levels of calcium observed in the leachate

relates to the low levels of calcium detected in a sample of Tutuka fly ash analysed by XRF, section 4.5.2. Izquierdo and Querol, (2011) suggests that calcium is the most readily released cation and even though calcium is not an element of environmental concern it influences the pH of ash-water systems. A lot of trace elements exhibit pH-dependent solubility and calcium, and therefore plays a pivotal role in the environmental quality of ash. Toxic trace elements that are released depend on the pH and consequently indirectly on the amount of calcium (Izquierdo and Querol, 2011).

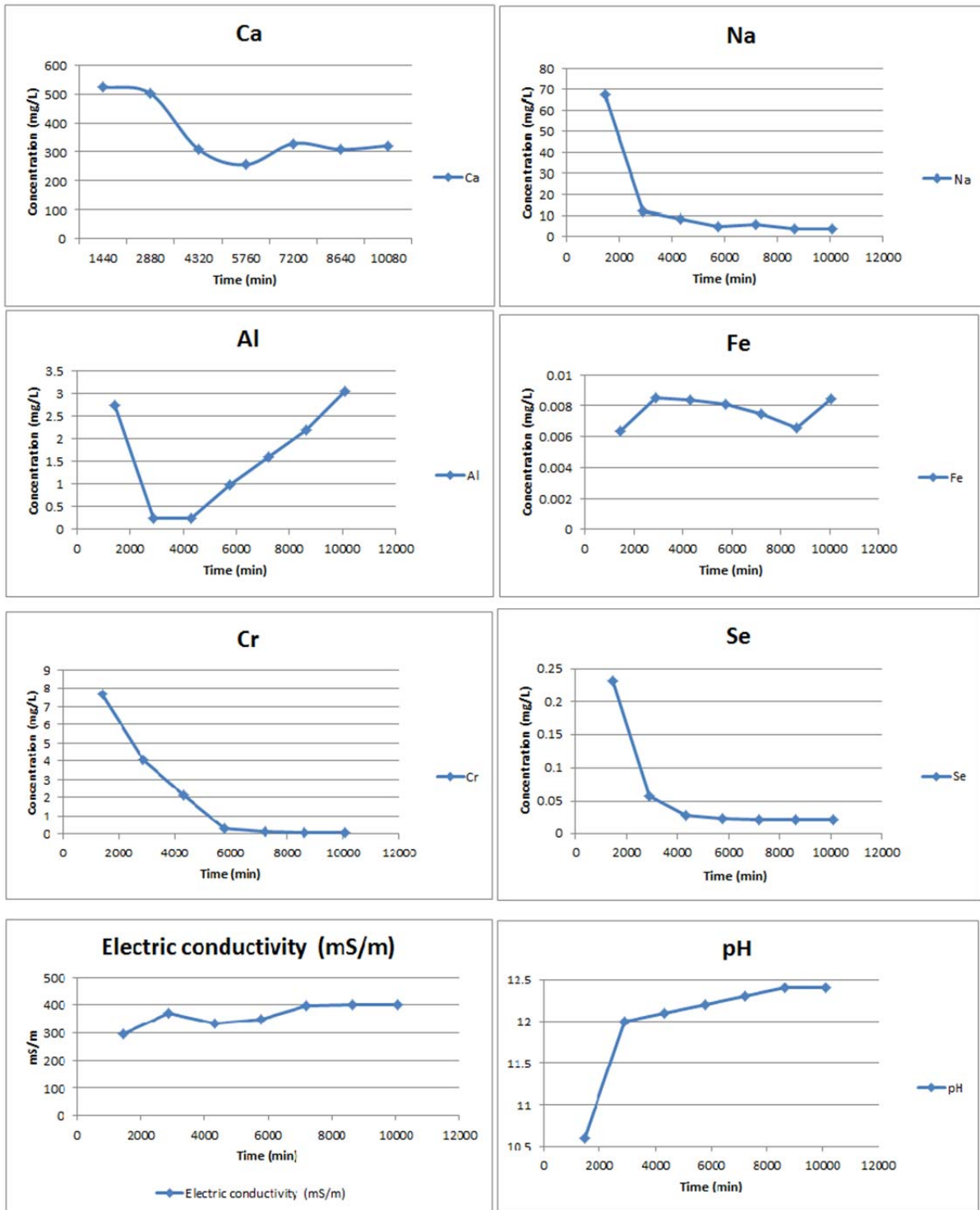


Figure 4-10 Parametric measurements for LSM 1 (Dura-Pozz fly ash) with time

The same declining trend in calcium concentration can also be seen in LSM 1 (Dura-Pozz fly ash) with moderate levels of less than 600 mg/L. The calcium levels are relatively high in LSM 7 (fly ash with additives 3%lime / 3%gypsum). Both lime and gypsum contain calcium and since calcium is highly soluble in water elevated levels

can be observed in the leachate. This indicates that not all the calcium added reacted to form cementitious compounds with the ash but some was left as free lime.

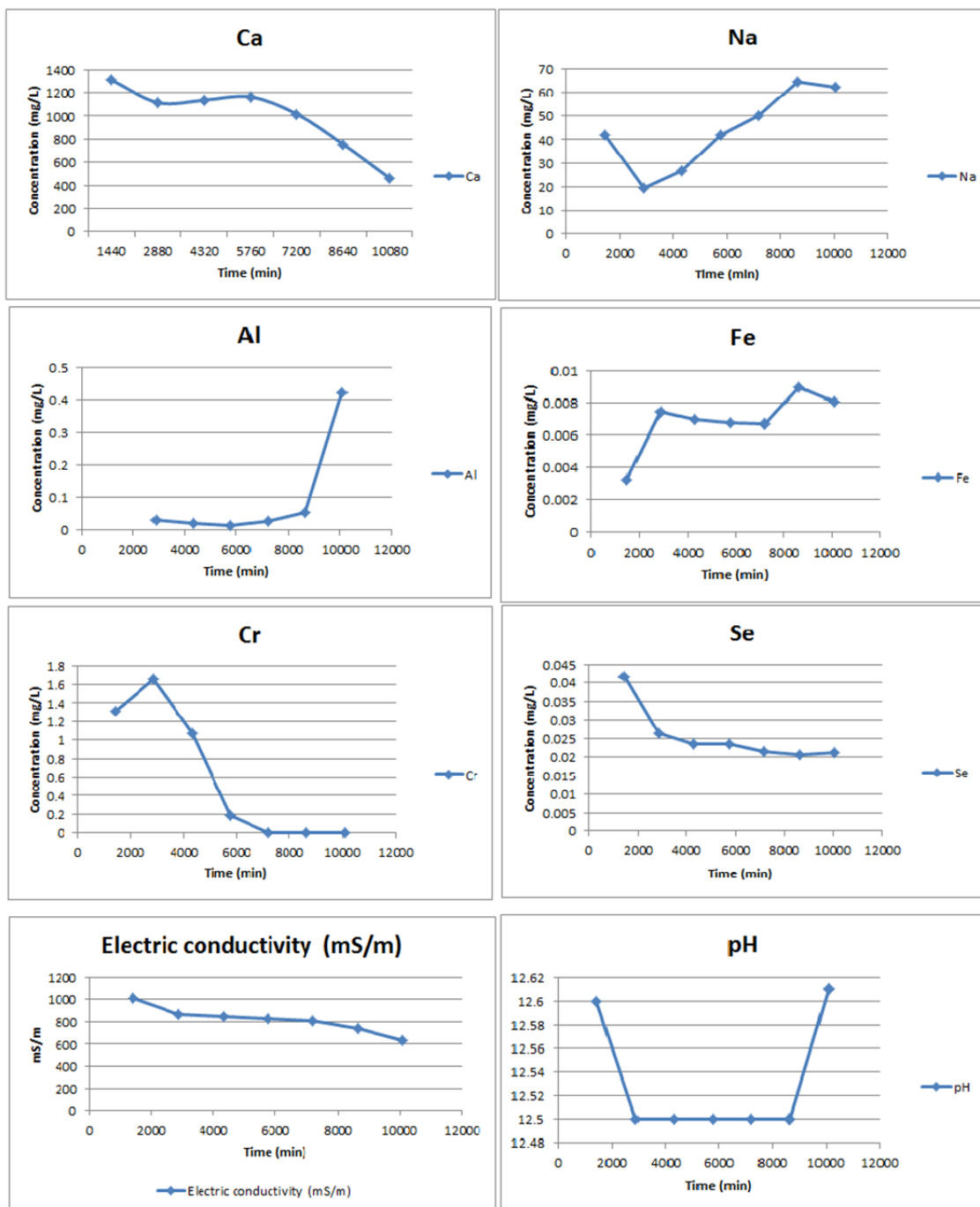


Figure 4-11 Parametric measurements for specimen LSM 7 with time

With high amounts of calcium, LSM 7 also has a higher pH (≥ 12.5) than both LSM 1 and LSM 10. The pH of LSM 10 begins at 9.83 and that of LSM 1 at 10.6 but they both show an increasing trend as more alkaline leachate develops in the later stages

of leaching. This is possibly due to the flushing out of more acidic elements like sulphates in the specimens, Appendix A-5.

During leaching sodium appears to have an abrupt decrease in concentration at the beginning followed by a period of constant concentration with subsequent leaching. This behaviour is similar to that observed for calcium and seems to be pH dependent. The graphs of pH and sodium display similar trends but the opposite effect is observed, as a decline in sodium concentration is coupled with an increase in pH especially for LSM 1 and LSM 10. There is a general increasing trend in aluminium concentration with subsequent leaching in all the specimens but this increasing trend is of a small magnitude as the highest aluminium concentration observed is 2.74 mg/L in LSM 1. This is strange given the high levels of aluminium recorded with the XRF analysis, section 4.5.2. Izquierdo and Querol, (2011) suggested that even though aluminium is normally enriched in fly ash, it is poorly leached due to the slow dissolution rates of the glassy matrix and the crystalline aluminosilicate phases. Iron is also present in low levels throughout leaching with average concentrations as low as 0.007 mg/L, 0.007 mg/L, and 0.014 mg/L for specimens LSM 1, LSM 7 and LSM 10 respectively.

It is usually not the major elements that are of environmental concern with regard to groundwater contamination since most of them are poorly leached and fall within regulatory thresholds. Some trace elements are however of environmental concern as they are leached from fly ash in concentrations above regulatory thresholds (Izquierdo and Querol, 2011). Chromium has a declining trend in all the specimens with subsequent leaching but the levels observed at early stages are more than the set thresholds by environmental protection agencies. These concentration levels are still relatively low when compared to other elements like calcium but since hexavalent chromium is known to be a carcinogen these levels are of a health and environmental concern. In South Africa the leachable concentration threshold limit for total chromium is set at 1.0 mg/L (Affairs, 2011). The total chromium levels are way over this threshold in the early stages of leaching with chromium concentrations as high as 7.56 mg/L and 7.65 mg/L for LSM 10 (Tutuka fly ash) and LSM 1 (Dura-Pozz fly ash) leachates respectively. An addition of lime and gypsum appears to have stabilised the fly ash with respect to its leachability of chromium as the highest

concentration observed is 1.65 mg/L. This value is however still slightly above the threshold value of 1.0 mg/L.

Selenium as a trace element has low concentrations but just like chromium it is considered an environmental hazard and its concentrations are therefore of great concern. The leachable concentration threshold limit for selenium is set at 0.01 mg/L in South Africa (Affairs, 2011). Selenium concentration is particularly high in Dura-Pozz fly ash (0.23 mg/l) in early leachate when compared to Tutuka fly ash (0.04 mg/L). This could be due to the coal make-up since selenium is a strongly enriched element in coal (Izquierdo and Querol, 2011). The addition of lime and gypsum appear to have restricted the mobility of selenium in the fly ash as observed in LSM 7 that has lower concentrations of selenium in the initial phases of leaching when compared to LSM 1.

The electrical conductivity has a declining trend in all specimens with Tutuka fly ash leachate having the lowest values throughout. Even though Tutuka fly ash is conditioned with effluent water during processing and also at the landfill for dust suppression the electrical conductivity remains low in all leachate samples. The electrical conductivity for Dura-Pozz fly ash remains high even in LSM 7. It seems like the addition of lime and gypsum elevated the electrical conductivity with values as high as 1013 mS/ m observed at the initial stages of LSM 7 leachate. This could be that calcium and sulphate ions from lime and gypsum have not fully reacted with the fly ash and remain in solution thereby increasing the electrical conductivity.

4.5 Physical, chemical and mineralogical compositions

Particle size distribution information on Dura-Pozz fly ash was provided by the supplier, Ash Resources (Pty) Ltd. The cumulative graph of Dura-Pozz fly ash particle size with volume percentage is included in Appendix A-6. The graph shows over 85% of Dura-Pozz fly ash falls below 45 µm. Muriithi, (2009) made particle size fractions determinations on Tutuka fly ash and observed that it has a coarser fraction distribution with 54.84% falling below 75 µm. These observations are consistent with the outcomes by Kruger, (2003) who reported that the amount of fly ash retained on a 45 µm is usually less than 10% but for finer fly ash such as Dura-Pozz fly ash is much higher. Kruger, (2003) also found the surface area to be in the range of 3500

to $4000 \text{ cm}^2\text{g}^{-1}$ for South African fly ash marketed as cement extender such as Dura-Pozz fly ash. This large surface area renders fly ash as a good absorbent that can be utilised in processes like flue-gas desulphurization and production of zeolites (Ahmaruzzaman, 2009).

4.5.1 Morphology analysis by Scanning Electron Microscope (SEM)

Scanning electron microscope (SEM) analyses were carried out on samples taken from the compacted specimen from the constant head test permeameters after 7 days of leaching as discussed in section 3.8. The procedure that was followed for SEM analysis was described in section 3.5.3. Energy dispersive spectroscopy (EDS) analyses were also conducted on specific spots on the samples in the SEM. Scanning electron micrograms depicting the morphology of samples LSM 1, LSM 7, and LSM 10 are shown in Figure 4-12 with the corresponding EDS spot analysis.

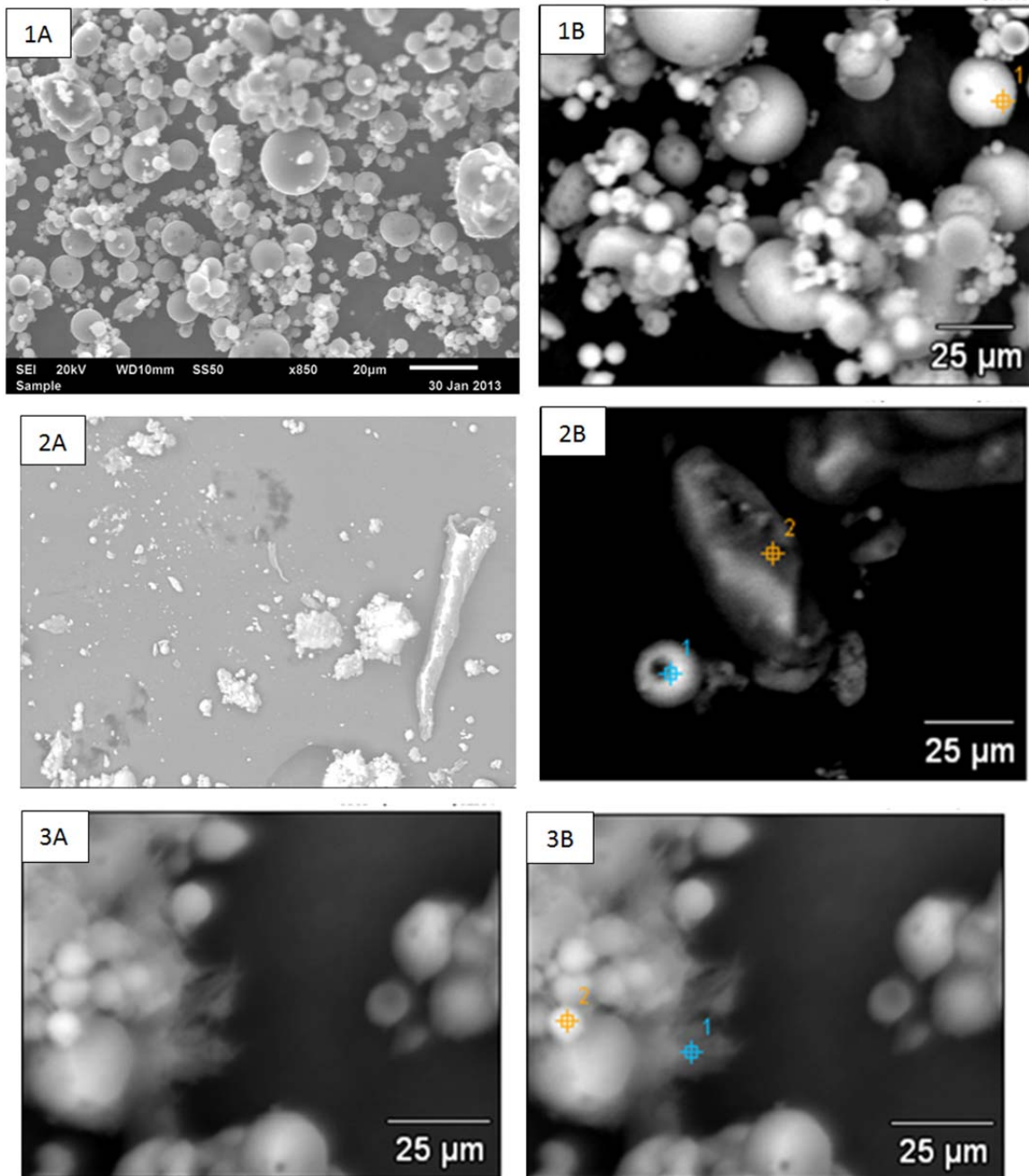


Figure 4-12 SEM-EDS micrograph of Dura-Pozz fly ash (1A & 1B) and Tutuka fly ash (2A & 2B) and sample LSM 7 (3A & 3B)

SEM images of LSM 1 as shown in Figure 4-12(1A-B) show predominantly spherical particles. The size of the particles fluctuates but is generally less than 50 µm. This size distribution agrees with the particle size distribution graph of Dura-Pozz fly ash presented in Appendix A-1 where more than 85 % of particles were below 45 µm. Bin-Shafique et al., (2003) suggested that since fly ash particles are solidified while in suspension with the flue gas their shape is generally spherical and are extremely small in size. There is clustering and rod like particles are observed in Figure 4-12

2A and Figure 4-12 2B. Clustering of fly ash particles is a possible indicator of high temperature sintering reactions (Saikia et al., 2006). A lot of fibrous material is observed in Figure 4-12 3A and Figure 4-12 3B. Since fly ash particles are generally spherical this fibrous substance is possibly a secondary phase.

SEM-EDS spot analyses are presented in Table 4-4. The SEM-EDS spot analysis of a spherical particle shown in Figure 4-12 1B indicate a phase with major compounds Al_2O_3 and SiO_2 , Table 4-4, therefore this phase could possibly be an aluminosilicate like mullite. The SEM-EDS spot analysis of spots 1 and 2 in Figure 4-12 2B also show a phase with major compounds Al_2O_3 and SiO_2 which could also possibly be mullite, but spot 2 is likely to be quartz due to the exceedingly high SiO_2 percentage. The SEM-EDS spot analysis of spots 1 in Figure 4-12 3B emanates from a fibrous material which shows high levels of compounds CaO , Al_2O_3 , SiO_2 and SO_3 . This phase can possibly be ettringite, which is a hydrous calcium aluminium sulphate mineral that is generally associated with addition of lime and gypsum to fly ash or concrete and also has a fibrous morphology. The SEM-EDS spot analysis of spots 2 in Figure 4-12 3B show a phase which has high levels of compounds CaO , Al_2O_3 and SiO_2 . Since LSM 7 has lime added to fly ash, it is possibly a Ca-aluminosilicate which is one of the two cementitious gels associated with the hydration reaction of pozzolans with lime.

Table 4-4 SEM-EDS spot analysis of LSM 1, LSM 7 and LSM 10 in compound %

	MgO	Al_2O_3	SiO_2	SO_3	K_2O	CaO	TiO_2	Fe_2O_3	Na_2O	F	P_2O_5	MoO_3
LSM 1 (1B) point 1	0.41	34.88	46.28	0.45	1.64	3.93	6.25	6.15	-	-	-	-
LSM 10 (2B) point 1	0.71	38.69	53.42	-	0.85	2.59	0.56	1.62	1.57	-	-	-
LSM 10 (2B) point 2	0.56	10.33	82.88	-	0.74	2.20	0.36	1.35	1.59	-	-	-
LSM 7 (3B) point 1	0.42	19.40	26.65	4.61	0.77	40.66	1.02	2.40	-	4.07	-	-
LSM 7 (3B) point 2	0.36	14.35	18.13	-	0.42	41.52	1.41	1.67	0.17	-	20.18	1.80

4.5.2 Chemical composition by X-ray Fluorescence (XRF)

The elemental composition of LSM 1 (Dura-Pozz fly ash) and LSM 10 (Tutuka fly ash) was carried out as described in section 3.5.2. The results of major elements are presented in Table 4-5.

Table 4-5 XRF analysis results for major elements in %(wt/wt)

Elements	Dura-Pozz Fly ash	Tutuka Fly ash
SiO ₂	54.11%	54.85%
TiO ₂	1.66%	1.36%
Al ₂ O ₃	32.20%	24.20%
Fe ₂ O ₃	3.33%	5.33%
MgO	1.11%	1.54%
CaO	4.68%	4.79%
Na ₂ O	0.21%	0.70%
K ₂ O	0.76%	0.80%
P ₂ O ₅	0.48%	0.12%
SO ₃	0.36%	0.38%
MnO (Cal)	0.01%	0.02%
LOI (%)	0.64%	5.58%
Total %	99.55%	99.66%

The results of the major elements presented in Table 4-5 show that both Tutuka fly ash and Dura-Pozz fly ash have SiO₂, Al₂O₃, CaO and Fe₂O₃ as their major elements. The sum of the percentage composition of SiO₂, Al₂O₃ and Fe₂O₃ is more than 70% and according to the classification prescribed by the American Society for Testing and Materials (ASTM-C618, 1993) classify both fly ashes as class F fly ash. The CaO percentage is less than 10% for both fly ashes which is also a rating benchmark for class F fly ash (ASTM-C618, 1993). There is a higher LOI (loss on ignition) value for Tutuka fly ash (5.58%) than Dura-Pozz fly ash (0.64%) and this may be due to variations in boiler performance in the different power stations.

The results of trace elements for both Tutuka fly ash and Dura-pozz fly ash are presented in Table 4-6. Cr, Sr, Zr, Ba and V appear to be the most abundant trace elements in both fly ashes. Cr and Ba have the highest concentrations of all the other trace elements. Cr levels were observed to be higher than the regulatory threshold in leachate collected from constant head tests of specimens of Tutuka fly ash and Dura-pozz fly ash, section 4.4. Izquierdo and Querol, (2011) suggest that while the alkalinity of fly ash reduces the release of some elements of environmental concern such as Co, Cu, Hg, Ni, Pb, Sn and Zn it also promotes the release of oxyanionic elements like As, B, Cr, Mo, Sb, Se, V and W. The leachate results of LSM 1, LSM 7, and LSM 10 presented in appendix A-5 show levels above the regulatory threshold for Mo, Cr, Se and Ba.

Table 4-6 XRF results for trace elements (in part per million)

Element	Tutuka (ppm)	FA	Dura-Pozz FA (ppm)
Sc	ND	0	
V	128	143	
Cr	722	755	
Co	8	7	
Ni	26	25	
Cu	12	13	
Zn	12	15	
As	ND	7	
Br	5	5	
Rb	3	1	
Sr	312	235	
Y	30	30	
Zr	382	442	
Nb	ND	7	
Mo	ND	ND	
Cd	ND	ND	
Sn	64	64	
Sb	ND	ND	
Ba	823	972	
Tl	0	2	
Pb	66	68	
Th	28	28	
U	2	3	

ND – Not determined

4.5.3 Mineralogical composition by X-ray Diffraction (XRD)

Mineralogical analyses were carried out on samples taken from the compacted specimens of the constant head test permeameters after 7 days of leaching as discussed in section 3.8. Samples LSM 1 to LSM 10 were analysed using XRD using the procedure described in section 3.5.1. The diffractograms of LSM 1 and LSM 7 are presented in Figure 4-13 and Figure 4-14 respectively. The bump seen in both figures is representative of the presence of a glass phase (Ward and French, 2006).

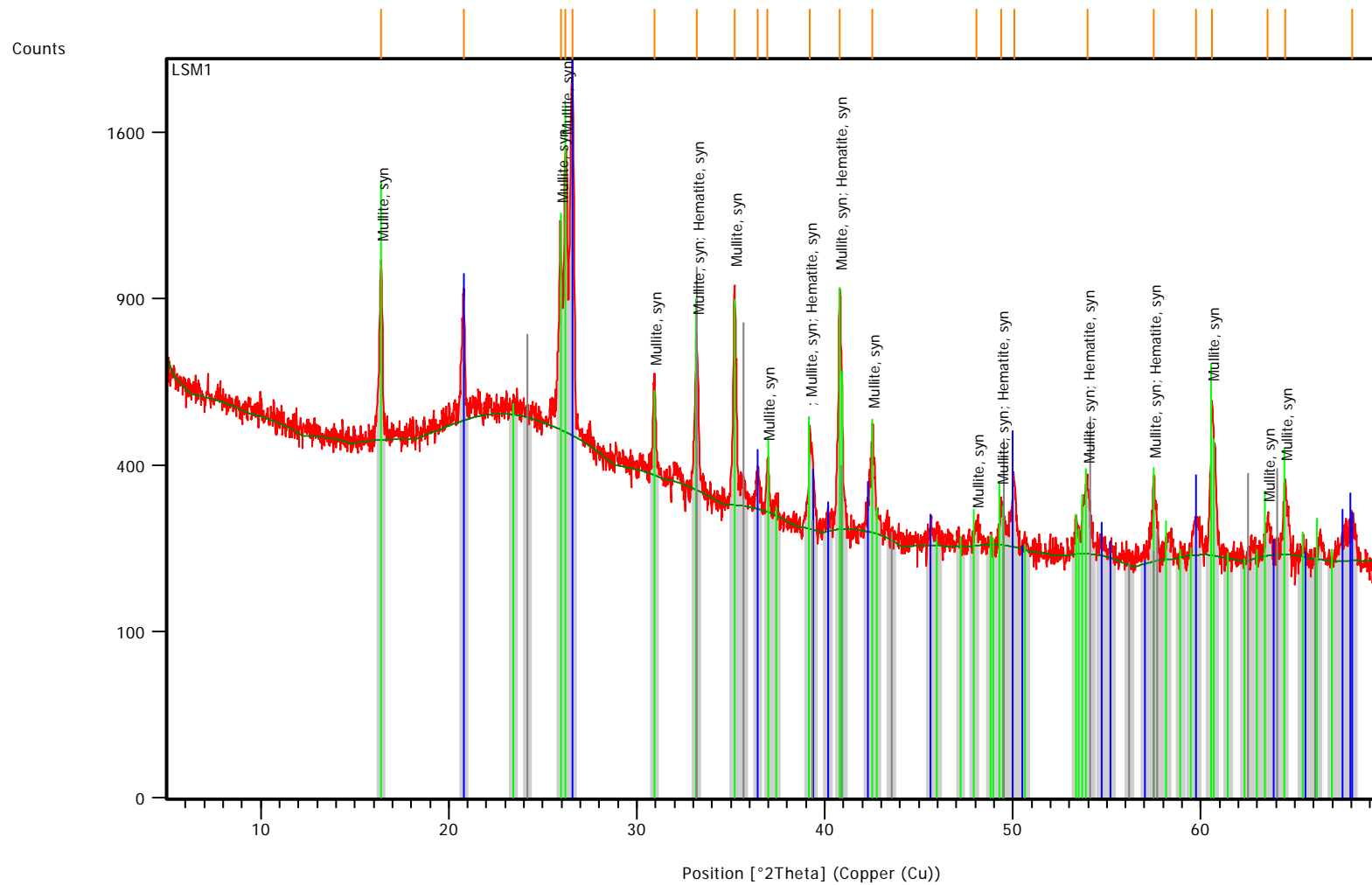


Figure 4-13 Diffractogram of sample LSM 1 showing mineral formations

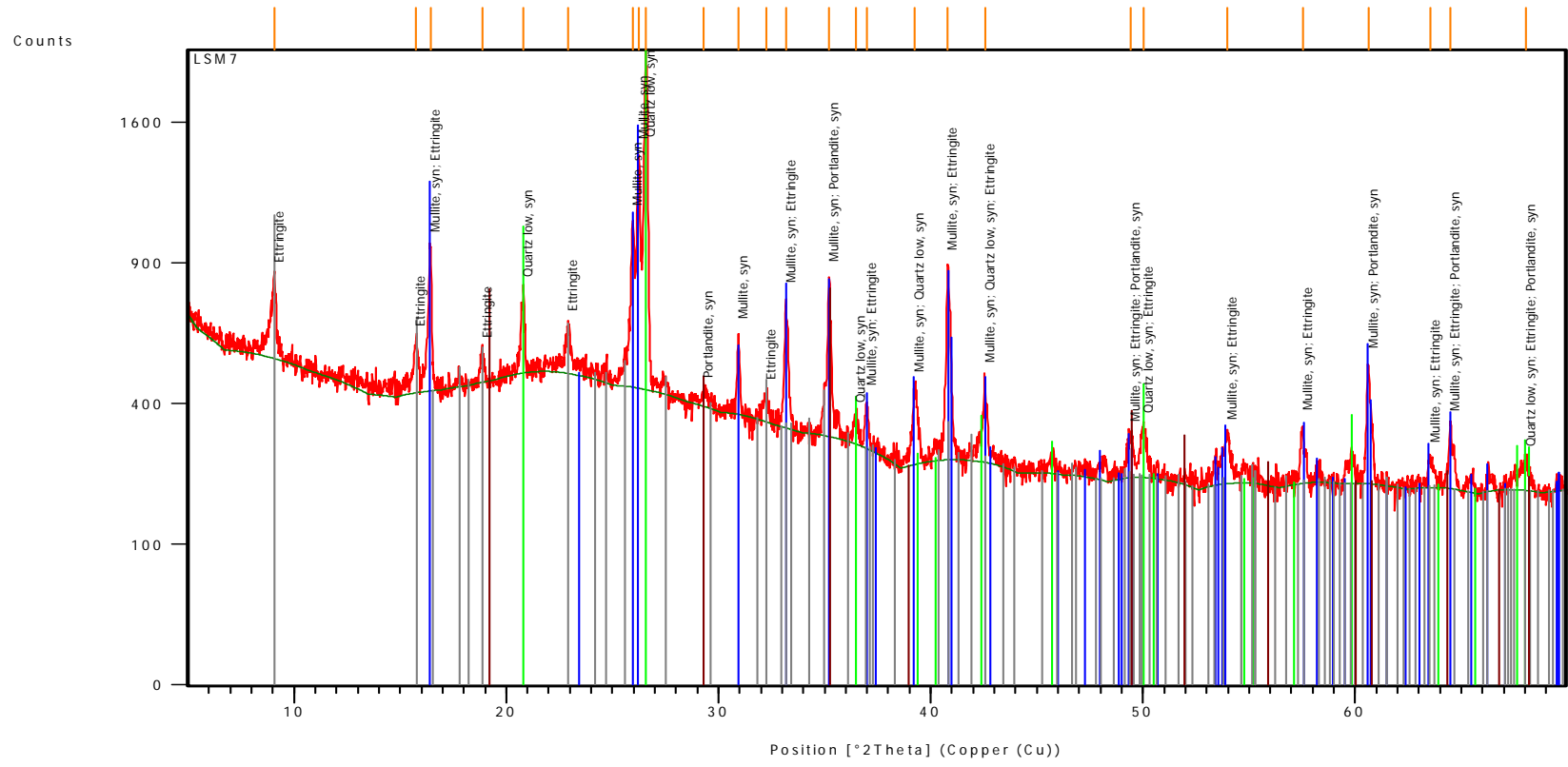


Figure 4-14 Diffractogram of sample LSM 7 showing mineral formations

The results of the phases detected by XRD for specimens LSM 1 to LSM 10 are summarized in Table 4-7. The phases that were identified, but had lower peak intensities were labelled as minor minerals.

Table 4-7 Mineralogical analyses results from XRD

Sample name	Fly ash	%Lime	%Gypsum	Major mineral	Minor mineral
LSM1	Dura-Pozz fly ash	0%	0%	Quarts, mullite	Hematite
LSM2	Dura-Pozz fly ash	1%	1%	Quarts, mullite	Hematite
LSM3	Dura-Pozz fly ash	3%	1%	Quarts, mullite	Ettringite
LSM4	Dura-Pozz fly ash	6%	1%	Quarts, mullite	Hematite, Ettringite
LSM5	Dura-Pozz fly ash	10%	1%	Quarts, mullite	Coestite, Portlandite
LSM6	Dura-Pozz fly ash	1%	3%	Quarts, mullite	Hematite, Gypsum
LSM7	Dura-Pozz fly ash	3%	3%	Quarts, mullite	Ettringite, Portlandite
LSM8	Dura-Pozz fly ash	6%	3%	Quarts, mullite	Ettringite, Portlandite, Hematite
LSM9	Dura-Pozz fly ash	10%	3%	Quarts, mullite	Ettringite, Calcite
LSM10	Tutuka Fly ash	0%	0%	Quarts, mullite	Coesite

Dura-Pozz fly ash (LSM 1) and Tutuka fly ash (LSM 10) have similar major phases of quartz and mullite but LSM 1 has hematite as a minor mineral, whereas LSM 10 is coesite Table 4-7. These XRD outcomes validate the XRF results where SiO₂ and Al₂O₃ were found to be major elements for both Dura-Pozz fly ash and Tutuka fly ash. These elements (Al and Si) form a main component of the major minerals detected in XRD. The addition of lime and gypsum in varying amounts appears to have resulted in an array of secondary minerals as seen in specimens LSM 2 to LSM 9. The diffractogram of LSM 7 on Figure 4-14 shows mineral phases ettringite and portlandite which were not identified in LSM 1 (Figure 4-13). These secondary phases are also observed in other Dura-Pozz admixtures as seen in Table 4-7. It appears that ettringite formation is influenced by lime percentage as all samples with lime content of more than 3% added contained ettringite except for LSM 5. Secondary minerals can possibly reduce the size of the pore spaces that water flows through thereby reducing the hydraulic conductivity, section 4.3.

4.5.4 Quantitative analysis by QEMSCAN

Quantitative analyses were carried out using QEMSCAN (Quantitative evaluation of minerals by scanning electron microscopy). Block samples from the compacted specimens taken from the constant head test permeameters after 7 days of leaching (as discussed in section 3.8) were used subjected to QEMSCAN analysis. A sample of Dura-Pozz (LSM 1) was also analysed using QEMSCAN, but the sample could however not be analysed as a block since the material lacked strength and crumbled during cutting, see Figure 3-11. A powdered sample of LSM 1 was then used.

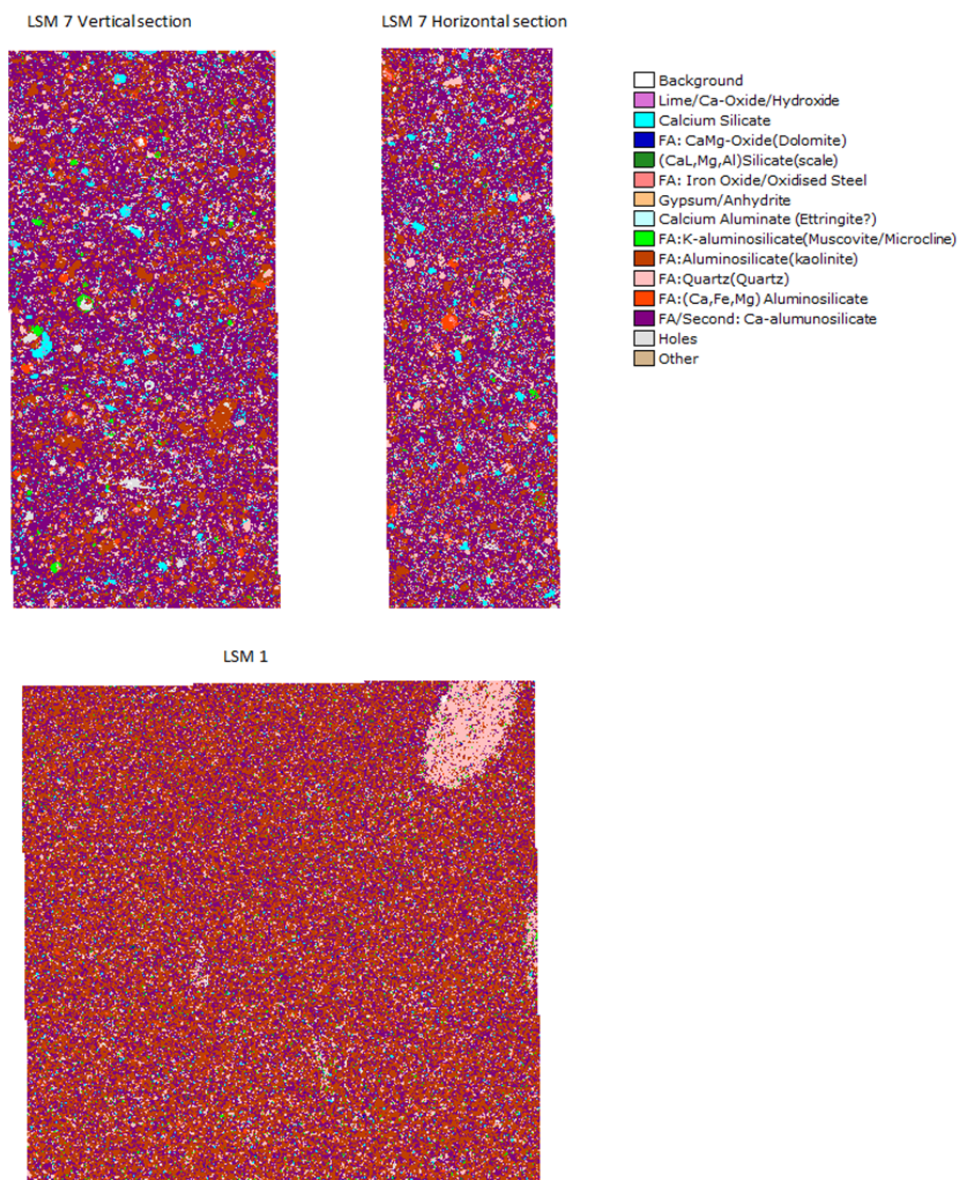


Figure 4-15 QEMSCAN false colour images of vertical and horizontal block samples of LSM 7 (top) and a powdered sample of LSM 1 (bottom)

The Dura-Pozz fly ash (LSM 1) sample was found to be extremely fine as seen in Figure 4-15 and it was characterised by high proportion of aluminosilicate and calcium aluminosilicate see Table 4-8. The addition of lime and gypsum resulted in an increase in, the proportion of calcium silicate, Ca-aluminosilicate and gypsum relative to the LSM 1 mineralogy. This can be seen in both the vertical and horizontal blocks of LSM 7 as shown in Figure 4-15 and Table 4-8. It is possible that these phases are indicative of exceedingly fine lime/gypsum in contact with aluminosilicate and quartz from the fly ash or it could be an amorphous secondary phase which had formed. If it was not amorphous, then XRD results should have detected a calcium silicate and or Ca-aluminosilicate (Table 4-7).

QEMSCAN did not detect any appreciable amounts of ettringite in all the samples analysed. It is possible that ettringite being a secondary mineral is finer than the QEMSCAN beam resolution of 3 microns.

Table 4-8 QEMSCAN results showing qualitative results of mineral phases

Volume-%	Fly Ash	Vertical Section	Horizontal section
Lime/Ca-Oxide/Hydroxide (Portlandite)	0.3	0.6	0.7
Calcium Silicate	1.0	3.2	3.6
FA: CaMg-Oxide(Dolomite)	0.2	0.2	0.2
(CaL,Mg,Al)Silicate(scale)	0.5	0.4	0.3
FA: Iron Oxide/Oxidised Steel	0.3	0.4	0.5
Gypsum/Anhydrite	0.2	1.2	2.1
Calcium Aluminate (Ettringite)	0.00	0.01	0.02
FA:K-aluminosilicate(Muscovite/Microcline)	1.3	0.7	0.9
FA:Aluminosilicate(kaolinite)("mullite")	47.4	24.5	23.4
FA:Quartz(Quartz)	9.8	6.9	7.2
FA:(Ca,Fe,Mg) Aluminosilicate	3.3	2.8	3.7
FA/Second: Ca-alumunosilicate	35.8	58.5	56.9
Other	0.1	0.6	0.5

4.5.5 Texture analysis

Soil texture analysis of Dura-Pozz fly ash (LSM 1) and Tutuka fly ash (LSM 10) were carried out using the procedure described in section 3.7. The results are presented in Table 4-9.

Table 4-9 Soil texture results showing different texture as % wt/wt

Sample	TEXTURE						
	Silt + Clay			Sand			
	Coarse Silt %	Fine Silt %	Clay %	Coarse %	Med %	Fine %	V.Fine %
LSM 1	15.8	40.0	27.5	2.6	2.9	3.3	7.7
LSM 10	10	26	16	7.08	4.36	16.08	19.68

Dura-Pozz fly ash (LSM 1) appears to have much finer fractions of silt and clay than Tutuka fly ash (LSM 10). This fine texture was also seen in QEMSCAN images in section 4.5.4. Particle size distribution also revealed that over 85% of Dura-Pozz fly ash falls below 45 µm, Appendix A-6. The sum of the sand fractions in LSM 10 is 47.2% which is exceedingly high when compared to that of LSM 1 (16.5%). Clay fraction of LSM 1 was higher at 27.5% when compared to the 16% of LSM 10. A substantial amount of Kaolinite, a clay mineral, was found in the LSM 1 and LSM 7 samples analysed with QEMSCAN, Table 4-8. Clay minerals usually have cation exchange abilities that play an important role in environmental applications, such as liners for waste disposal (Nesse, 1999).

4.5.6 Cation exchange capacity

Cation exchange capacity of specimens LSM 1 to LSM 10 was conducted using the procedure described in section 3.6. The test was conducted at a pH of 7 but for specimen LSM 7 the pH was varied to see if CEC is affected by pH. The first stage of CEC determinations involves washing with a 1N ammonium acetate solution and from the leachate the exchangeable cation concentrations were determined and results are summarised in Figure 4-16. The results of the cation exchange capacity are presented in Figure 4-17.

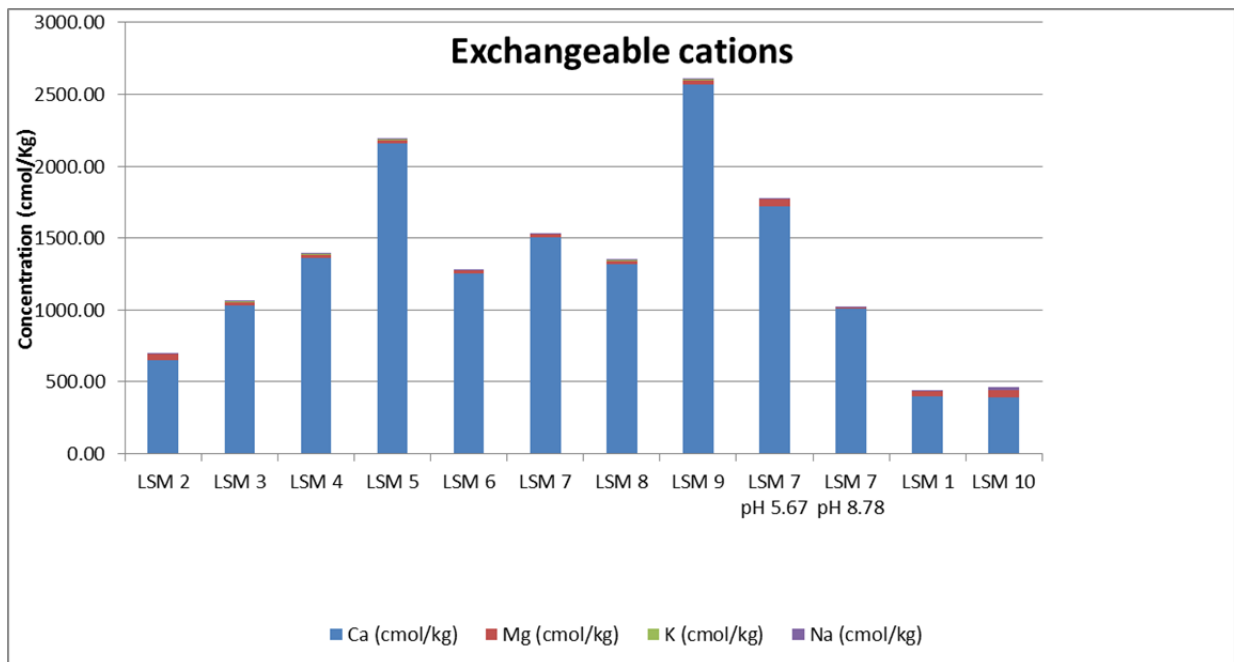


Figure 4-16 Exchangeable cation determined during CEC determinations

Calcium appears to be the most readily exchanged cation of all the cations analysed. This is possibly due to the high solubility that calcium has when compared to these other cations. LSM 5 and LSM 9 which both have an added calcium content of 10%, have the highest proportions of leached calcium. It is possible that the calcium in these two specimens is in excess and hence did not form cementitious compounds with the ash, therefore it is easily leached out by the 1N ammonium acetate solution. The other cations are detected in very low concentrations. This could be an indication that they are tightly bound in the crystal lattices of the different mineral phases and are therefore shielded from competing cations in solution or they could be in small amounts in the sample analysed. The concentrations of exchangeable cations were slightly affected by changes in pH, as LSM 7 at pH 5.67 gave a higher concentration of exchangeable cations than at the pH of 7. The increase in pH had a reverse effect with LSM 7 at 8.78 having a lower concentration of exchangeable cations.

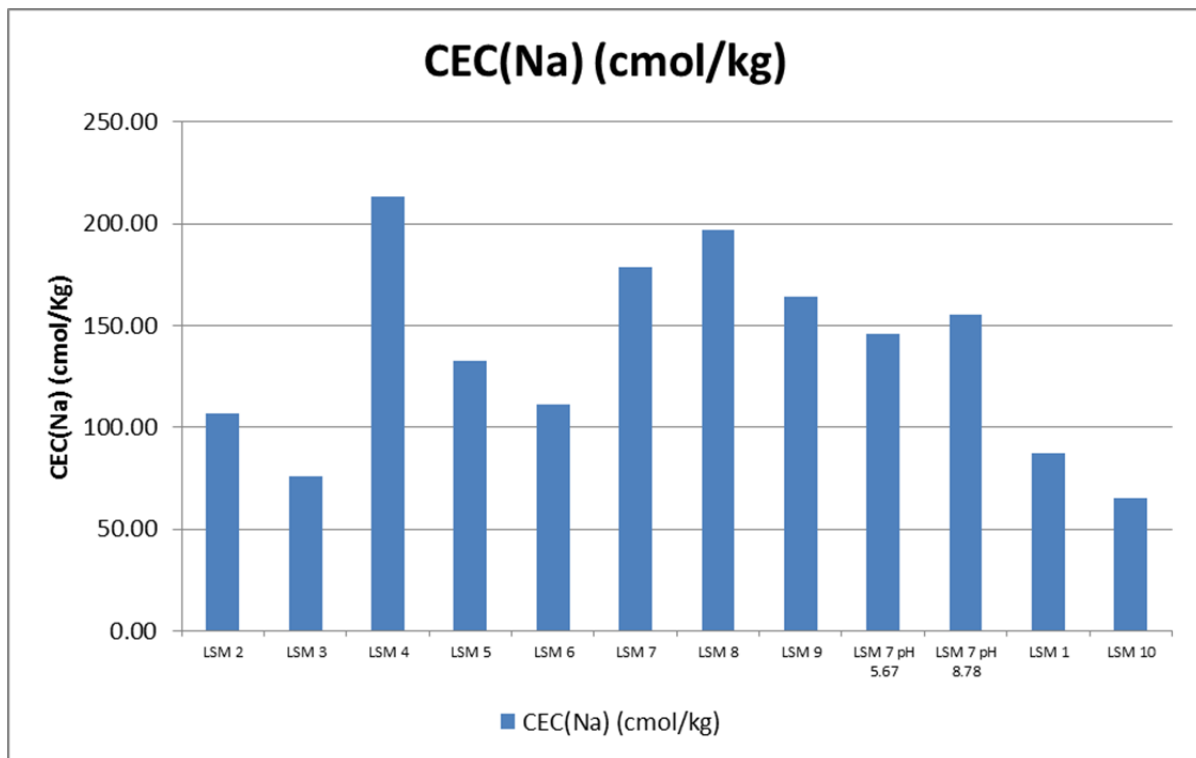


Figure 4-17 Cation exchange capacity determined as (Na) (cmol/Kg)

The cation exchange capacity of LSM 1 and LSM 10 were amongst lowest of all the samples with LSM 3 the only admixture sample lower than LSM 1, with LSM 10 as the lowest of all the samples. It appears that an addition of lime and gypsum had an increasing effect on the CEC of fly ash. This is possibly due to secondary minerals that add a CEC influence to the overall CEC of the specimen. Varying of pH for LSM 7 had a lowering effect on the CEC for both basic and acidic solutions.

4.6 Performance of multi-layer liner system

The composition of LSM 7 was selected as the most optimum admixture composition due to its prominent performance in all of the tests employed in this study. This admixture composition was therefore used in the evaluation of a multi-layer liner system. This system was made up of stacked layers of low hydraulic conductivity layers (LSM 7) mixed with high hydraulic conductivity layers (gravel acting as capillary breaks). Two systems compacted at different rates were used to evaluate the performance of the multi-layer liner system. The first multi-layer liner system was compacted at full compaction as described in section 3.8 and will be referred to as MLF. The second multi-layer liner system was compacted at a quarter compaction

rate and will be referred to as MLQ. The layer loading of the two compaction rates are shown in Figure 4-18 and Figure 4-19 representing MLF and MLQ respectively.

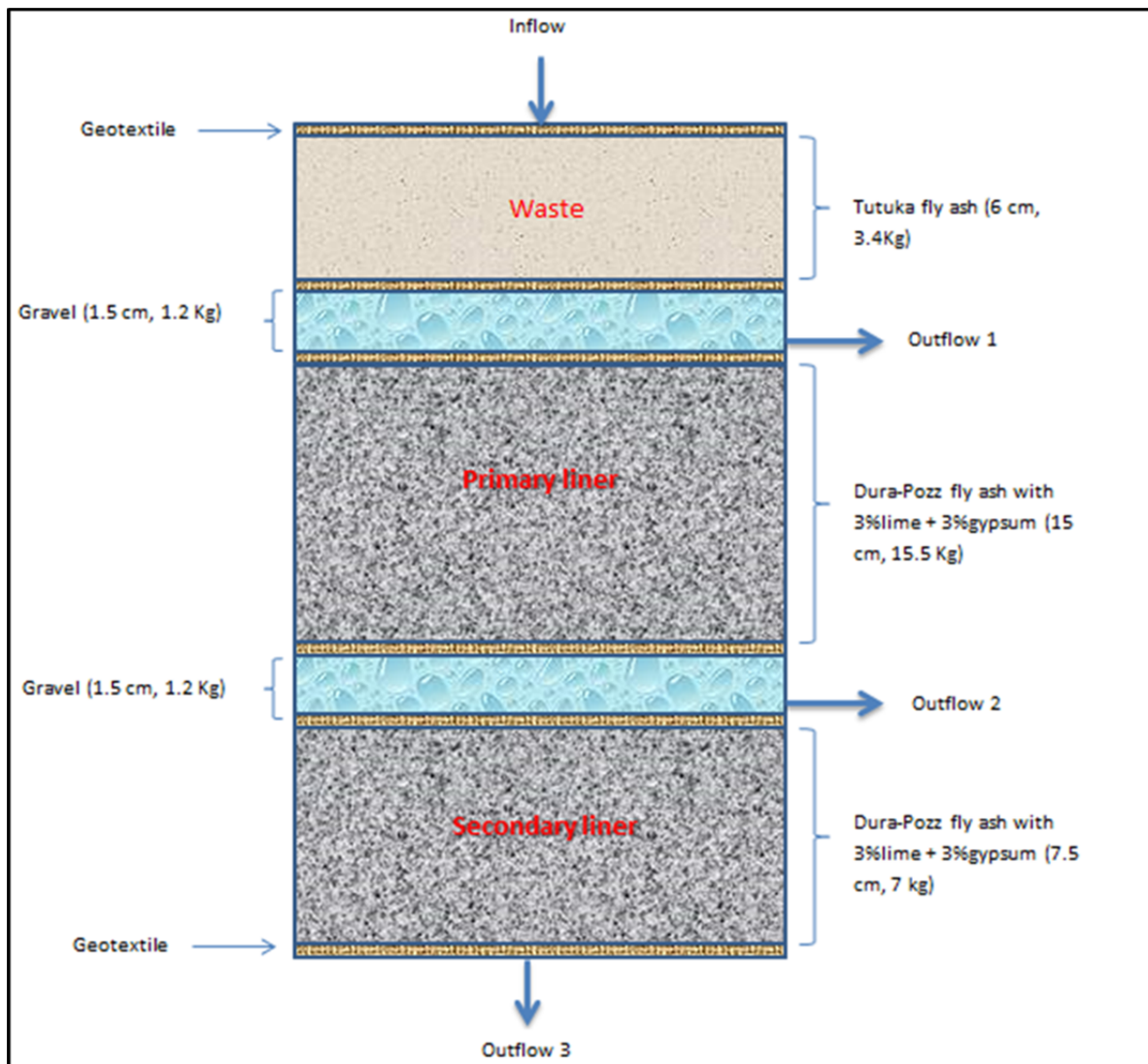


Figure 4-18 Graphical representation of multi-layer liner system at full compaction (MLF)

Since MLF was compacted at a higher compaction rate, more of the fly ash admixture was compacted per layer as compared to MLQ, see Figure 4-18 and Figure 4-19. MLF had 7.5 kg of fly ash admixture compacted into the secondary liner while MLQ had only 5.6 kg. The primary liner of MLF had 15.5 kg while MLQ had 13.7 kg of fly ash admixture compacted.

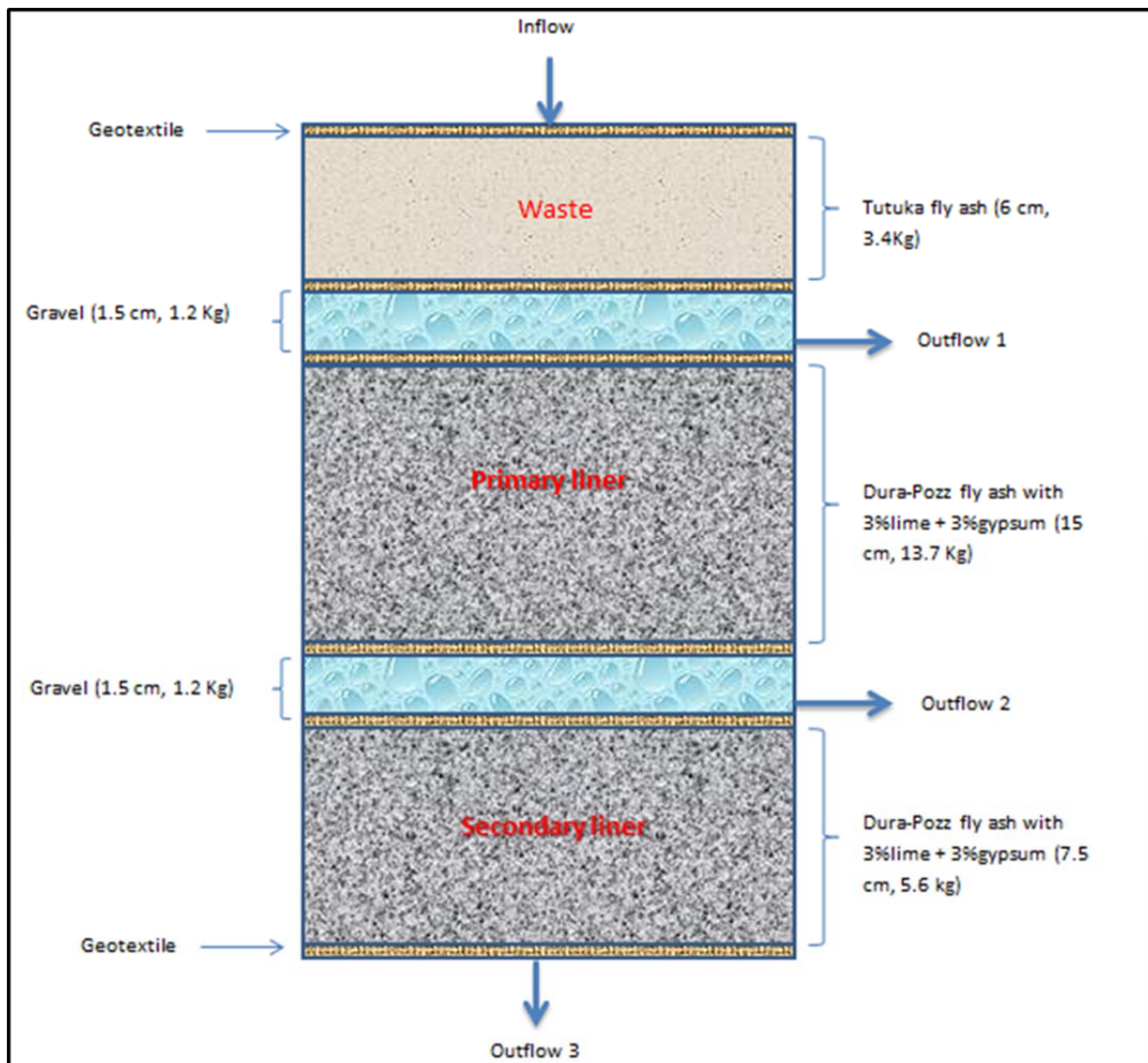


Figure 4-19 Graphical representation multi-layer liner system at a quarter compaction

A volume of 20L of brine water was injected once a day through the inflow point above the permeameter and water was collected at different outflow points. A water balance was conducted on a daily basis for both MLF and MLQ. The results of the water balance of MLF are presented in Table 4-10 and that of MLQ in Table 4-11.

Table 4-10 Water balance of MLF after cycles of 20L brine injections

Cycles	Brine injected (L)	Outflow 1 (L)	Outflow 2 (L)	Outflow 3 (L)	% Outflow 1	% Outflow 2	% Outflow 3
1	20	19.7	0	0	98.50%	0.00%	0.00%
2	20	19.5	0	0	97.50%	0.00%	0.00%
3	20	19.7	0	0	98.50%	0.00%	0.00%
4	20	19.6	0	0	98.00%	0.00%	0.00%
5	20	19.8	0.3	0	99.00%	1.52%	0.00%
6	20	19.4	0.53	0	97.00%	2.73%	0.00%
7	20	19.5	1.21	0	97.50%	6.21%	0.00%
Total	140	137.2	2.04	0	Average 98.00%	1.49%	0.00%

98% of leachate was collected in outflow point 1 and 1.49% in outflow point 2 in the MLF system while 95.8% of the leachate was collected in outflow point 1 and 2.9% in outflow point 2 in MLQ. It appears that compaction rate does influence the performance of the system as more leachate was collected in outflow point 2 in MLQ than in MLF. The primary liner of MLQ was also more porous than that of MLF. No leachate was collected in outflow 3 in both systems.

Table 4-11 Water balance of MLQ after cycles of 20L brine injections

Cycles	Brine injected (L)	Outflow 1 (L)	Outflow 2 (L)	Outflow 3 (L)	% Outflow 1	% Outflow 2	% Outflow 3
1	20.0	19.1	0.0	0.0	95.50%	0.00%	0.00%
2	20.0	19.3	0.0	0.0	96.50%	0.00%	0.00%
3	20.0	19.2	0.0	0.0	96.00%	0.00%	0.00%
4	20.0	18.9	0.5	0.0	94.50%	2.38%	0.00%
5	20.0	19.2	0.9	0.0	96.00%	4.69%	0.00%
6	20.0	19.3	1.2	0.0	96.50%	5.96%	0.00%
7	20.0	19.1	1.5	0.0	95.50%	7.59%	0.00%
Total	140.0	134.1	4.0	0.0	Average 95.79%	2.95%	0.00%

The water balance was done in such that the difference between inflowing water and outflowing water was attributed to the holding capacity of the system, see equation 3.11. The holding capacity of MLF was determined as 0.76 L while that of MLQ as 1.9 L. MLF performed better than MLQ holding off 98% of the leachate and only 1.5% seeping through the primary liner while MLQ was able to hold of 95.8 % of the leachate and had 2.9% of the leachate seeping through the primary liner.

The results of the continuous percolation test are presented in Table 4-12. The purpose of running a constant flow through the system was to determine how the multi-liner performed with constant flow conditions.

Table 4-12 Water balance of 30 day continuous brine circulation

	Brine injected (L)	Outflow 2 (L)	Outflow 3 (L)		% Outflow 2	% Outflow 3
MLF after 30 days	10	3.1	0.9	Average	31%	9%
MLQ after 30 days	10	5.3	1.2	Average	53%	12%

MLF had 31% of leachate seeping through the primary liner and 9% seeping through the secondary liner while MLQ had 53% seepage through the primary liner and 12% in the secondary liner. These results are similar to the daily percolation results and show that compaction rate plays an important role in the performance of a liner system. Leachate seeped through the secondary liner in both systems.

4.7 General discussion

The tests results reveal various characteristics of fly ash and how it performs as a liner material. Fly ash on its own proved to have a low strength as the unconfined compression strength test could not be determined for specimens containing only fly ash samples. These specimens collapsed when inserted in a water bath and could not stand unsupported by the mould. The XRF results found both Dura-Pozz fly ash and Tutuka fly ash to be class F fly ashes. Class F fly ash has little or no cementitious value (Bin-Shafique et al., 2003) and therefore lacks the ability to bind materials in order to form strong cohesive substances. An addition of lime and gypsum induced strength on fly ash with varying amounts of strength as illustrated by the unconfined compression strength tests and indirect tensile strength tests. The amount of additives added to the fly ash seemed to influence the ultimate strength the material obtained, as high levels of lime (10%) seemed to exhibit a lower unconfined compression strength. Gypsum proved to influence the strength more than lime as samples with 3% gypsum had higher unconfined compression strength values than those with the same amount of lime but at 1% gypsum. Curing time also had an influence on strength, as samples placed in a water bath for 7 days generally had a lower strength than their counterparts that were cured just for 4 hours. The

composition mixture of 3% lime and 3% gypsum proved to be the most optimum fly ash admixture in terms of strength performance and costing outlook.

Hydraulic conductivity had a general decreasing trend with time for all specimens even for fly ash without any additives added. Lime addition seemed to generally have little effect on the hydraulic conductivity as lime addition in the range of 1% to 10% did not have a lower hydraulic conductivity when compared to a specimen of fly ash without additives. In fact in a case where lime seemed to be in excess (10% lime) the hydraulic conductivity was over two times higher after 7 days when compared to that of fly ash alone. Gypsum proved to have an influence on hydraulic conductivity as specimens with 3% gypsum had a lower hydraulic conductivity than specimens with only 1% gypsum even though the lime content was carried out in the same manner. Admixture of 3% lime and 3% gypsum had the lowest hydraulic conductivity at the end of 7 days and once again proved to be the optimum compositional fly ash admixture. This admixture's hydraulic conductivity was further tested with brine water and demineralized water over a lengthier period of 60 days. This was done to determine how this admixture can perform under real life scenarios with brine water acting as toxic leachate that is generated in ash dumps. The brine water-hydraulic conductivity test had a lower K value at the end of 60 days than demineralized water. This proved to some extent that the 3% lime/3% gypsum admixture can contend with real life situations as a liner material. This admixture hydraulic conductivity resilience was further subjected to wet/dry cycles to determine if there would be an adjustment in hydraulic conductivity. The change in hydraulic conductivity was negligible even with reduced amounts in latter cycles. The secondary mineral ettringite was detected by XRD, mostly in fly ash with 3% gypsum added. Secondary minerals can possibly limit flow as they reduce the void areas in specimens of fly ash. Consequently all the specimens that had ettringite detected by XRD had a lower hydraulic conductivity than LSM 1 except for LSM 3.

An addition of lime and gypsum appeared to have stabilised fly ash in terms of its leachability of certain toxic elements. Cr concentration levels were found to be 7 times more than the regulatory limit in the leachates of both Dura-Pozz fly ash and Tutuka fly ash. The highest Cr concentration level in LSM 7 was less than twice the regulatory limit. The Department of Water Affairs set thresholds for leachate values from Part 2 section 6 of Government Gazette notice 34415 of 1 July 2011 and LSM 7

was classified according this notice, with a risk profile of LSM 7 presented in Table 4-13.

Table 4-13 Risk profile of leachate from LSM7 according to Government Gazette notice 34415 of 1 July 2011

LCT _i , LCT ₀ , LCT and TCT Threshold	Type 0	Type 1	Type 2	Type 3	Type 4
Criteria	LC > LCT ₂ or TC > TCT ₂	LCT ₁ < LC ≤ LCT ₂ , or TCT ₁ < TC	LCT ₀ < LC ≤ LCT ₁ and TC ≤ TCT ₁	LCT _i < LC ≤ LCT ₀ and TC ≤ TCT ₀	TC < 20*LCT _i , or LC ≤ LCT _i and TC ≤ TCT _i
B, Boron				Type 3	
Cd, Cadmium					Type 4
Cr, Chromium				Type 3	
Cu, Copper					Type 4
Mo, Molybdenum				Type 3	
Pb, Lead				Type 3	
Se, Selenium				Type 3	

The highest classification for LSM 7 is type 3 waste and according to Government Gazette notices 432 and 433 of 2011 should be disposed of in a Class **G:B⁺** landfills that has a single liner system. According to this classification a geomembrane or a geosynthetic clay liner should be placed at the base preparation layer if fly ash is to be used as a liner material. This will ensure that any leaching from the fly ash liner is contained and does not seep into the underlying soils.

4.8 Summary

The main property of a liner material is to have a low hydraulic conductivity. The hydraulic conductivity of fly ash was generally reduced by addition of lime and gypsum. Hydraulic conductivity of 2.27×10^{-9} m/s was obtained during a constant head test with brine water. This value is less than the value prescribed by the legislative guidelines for a hazardous waste liner, in South Africa. The formation of secondary minerals was detected in fly ash and it is plausible that these minerals block the flow pathways which could explain why hydraulic conductivity reduces with time in fly ash.

It is possible that secondary minerals also precipitate out some of the trace elements in fly ash. A reduction in chromium concentrations was observed in leachate

emanating from a fly ash admixture with 3% lime and 3% gypsum but since fly ash was found to also have cation exchange capacity this reduction could be from the ionic exchange in the clay fractions of fly ash. This admixture composition was also found to be able to restrain over 95% of leachate when used in a multi-layered system.

The next chapter provides the conclusion and recommendations resulting from this study.

5 Conclusion and Recommendations

This chapter provides the key findings from this research and how it relates to the specific objectives of the study. Recommendations for supplementary research are also outlined.

5.1 Conclusion

There is a noticeable improvement in the engineering and chemical properties of fly ash with the addition of lime and gypsum. This increases its desirability to be used as a possible liner material. The following conclusions are derived from the study:

- An addition of lime and gypsum increases the strength of fly ash. However this increase in strength was reduced when lime was used in excess.
- An addition of lime and gypsum reduces the optimum water content at which the maximum dry density is obtained for fly ash. This shows that an addition of lime and gypsum has a lubrication effect on fly ash therefore improving its durability in the liner system.
- An addition of lime and gypsum decreases the hydraulic conductivity of fly ash. The reduction in hydraulic conductivity depends to a greater extent on gypsum addition than on lime content. A hydraulic conductivity of 2.27×10^{-9} m/s was determined for an admixture of Dura-Pozz fly ash mixed with 3% lime and 3% gypsum. This value qualifies for a H:h liner system prescribed for lining hazardous waste by the South African legislative guidelines.
- The formation of secondary minerals in fly ash is heightened by an addition of lime and gypsum. However ettringite was more prevalent in samples with 3% gypsum than those with 1% added.
- Addition of lignosulphonate increases the plasticity index of fly ash to acceptable values prescribed for liners materials, according to South African legislative guidelines.
- A water balance of a multi-layer liner system showed that 95% of leachate that had passed through a layer of waste (untreated Tutuka fly ash) was successfully restricted by a primary liner made up of a fly ash admixture with 3% lime and 3% gypsum.

- An addition of lime and gypsum reduced the leachability of some trace elements found in fly ash.
- Fly ash has appreciable quantities of clay minerals as determined by QEMSCAN and texture analysis. Clay minerals are known to have cation exchange capacities. The cation exchange capacity of fly ash was slightly increased by an addition of lime and gypsum.

5.2 Recommendations

- The materials used in this study are to a large extent products that are accessible to coal power stations. It is recommended that power utility companies like Eskom and Sasol should incorporate the findings of this study into their future plans regarding ash landfill lining.
- South African fly ash is alkaline in nature and can have widespread application in lining acidic waste such as mining tailings that produce acid mine drainage
- Laboratory testing of hydraulic conductivities are not always duplicated in the field. In order to determine actual hydraulic conductivity values a test pad should be used.
- Geochemical modelling with PHREEQC should be used to check how the redox conditions will affect the liner material in the future as a result of weathering processes. Advection and dispersivity should be investigated as it relates to porosity changes and hydraulic conductivity.
- Longer leaching tests, (> 1 year), under different hydraulic heads should be assessed to check the performance of the liner system. Solutions of varying pH should be included in these percolation tests as pH is a factor that affects the leachability of certain elements.
- Fly ash contains trace amounts of toxic elements such as, Cr, and as a liner material should have a geomembrane or geosynthetic clay liner. This is in order to limit toxic leachate from seeping into the sub-surface. Both multi-liner systems used in this study had seepage through their secondary liners.
- Further research should be conducted on the mechanisms of lignosulphonate leaching on fly ash. This is due to the fact that lignosulphonate was observed

to increase the plasticity index of fly ash but failed to be retained in the fly ash mixture with subsequent leaching.

- The impressive clay fractions found in fly ash, warrants further investigations into how to increase the cation exchange capacity. Fulvic and humic acid can be investigated as additives that can possibly increase the cation exchange capacity of fly ash.

References

- AFFAIRS, D. O. E. 2010. NATIONAL ENVIRONMENTAL MANAGEMENT ACT: ENVIRONMENTAL IMPACT ASSESSMENT REGULATIONS In: AFFAIRS, D. O. E. (ed.) 33306.
- AFFAIRS, D. O. E. 2011. Draft standard for assessment of waste for landfill disposal. In: AFFAIRS, D. O. E. (ed.) 433. Pretoria: Government Gazette.
- AGYEI, N. M., STRYDOM, C. A. & POTGIETER, J. H. 2000. An investigation of phosphate ion adsorption from aqueous solution by fly ash and slag. *Cement and Concrete Research*, 30, 823-826.
- AHMARUZZAMAN, M. 2009. A review on the utilization of fly ash. *Progress in Energy and Combustion Science*, 36, 2010, 327–363.
- ASH-RESOURCES. 2013. Ash resources: materials for today and the future [Online]. Available: <http://www.ash.co.za/upload/File/Super%20Pozz.pdf> [Accessed 17 July 2013 2013].
- ASTM-C618 1993. ASTM standard specification for coal fly ash and raw or calcined natural pozzolan for use in concrete (C618-12a). In: *Annual book of ASTM standards, concrete and aggregates*, vol. 04.02. American Society for Testing Materials.
- BATABYAL, D., SAHU, A. & CHAUDHURI, S. K. 1995. Kinetics and mechanism of removal of 2,4-dimethyl phenol from aqueous solutions with coal fly ash. *Separations Technology*, 5, 179-186.
- BAYAT, B. 2002. Comparative study of adsorption properties of Turkish fly ashes II. The case of chromium (VI) and cadmium (II). *Journal of Hazardous Materials*, B95, 275-290.
- BIN-SHAFIQUE, M. S., BENSON, C. H. & EDIL, T. B. 2003. leaching of heavy metals from fly ash stabilized soils used in highway pavements. *Combustion Byproducts Recycling Consortium*.
- BLISSETT, R. S. & ROWSON, N. A. 2012. A review of the multi-component utilisation of coal fly ash. *Fuel*, 91(2012) 1-23.

CHRISTENSEN, T. H., COSSU, R. & STEGMANN, R. (eds.) 1992. Landfill leachate: An Introduction, London: Elsevier science publishers ltd.

CHU, V. T. H. 2010. A Self-Learning Manual Mastering Different Fields of Civil Engineering Works (VC-Q&A Method) [Online]. [Accessed 07 July 2013 2013].

COKCA, E. & YILMAZ, Z. 2003. Use of rubber and bentonite added fly ash as a liner material. Waste Management, 24, 153-164.

COMMITTEE, N.-A. S. A. W. 1990. Handbook of Standard Soil-Testing Methods for Advisory Purposes, Pretoria, Soil Science Society of South Africa.

DANIEL, D. E. (ed.) 1993. Geotechnical Practice for Waste Containment, London: Chapman & Hall.

DAVINI, P. 1996. Investigation of the SO₂ adsorption properties of Ca(OH)₂-fly ash systems. Fuel, 75, 713-716.

DWAF. 1998a. Guidelines for leachate control [Online]. Department of Water Affairs. Available: www.dwaf.gov.za/Documents/Policies/WDD/LeachateControl.pdf [Accessed 21 April 2013].

DWAF 1998b. minimum requirements for waste disposal by landfill. second ed. Department of Water Affairs, Pretoria.

ESKOM. 2011. Intergrated Report 2011 [Online]. Available: www.eskom.co.za/annreport11 [Accessed 6 February 2013].

ESKOM. 2012. Eskom intergrated report 2012 [Online]. Available: www.eskom.co.za/annreport12 [Accessed 10 July 2013 2013].

FATOBA, O. O. 2007. Chemical compositions and leaching behaviour of some South African fly ashes. Magister Scientiae in Chemistry, University of the Western Cape.

FETTER, C. W. 1993. Contaminant hydrogeology, Love Grove, Illinois, Waveland Press, Inc.

FREEZE, R. A. & CHERRY, J. A. 1979. Groundwater, Englewood Cliffs, NY, Prentice Hill.

GITARI, W. M. 2006. Evaluation of the Leachate Chemistry and Contaminants Attenuation in Acid Mine Drainage by Fly Ash and its derivatives. Ph. D., University of the Western Cape.

GITARI, W. M., PETRIK, L. F., ETCHEBERS, O., KEY, D. L. & OKUJENI, C. 2008. Utilization of fly ash for treatment of coal mines wastewater: Solubility controls on major inorganic contaminants. *Fuel*, 87, 2450 - 2462.

GUPTA, G. & TORRES, N. 1998. Use of fly ash in reducing toxicity of and heavy metals in wastewater effluent. *Journal of Hazardous Materials*, 57, 243-248.

HAFNER, B. 2013. Energy Dispersive Spectroscopy on the SEM: A Primer [Online]. Minnesota: University of Minnesota. Available: [http://www.charfac.umn.edu/instruments/eds_on_sem_primer .pdf](http://www.charfac.umn.edu/instruments/eds_on_sem_primer.pdf) [Accessed 27 July 2013 2013].

HANSEN, Y., NOTTEN, P. J. & PETRIE, J. G. 2002. The environmental impact of ash management in coal-based power generation. *Applied Geochemistry*, 17, 1131-1141.

HOWER, J. C. 2012. Petrographic examination of coal-combustion fly ash. *International Journal of Coal Geology*, 92, 90-97.

HUGHES, K. L., CHRISTY, A. D. & HEIMLICH, J. E. 2013. Landfill Types and Liner Systems [Online]. Ohio: The Ohio State University. Available: <http://ohioline.osu.edu/cd-fact/pdf/0138.pdf> [Accessed 8 May 2012].

IYER, R. 2002. The surface chemistry of leaching coal fly ash. *Journal of Hazardous Materials*, 93, 321-329.

IZQUIERDO, M. & QUEROL, X. 2011. Leaching behaviour of elements from coal combustion fly ash: An overview. *International Journal of Coal Geology*, 94, 54-66.

KAROL, R. H. 1955. Engineering properties of soils, Civil engineering and engineering mechanics series, New York, Prentice-Hall.

KIKUCHI, R. 1999. Application of coal ash to environmental improvement Transformation into zeolite, potassium fertilizer, and FGD absorbent. *Resources, Conservation and Recycling*, 27, 333-346.

KRUGER, J. E. 2003. SOUTH AFRICAN FLY ASH: A CEMENT EXTENDER. The South African Coal Ash Association.

KRUSEMAN, G. P. & RIDDER, N. A. D. 2000. Analysis and evaluation of pumping test data, Netherlands, International Institution for Land Reclamation and Improvement.

KUKIER, U., ISHAK, C. F., SUMNER, M. E. & MILLER, W. P. 2003. Composition and element solubility of magnetic and non-magnetic fly ash fractions. *Environmental Pollution*, 123, 255–266.

LÁBÁR, J. L. 2002. Introduction to electron microscopes: electron optics, interactions and signals. Research Institute for Technical Physics and Materials Science, H-1121, 29-33.

MADZIVIRE, G., PETRIK, L. F., GITARI, W. M., OJUMU, T. V. & BALFOUR, G. 2010. Application of coal fly ash to circumneutral mine waters for the removal of sulphates as gypsum and ettringite. *Minerals Engineering*, 23, 252–257.

MCCARTHY, M. J., CSETENYI, L. J., SACHDEVA, A. & DHIR, R. K. 2011. Identifying the role of fly ash properties for minimizing sulfate-heave in lime-stabilized soils. 92, 27-36.

MILLER, W. L., OPENSHAW, S. C., BOLCH, W. E. & BLOOMQUIST, D. 1992. Utilization of coal ash. Florida center for solid and hazardous waste management. Florida: Department of Environmental Engineering Sciences.

MURIITHI, G. N. 2009. CO₂ sequestration using brine impacted fly ash. Magister Scientiae Dissertation, University of the Western Cape.

NESSE, W. D. 1999. Introduction to mineralogy, Oxford.

NHAN, C. T., GRAYDON, J. W. & KIRK, D. W. 1996. Utilizing coal fly ash as a landfill barrier material. *Waste Management*, 16, 587-595.

NOCHAIYA, T., WONGKEO, W. & CHAIPANICH, A. 2009. Utilization of fly ash with silica fume and properties of Portland cement-fly ash-silica fume concrete. Construction material research unit.

PALMER, B. G., EDIL, T. B. & BENSON, C. H. 2000. Liners for waste containment constructed with class F and C fly ashes. *Journal of Hazardous Materials*, 76, 193-216.

PALMER, C. M. 1996. *Principles of contaminant hydrogeology*, Florida, CRC Press.

PEREZ-LOPEZ, R., NIETO, J. M. & ALMODOVAR, G. R. D. 2007. Utilization of fly ash to improve the quality of the acid mine drainage generated by oxidation of a sulphide-rich mining waste: Column experiments. *Chemosphere*, 67, 1637–1646.

QUEROL, X., PLANA, F., ALASTUEY, A. & LOPEZ-SOLER, A. 1997. Synthesis of Na-zeolites from fly ash. *Fuel*, 76, 793-799.

RAYMOND, S. 1961. Pulverized fuel ash as embankment material 19, 515 - 536.

REKNES, K. 2004. the chemistry of lignosulphonate and the effect on performance of lignosulphonate base plasticizers and superplasticizers. 29th conference on our world in concrete & structures. Singapore.

RIO, S. & DELEBARRE, A. 2003. Removal of mercury in aqueous solution by fluidized bed plant fly ash. *Fuel*, 82, 153-159.

ROBERTS, D. L. 2008. CHROMIUM SPECIATION IN COAL COMBUSTION BYPRODUCTS: CASE STUDY AT A DRY DISPOSAL POWER STATION IN MPUMALANGA PROVINCE, SOUTH AFRICA. Doctor of Philosophy, University of Witwatersrand.

SAIKIA, N., KATO, S. & KOJIMA, T. 2006. Compositions and leaching behaviours of combustion residues, *Fuel*, 85, 264-271.

SANTOS, F., LI, L., LI, Y. & AMINI, F. 2011. Geotechnical properties of fly ash and soil mixtures for use in highway embankments. World of coal ash (WOCA) conference. Denver, CO, USA: Department of civil and environmental science.

SCHWARTZ, F. W. & ZHANG, H. 2003. *Fundamentals of groundwater*, New York, Chichester, Wiley.

SIVAPULLAIAH, P. & BAIG, A. A. 2011. Gypsum treated fly ash as a liner for waste disposal facilities. *Waste Management*, 31, 359-369.

TANAKA, H., FUJII, A., FUJIMOTO, S. & TANAKA, Y. 2007. Microwave-Assisted Two-Step Process for the Synthesis of a Single-Phase Na-A Zeolite from Coal Fly Ash. *Advanced Powder Technology*, 19, 83–94.

TISHMACK, J. K., OLEK, J. & DIAMOND, S. 1999. Characterization of High-Calcium Fly Ashes and Their Potential Influence on Ettringite Formation in Cementitious Systems. *Cement, Concrete, and Aggregates, CCAGDP*, 21, 82–92.

TMH1-A2. 1986. the determination of the liquid limit of soils by means of the flow curve method [Online]. Pretoria: CSIR. Available: <http://asphalt.csir.co.za/tmh/> [Accessed 22 July 2013 2013].

TMH1-A3. 1986. The determination of the plastic limit and plasticity index of soils [Online]. Pretoria: CSIR. Available: <http://asphalt.csir.co.za/tmh/> [Accessed 22 July 2013 2013].

TMH1-A4. 1986. The determination of the linear shrinkage of soils [Online]. Pretoria: CSIR. Available: <http://asphalt.csir.co.za/tmh/> [Accessed 21 July 2013 2013].

TMH1-A7. 1986. the determination of the maximum dry density and optimum moisture content of gravel, soil and sand [Online]. Pretoria: CSIR. Available: <http://asphalt.csir.co.za/tmh/> [Accessed 21 July 2013 2013].

TMH1-A14. 1986. The determination of the unconfined compressive strength of stabilized soils, gravels and sands [Online]. Pretoria: CSIR. Available: <http://asphalt.csir.co.za/tmh/> [Accessed 21 July 2013 2013].

TMH1-A16T. 1986. Tentative method for the determination of the indirect tensile strength of stabilized materials [Online]. Pretoria: CSIR. Available: <http://asphalt.csir.co.za/tmh/> [Accessed 21 July 2013 2013].

VASSILEV, S. V. & VASSILEVA, C. G. 2006. A new approach for the classification of coal fly ashes based on their origin, composition, properties, and behaviour. *Fuel*, 86, 1490-1512.

WANG, S., MILLER, A., LLAMAZOS, E., FONSECA, F. & BAXTER, L. 2006. Biomass fly ash in concrete: Mixture proportioning and mechanical properties. *Fuel*, 87, 365-371.

WANG, S., TERDKIATBURANA, T. & TADE, M. O. 2008. Single and co-adsorption of heavy metals and humic acid on fly ash. *Separation and Purification Technology*, 58, 353-358.

WARD, C. R. & FRENCH, D. 2006. Determination of glass content and estimation of glass composition in fly ash using quantitative X-ray diffractometry. *Fuel*, 85, 2268-2277.

Abstract

The engineering properties of a South African class F fly ash were studied as a potential base liner for a dry coal ash dump. In order to increase the unconfined compression strength, lime and gypsum were added to the fly ash while also aiding in reducing the hydraulic conductivity. Lime was added in the range of 1 to 10% while the gypsum amounts were varied at 1% and 3% per specimen. The constant head method was used to determine the hydraulic conductivity of compacted specimens in the laboratory. Gypsum was observed to have more influence in reducing the hydraulic conductivity as specimens with 3% gypsum had a more reduced hydraulic conductivity than those with 1%. The variations in lime percentages did not appear to reduce the hydraulic conductivity but rather displayed higher values than fly ash specimens without additives when higher percentages of lime were used. A fly ash admixture of 3% lime and 3% gypsum was found to have the lowest hydraulic conductivity of 2.27×10^{-9} m/s after 60 days of percolating with brine water.

The unconfined compression strength also appeared to be more influenced by gypsum than lime percentages as specimens with 3% gypsum obtained higher strength values than those with 1% gypsum added. Unreacted lime was observed in specimens with higher percentages of lime added and these specimens also presented lower strength values. The addition of lime and gypsum was observed to have limited the release of some trace elements from fly ash. The secondary mineral ettringite was detected and could have possibly precipitated and captured out these toxic elements. An attempt was also made to increase the plasticity index of fly ash using lignosulphonate and values recommended by the South African legislative guidelines for liner materials were obtained. The plasticity was however not retained with subsequent leaching.

Two multi-layer liner systems were loaded under different compaction rates in permeameter cells with fitted inflow and outflow points. The primary liners of both systems were able to contain over 95% of leachate that percolated through a waste layer. Compaction rate was found to affect the liners performance as primary liners

with a higher compaction rate had less seepage than primary liner compacted at a lower rate. An addition of lime and gypsum improved the overall engineering properties of fly ash to levels accepted by the South African legislative guidelines for a liner material that is able to line hazardous waste. Even though concentrations of some trace elements in fly ash were reduced by addition of lime and gypsum the level of some of these trace elements remain above the threshold set by South African legislative guidelines and therefore remains a health and environmental concern.

Opsomming

Die ingenieurseienskappe van 'n Suid-Afrikaanse klas F-vliegas is ondersoek as 'n potensiële basis voering vir 'n droë steenkoolas-stortingsterrein. Kalk en gips is by vliegas gevoeg om die kompressiekrag te verhoog, terwyl dit ook bydra tot die vermindering van die hidrouliese geleiding. Kalk is bygevoeg in die reeks van 1 tot 10%, terwyl die gipsgetalle gewissel het tussen 1% en 3% per monster. Die konstante drukmetode is gebruik om die hidrouliese geleiding van gekompakteerde monsters in die laboratorium te bepaal. Gips is waargeneem om 'n groter invloed te hê op die vermindering van die hidrouliese geleiding waar monsters met 3% gips 'n meer verminderde hidrouliese geleiding as dié wat met 1% gehad het. Die variasies in kalkpersentasies het skynbaar nie die hidrouliese geleiding verminder nie, maar het eerder hoër waardes getoon as vliegasmonsters sonder bymiddels wanneer hoër persentasies van kalk gebruik is. Dit is bevind dat 'n vliegasmengsel van 3% kalk en 3% gips die laagste hidrouliese geleiding van 2.27×10^{-9} m/s na 60 dae van perkolering met pekel water gehad het.

Dit blyk dat die kompressiedrukkrug ook meer beïnvloed word deur gips- as kalkpersentasies aangesien monsters met 3% gips hoër kragwaardes verkry het as dié met 1% gips bygevoeg. Onopgeloste kalk is waargeneem in monsters met 'n hoër persentasie van kalk en hierdie monsters het ook laer kragsterktewaardes. Dit is waargeneem dat die byvoeging van kalk en gips die vrylating van sommige spoorelemente van vliegas verlaag het. Die sekondêre mineraal ettringiet is waargeneem en kon moontlik die giftige elemente uitgeskakel het. 'n Poging is ook aangewend om die plastisiteitsindeks van vliegas te vermeerder deur die gebruik van lignosulfonaat en waardes aanbeveel deur die Suid-Afrikaanse wetgewende riglyne vir die voeringmateriaal. Die plastisiteit is egter nie met die daaropvolgende uitloging behou nie.

Twee multi-laag voeringstelsels is gelaai onder verskillende kompaktetariëwe in permumeter-selle met ingeboude en uitvloeipunte. Die primêre voerings van beide stelsels was in staat om meer as 95% van logings wat deur 'n afvallaag geperkoleer is, te bevat. Daar is bevind dat die kompaktiekoers die voerings se prestasie beïnvloed, aangesien die primêre voerings met 'n hoër kompaktiekoers minder sydeling het as primêre voerings wat teen 'n laer koers kompakteer. Oor die

algemeen het die toevoeging van kalk en gips die fisiese eienskappe van vliegas verbeter tot vlakke wat volgens die Suid-Afrikaanse wetgewende riglyne aanvaarbaar is vir voeringmateriaal wat in staat is om die deursypeling van gevaarlike afval te inhibeer. Selfs al is konsentrasies van sekere spoorelemente in vliegas verminder deur die byvoeging van kalk en gips, is die vlak van 'n sommige van hierdie spoorelemente steeds bo die grens wat deur die Suid-Afrikaanse wetgewende riglyne daargestel is, en dus bly 'n gesondheids- en die omgewingsbekommernis.

Appendices

Appendix A-1

%Lime	%Gypsum	UCS 4 hours	Average
1%	1%	2475.6	2152.5
3%	1%	2251.2	2182
6%	1%	2265.7	2098.3
10%	1%	2399.9	2093.7
1%	3%	3203	2756.6
3%	3%	4588	4169.7
6%	3%	4680.4	4481.9
10%	3%	4658.6	4600.7
%Lime	%Gypsum	UCS 7 days	Average
1%	1%	2010.2	1578.5
3%	1%	2156.8	1716.7
6%	1%	2195.2	683.8
10%	1%	2635.1	1817.4
1%	3%	1784.4	1324.8
3%	3%	4329.9	3124.7
6%	3%	2731.2	2661
10%	3%	3803.4	2318
%Lime	%Gypsum	ITS	Average
1%	1%	810.71	475.46
3%	1%	607.61	471.99
6%	1%	725.04	609.34
10%	1%	655.4	534.84
1%	3%	446.08	304.67
3%	3%	719.51	632.78
6%	3%	1376.57	1202.71
10%	3%	534.64	392.95

Sample name	Sample composition	%Lime	%Gypsum	Sample composition	UCS (4hrs curing)(KPa)	ITS (KPa)	UCS (7days curing) (KPa)
LSM2	Dura-Pozz fill fly ash	1%	1%	LSM2 (1% L / 1% G)	2314.05	643.085	1794.35
LSM3	Dura-Pozz fill fly ash	3%	1%	LSM3 (3% L / 1% G)	2216.6	539.8	1936.75
LSM4	Dura-Pozz fill fly ash	6%	1%	LSM6 (% L / 1% G)	2182	667.19	1439.5
LSM5	Dura-Pozz fill fly ash	10%	1%	LSM10 (% L / 1% G)	2246.8	595.12	2226.25
LSM6	Dura-Pozz fill fly ash	1%	3%	LSM1 (% L / 3% G)	2979.8	375.375	1554.6
LSM7	Dura-Pozz fill fly ash	3%	3%	LSM3 (% L / 3% G)	4378.85	675.145	3727.3
LSM8	Dura-Pozz fill fly ash	6%	3%	LSM6 (% L / 3% G)	4581.15	1289.64	2696.1
LSM9	Dura-Pozz fill fly ash	10%	3%	LSM10 (% L / 3% G)	4629.65	463.795	3060.7

Appendix A-2

The following equation was used to calculate the hydraulic conductivity (K):

$$K = \frac{QL}{AH}$$

Where Area (A) = 0.008653 m³

Discharge = Volume / time

Dura-Pozz FA						
volume (ml)	time (sec)	Volume"	Discharge Q	Length/head	Area	K (m/s)
320	86400	0.00032	3.7037E-09	0.148648649	0.008653	6.36E-08
265	86400	0.000265	3.06713E-09	0.148648649	0.008653	5.27E-08
265	86400	0.000265	3.06713E-09	0.148648649	0.008653	5.27E-08
225	86400	0.000225	2.60417E-09	0.148648649	0.008653	4.47E-08
185	86400	0.000185	2.1412E-09	0.148648649	0.008653	3.68E-08
190	86400	0.00019	2.19907E-09	0.148648649	0.008653	3.78E-08
170	86400	0.00017	1.96759E-09	0.148648649	0.008653	3.38E-08

1%l + 1%g						
volume (ml)	time (sec)	Volume"	Discharge Q	Length/head	Area	K (m/s)
385	86400	0.000385	4.45602E-09	0.148648649	0.008653	7.65493E-08
315	86400	0.000315	3.64583E-09	0.148648649	0.008653	6.26312E-08
260	86400	0.00026	3.00926E-09	0.148648649	0.008653	5.16956E-08
205	86400	0.000205	2.37269E-09	0.148648649	0.008653	4.076E-08
170	86400	0.00017	1.96759E-09	0.148648649	0.008653	3.3801E-08
175	86400	0.000175	2.02546E-09	0.148648649	0.008653	3.47951E-08
125	86400	0.000125	1.44676E-09	0.148648649	0.008653	2.48537E-08

1%l + 3%g						
volume (ml)	time (sec)	Volume"	Discharge	Length/head	Area	K (m/s)
465	86400	0.000465	5.38E-09	0.148648649	0.008653	9.25E-08
370	86400	0.00037	4.28E-09	0.148648649	0.008653	7.36E-08
370	86400	0.00037	4.28E-09	0.148648649	0.008653	7.36E-08
290	86400	0.00029	3.36E-09	0.148648649	0.008653	5.77E-08
200	86400	0.0002	2.31E-09	0.148648649	0.008653	3.98E-08
220	86400	0.00022	2.55E-09	0.148648649	0.008653	4.37E-08
190	86400	0.00019	2.2E-09	0.148648649	0.008653	3.78E-08

6% l + 1% g						
volume (ml)	time (sec)	Volume"	Discharge Q	Length/head	Area	K (m/s)
500	86400	0.0005	5.78704E-09	0.148648649	0.008653	9.94E-08
520	86400	0.00052	6.01852E-09	0.148648649	0.008653	1.03E-07
275	86400	0.000275	3.18287E-09	0.148648649	0.008653	5.47E-08
260	86400	0.00026	3.00926E-09	0.148648649	0.008653	5.17E-08
260	86400	0.00026	3.00926E-09	0.148648649	0.008653	5.17E-08
195	86400	0.000195	2.25694E-09	0.148648649	0.008653	3.88E-08
245	86400	0.000245	2.83565E-09	0.148648649	0.008653	4.87E-08

10% l + 1% g						
volume (ml)	time (sec)	Volume"	Discharge Q	Length/head	Area	K (m/s)
700	86400	0.0007	8.10185E-09	0.148648649	0.008653	1.39E-07
750	86400	0.00075	8.68056E-09	0.148648649	0.008653	1.49E-07
375	86400	0.000375	4.34028E-09	0.148648649	0.008653	7.46E-08
390	86400	0.00039	4.51389E-09	0.148648649	0.008653	7.75E-08
445	86400	0.000445	5.15046E-09	0.148648649	0.008653	8.85E-08
340	86400	0.00034	3.93519E-09	0.148648649	0.008653	6.76E-08
350	86400	0.00035	4.05093E-09	0.148648649	0.008653	6.96E-08

1% l + 3% g						
volume (ml)	time (sec)	Volume"	Discharge Q	Length/head	Area	K (m/s)
950	86400	0.00095	1.09954E-08	0.148648649	0.008653	1.89E-07
610	86400	0.00061	7.06019E-09	0.148648649	0.008653	1.21E-07
520	86400	0.00052	6.01852E-09	0.148648649	0.008653	1.03E-07
380	86400	0.00038	4.39815E-09	0.148648649	0.008653	7.56E-08
240	86400	0.00024	2.77778E-09	0.148648649	0.008653	4.77E-08
175	86400	0.000175	2.02546E-09	0.148648649	0.008653	3.48E-08
95	86400	0.000095	1.09954E-09	0.148648649	0.008653	1.89E-08

3% l + 3% g						
volume (ml)	time (sec)	Volume"	Discharge Q	Length/head	Area	K (m/s)
420	86400	0.00042	4.86111E-09	0.148648649	0.008653	8.35E-08
350	86400	0.00035	4.05093E-09	0.148648649	0.008653	6.96E-08
275	86400	0.000275	3.18287E-09	0.148648649	0.008653	5.47E-08
160	86400	0.00016	1.85185E-09	0.148648649	0.008653	3.18E-08
70	86400	0.00007	8.10185E-10	0.148648649	0.008653	1.39E-08
65	86400	0.000065	7.52315E-10	0.148648649	0.008653	1.29E-08
45	86400	0.000045	5.20833E-10	0.148648649	0.008653	8.95E-09

6%I+3%g						
volume (ml)	time (sec)	Volume"	Discharge Q	Length/head	Area	K (m/s)
470	86400	0.00047	5.43981E-09	0.148648649	0.008653	9.34498E-08
410	86400	0.00041	4.74537E-09	0.148648649	0.008653	8.152E-08
275	86400	0.000275	3.18287E-09	0.148648649	0.008653	5.46781E-08
240	86400	0.00024	2.77778E-09	0.148648649	0.008653	4.7719E-08
220	86400	0.00022	2.5463E-09	0.148648649	0.008653	4.37425E-08
120	86400	0.00012	1.38889E-09	0.148648649	0.008653	2.38595E-08
50	86400	0.00005	5.78704E-10	0.148648649	0.008653	9.94147E-09

10%I+3%g						
volume (ml)	time (sec)	Volume"	Discharge Q	Length/head	Area	K (m/s)
600	86400	0.0006	6.94444E-09	0.148648649	0.008653	1.19E-07
450	86400	0.00045	5.20833E-09	0.148648649	0.008653	8.95E-08
400	86400	0.0004	4.62963E-09	0.148648649	0.008653	7.95E-08
270	86400	0.00027	3.125E-09	0.148648649	0.008653	5.37E-08
120	86400	0.00012	1.38889E-09	0.148648649	0.008653	2.39E-08
70	86400	0.00007	8.10185E-10	0.148648649	0.008653	1.39E-08
65	86400	0.000065	7.52315E-10	0.148648649	0.008653	1.29E-08

Appendix A-3

Sample ID	
Brine	
pH @ 25 °C	8.36
Conductivity μ S/cm	10200
Element	mg/l
Alkalinity Total CaCO ₃	558
Aluminium as Al	<0.005
Barium as Ba	0.04
Beryllium as Be mg/l <0.005	<0.005
Boron as B mg/l 4.9	4.9
Cadmium as Cd mg/l <0.005	<0.005
Cobalt as Co	<0.005
Chromium as Cr	0.05
Copper as Cu	<0.06
Iron as Fe	<0.005
Manganese as Mn	0.02
Molybdenum as Mo	0.17
Nickel as Ni	<0.005
Lead as Pb	<0.010
Strontium as Sr	6
Zinc as Zn	0.03

MALVERN MASTERSIZER

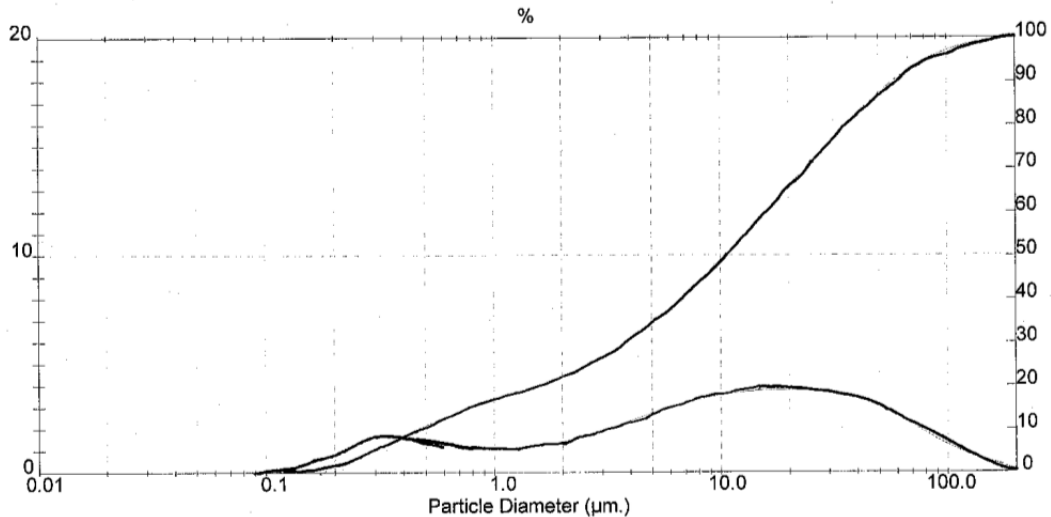
Result: Histogram Report

Sample Details		
Sample ID: DURAPOZZ	Run Number: 1	Measured: Mon Jul 15 2013 20:52PM
Sample File: DURAPOZZ	Record Number: 29825	Analysed: Mon Jul 15 2013 20:52PM
Sample Path: C:\SIZERS\DATA\		Result Source: Analysed
Sample Notes: DURAPOZZ DAILY SAMPLE		
DATE: 15/07/2013		
NIGHT SHIFT (07/15L/01)		
SAMPLE: 01 (15G13D)		

System Details			
Range Lens: 300RF mm	Beam Length: 2.40 mm	Sampler: None	Obscuration: 15.2 %
Presentation: 3OHD	[Particle R.I. = (1.5295, 0.1000);	Dispersant R.I. = 1.3300]	Residual: 0.518 %
Analysis Model: Polydisperse			
Modifications: None			

Result Statistics			
Distribution Type: Volume	Concentration = 0.0081 %Vol	Density = 2.180 g / cub. cm	Specific S.A. = 1.7014 sq. m / g
Mean Diameters:	D (v, 0.1) = 0.46 um	D (v, 0.5) = 10.50 um	D (v, 0.9) = 58.07 um
D [4, 3] = 21.68 um	D [3, 2] = 1.62 um	Span = 5.484E+00	Uniformity = 1.731E+00

Size (um)	Volume Under %	Size (um)	Volume Under %	Size (um)	Volume Under %	Size (um)	Volume Under %
0.400	8.51	6.50	39.36	19.00	64.49	80.00	94.77
0.500	10.88	7.00	40.89	20.00	65.77	85.00	95.46
0.600	12.66	7.50	42.37	21.00	66.98	90.00	96.06
0.700	14.01	8.00	43.77	22.00	68.14	95.00	96.57
0.800	15.08	8.50	45.12	23.00	69.24	100.00	97.02
0.900	15.98	9.00	46.41	24.00	70.30	110.00	97.74
1.00	16.76	9.50	47.65	25.00	71.31	120.00	98.29
1.50	19.78	10.00	48.84	30.00	75.76	130.00	98.71
2.00	22.21	10.50	49.99	35.00	79.41	140.00	99.04
2.50	24.43	11.00	51.09	40.00	82.46	150.00	99.31
3.00	26.55	12.00	53.18	45.00	85.03	160.00	99.52
3.50	28.60	13.00	55.12	50.00	87.19	170.00	99.69
4.00	30.58	14.00	56.93	55.00	89.02	180.00	99.82
4.50	32.49	15.00	58.63	60.00	90.57	190.00	99.90
5.00	34.32	16.00	60.22	65.00	91.88	200.00	99.94
5.50	36.07	17.00	61.73	70.00	93.00		
6.00	37.75	18.00	63.15	75.00	93.95		



Malvern Instruments Ltd.
 Malvern, UK
 Tel: +[44] (0)1684-892456 Fax: +[44] (0)1684-892789

Mastersizer S Ver. 2.19
 Serial Number: 33544-20

P.
 16 Jul 13 1'

